Fall 12-19-2020

Improved Statistical Methods for Time-series and Lifetime Data

Xiaojie Zhu
Southern Methodist University, xiaojiez@smu.edu

IMPROVED STATISTICAL METHODS FOR

TIME-SERIES AND LIFETIME DATA

Approved by:

Dr. Hon Keung Tony Ng
Prof. of Statistical Science

Dr. Ian Harris
Assoc. Prof. of Statistical Science

Prof. Wayne A. Woodward
Prof. of Statistical Science

Dr. Pankaj Choudhary
Prof. of Mathematical Sciences

IMPROVED STATISTICAL METHODS FOR TIME-SERIES AND LIFETIME DATA

A Dissertation Presented to the Graduate Faculty of the

Dedman College

Southern Methodist University

in

Partial Fulfillment of the Requirements

for the degree of

Doctor of Philosophy

with a

Major in Statistical Science

by

Xiaojie Zhu

B. S. , Ocean Univ. of China
Ph.D., Texas A&M University

December 19, 2020

ACKNOWLEDGMENTS

This work could not have been accomplished without the wisdom of my advisor, Prof. Ng, along with wonderful professors in the Department of Statistical Science here at SMU. I hereby would like to thank my advisor, Professor Hon Keung Tony Ng for his constant guidance, great encouragement and supervision. I also would like to express my sincere gratitude to Professor Wayne Woodward for his valuable suggestions and critical insights in this dissertation. I also would like to thank Professor Ian Harris and Professor Pankaj Choudhary for their valuable guidance and comments. Last but not the least, my sincere thanks are also due to my friends and colleagues and the department faculty and staff for making my time at SMU a great experience.

I'm forever grateful to my family for being so supportive of me. I am grateful that my husband Bo Chen is my powerful and strong pillar of strength, that my lovely kids Maddie, Jacey and Wolfram cheer me up everyday, and that my selfless parents Benqiang Zhu, Suhuai Lu and my caring parents-in-law Xiuying Zhou, Lejun Chen are always there whenever I need help.

Zhu, Xiaojie

B. S. , Ocean Univ. of China
Ph.D., Texas A&M University

Improved Statistical Methods for
Time-Series and Lifetime Data

Advisor: Dr. Hon Keung Tony Ng

Doctor of Philosophy degree conferred December 19, 2020
Dissertation completed July 9, 2020

In this dissertation, improved statistical methods for time-series and lifetime data are developed. First, an improved trend test for time series data is presented. Then, robust parametric estimation methods based on system lifetime data with known system signatures are developed.

In the first part of this disseration, we consider a test for the monotonic trend in time series data proposed by Brillinger (1989). It has been shown that when there are highly correlated residuals or short record lengths, Brillinger's test procedure tends to have significance level much higher than the nominal level. This could be related to the discrepancy between the empirical distribution of the test statistic and the asymptotic normal distribution. Hence, different bootstrap-based procedures are proposed based on the Brillinger test statistic. The performances of proposed bootstrap test procedures are evaluated through an extensive Monte Carlo simulation study, and are compared to other trend test procedures in the literature.

In the second part of this dissertation, we consider the estimation of component reliability based on system lifetime data with known system signature using the minimum density divergence estimation method. Different estimation procedures based on the minimum density divergence estimation method are proposed. We also study the standard error estimation and interval estimation procedures for the proposed minimum density divergence estimator. Based on the proposed procedures, a Monte Carlo simulation study

is used to evaluate the performance of these proposed procedures and compare these procedures with the maximum likelihood estimation under different contaminated models. Then, a numerical example is presented to illustrate the minimum density divergence estimation method. In particular, we show that the proposed estimation procedures are robust to contamination and model misspecification.

TABLE OF CONTENTS

LIST OF FIGURES viii

LIST OF TABLES xii

CHAPTER

1. Introduction 1

    1.1. Introduction of Improved Test for Monotonic Trend in Time Series Data ... 2

    1.2. Introduction of Robust Parameter Estimation Based on System Lifetime Data 4

    1.3. Scope of The Dissertation 6

2. Improved Test for Monotonic Trend in Time Series Based on Resampling Method 8

    2.1. The Issue of Inflated Significance Levels 8

    2.2. Test Procedures Based on Bootstrap Methods 12

    2.3. Performance of the Proposed Procedures 15

        2.3.1. Significance Level 16

        2.3.2. Power 20

    2.4. Comparison with Other Trend Tests 22

    2.5. Illustrative Example 25

3. Robust Parameter Estimation of Component Lifetime Distribution based on System Lifetime with Known Signature 27

    3.1. System Lifetime Data 27

    3.2. Minimum Density Divergence Estimator for System Lifetime Data 29

        3.2.1. Minimum Density Divergence Estimator 29

        3.2.2. Standard Error Estimation and Confidence Intervals 33

            3.2.2.1. Based on The Theoretical Results from Basu et al. (1998) 33

3.2.2.2. Based on The Observed Fisher Information Matrix 36
3.2.2.3. Based on The Bootstrap Method 37
3.3. Monte Carlo Simulation Studies 38
3.3.1. Results for Estimation of Scale and Shape Parameters 39
3.3.1.1. Results for The MDE_S Procedure 39
3.3.1.2. Results for The MDE_C Procedure 49
3.3.1.3. Results for The MDE_P Procedure 52
3.3.2. Results for Estimating The Mean Component Lifetime 71
3.3.3. Results for Standard Error Estimation and Confidence Interval Estimation 75
3.3.3.1. Determining a Suitable Bootstrap Size for Standard Error Estimation 78
3.3.3.2. Performance of Standard Error Estimates 79
3.3.3.3. Performance of Confidence Intervals 79
3.4. Illustrative Example 83
4. Concluding Remarks and Future Research Directions 93
4.1. Concluding Remarks 93
4.1.1. Improved Test for Monotonic Trend in Time Series Data 93
4.1.2. Robust Parameter Estimation for System Lifetime Data 94
4.2. Future Research Directions 95
4.2.1. Improved Test for Monotonic Trend in Time Series Data 95
4.2.2. Robust Parameter Estimation for System Lifetime Data 97

LIST OF FIGURES

Figure Page

2.1 The empirical distributions of Brillinger's test statistic (blue solid curves) and the standard normal distributions (red solid curves) with different record lengths. (a) $T = 100$, (b) $T = 500$, (c) $T = 1000$ and (d) $T = 10000$. The black dash lines demonstrate the observed test statistic, the blue dash lines are the critical values for rejecting the null hypothesis based on the empirical distributions, the red dash lines are the critical value for rejecting the null hypothesis based on the asymptotic standard normal. 11

2.2 The variance of estimated significance and observed power for Procedure 1, Procedure 2, and Procedure 3 with different record lengths. The blue circle lines are for $T = 100$, the red star lines are for $T = 500$, and the purple cross lines are for $T = 1000$. 17

2.3 Estimated significance levels of the three proposed bootstrap-based procedures (black for Procedure 1, blue for Procedure 2 and red for Procedure 3) with parametric and nonparametric bootstrap methods, different record lengths and autocorrelation coefficients. The dots represent the values of the estimated significance levels and the error bars represent the Monte Carlo error. 19

2.4 (a) Estimated power of the three proposed bootstrap-based procedures (black for Procedure 1, blue for Procedure 2 and red for Procedure 3) for $S(t) = \sqrt{t}$ and signal-to-noise ratio of 1, with parametric (dots) and nonparametric (triangles)bootstrap methods. (b) Estimated power values of the three proposed bootstrap-based procedures (black for Procedure 1, blue for Procedure 2 and red for Procedure 3) for $S(t) = \sqrt{t}$ and parametric bootstrap method, with signal-to-noise ratios(S/N) of 0.25 (dots) and 4.0 (triangles). The dots and triangles represent the values of estimated power and the error bars represent the Monte Carlo error. 21

2.5 Global annual temperature anomaly (black solid line) from 1880 to 2016 with fifteen years running mean of annual data (blue dash line) 26

3.1 (a) a 4-component series-parallel III system ($\boldsymbol{s} = (1/4, 1/4, 1/2, 0)$, referred to as *system I*) and (b) a 4-component mixed parallel I system ($\boldsymbol{s} = (0, 1/2, 1/4, 1/4)$), referred to as *System II*. 29

3.2 Boxplot of 10000 estimates of scale parameters by the MDE_S procedure for the System I with the longer-life contamination model 40

3.3 Boxplot of 10000 estimates of scale parameters by the MDE_S procedure for the System I with the shorter-life contamination model 41

3.4 Boxplot of 10000 estimates of shape parameters by the MDE_S procedure for the System I with the longer-life contamination model 42

3.5 Boxplot of 10000 estimates of shape parameters by the MDE_S procedure for the System I with the shorter-life contamination model 43

3.6 Boxplot of 10000 estimates of scale parameters by the MDE_S procedure for the System II with the longer-life contamination model 44

3.7 Boxplot of 10000 estimates of scale parameters by the MDE_S procedure for the System II with the shorter-life contamination model 45

3.8 Boxplot of 10000 estimates of shape parameters by the MDE_S procedure for the System II with the longer-life contamination model 46

3.9 Boxplot of 10000 estimates of shape parameters by the MDE_S procedure for the System II with the shorter-life contamination model 47

3.10 Relative efficiencies of estimated scale parameter by the MDE_S procedure for the System I 50

3.11 Relative efficiencies of estimated shape parameter by the MDE_S procedure for the System I 50

3.12 Relative efficiencies of estimated scale parameter by the MDE_S procedure for the System II 51

3.13 Relative efficiencies of estimated shape parameter by the MDE_S procedure for the System II 51

3.14 Boxplot of 10000 estimates of scale parameters by the MDE_C procedure for the System I with the longer-life contamination model 53

3.15 Boxplot of 10000 estimates of scale parameters by the MDE_C procedure for the System I with the shorter-life contamination model 54

3.16 Boxplot of 10000 estimates of shape parameters by the MDE_C procedure for the System I with the longer-life contamination model 55

3.17 Boxplot of 10000 estimates of shape parameters by the MDE_C procedure for the System I with the shorter-life contamination model 56

3.18 Boxplot of 10000 estimates of scale parameters by the MDE_C procedure for the System II with the longer-life contamination model 57

3.19 Boxplot of 10000 estimates of scale parameters by the MDE_C procedure for the System II with the shorter-life contamination model 58

3.20 Boxplot of 10000 estimates of shape parameters by the MDE_C procedure for the System II with the longer-life contamination model 59

3.21 Boxplot of 10000 estimates of shape parameters by the MDE_C procedure for the System II with the shorter-life contamination model 60

3.22 Relative efficiencies of estimated scale parameter by the MDE_C procedure for the System I 61

3.23 Relative efficiencies of estimated shape parameter by the MDE_C procedure for the System I 61

3.24 Relative efficiencies of estimated scale parameter by the MDE_C procedure for the System II 62

3.25 Relative efficiencies of estimated shape parameter by the MDE_C procedure for the System II 62

3.26 Boxplot of 10000 estimates of scale parameters by the MDE_P procedure for the System I with the longer-life contamination model 63

3.27 Boxplot of 10000 estimates of scale parameters by the MDE_P procedure for the System I with the shorter-life contamination model 64

3.28 Boxplot of 10000 estimates of shape parameters by the MDE_P procedure for the System I with the longer-life contamination model 65

3.29 Boxplot of 10000 estimates of shape parameters by the MDE_P procedure for the System I with the shorter-life contamination model 66

3.30 Boxplot of 10000 estimates of scale parameters by the MDE_P procedure for the System II with the longer-life contamination model 67

3.31 Boxplot of 10000 estimates of scale parameters by the MDE_P procedure for the System II with the shorter-life contamination model 68

3.32 Boxplot of 10000 estimates of shape parameters by the MDE_P procedure for the System II with the longer-life contamination model 69

3.33 Boxplot of 10000 estimates of shape parameters by the MDE_P procedure for the System II with the shorter-life contamination model 70

3.34 Relative efficiencies of estimated scale parameter by the MDE_P procedure for the System I 72

3.35 Relative efficiencies of estimated shape parameter by the MDE_P procedure for the System I 72

3.36 Relative efficiencies of estimated scale parameter by the MDE_P procedure for the System II 73

3.37 Relative efficiencies of estimated shape parameter by the MDE_P procedure for the System II 73

3.38 Relative efficiencies of estimated mean component lifetime for the System I with the longer-life contamination model 76

3.39 Relative efficiencies of estimated mean component lifetime for the System I with the shorter-life contamination model 76

3.40 Relative efficiencies of estimated mean component lifetime for the System II with the longer-life contamination model 77

3.41 Relative efficiencies of estimated mean component lifetime for the system II with the shorter-life contamination model 77

3.42 Coefficient of variation of $\widehat{SE}_B$ for scale parameter as a function of the number of bootstrap samples B 80

3.43 Coefficient of variation of $\widehat{SE}_B$ for scale parameter as a function of the number of bootstrap samples B 80

4.1 Percentage of identifying a significant trend for testing the monotonic trend with (a) the smooth window for spectrum $L = 7$ and the moving average parameter V varying from 2 to 20 in interval of 2 and with (b) the moving average parameter $V = 5$ and the smooth window for spectrum L varying from 2 to 20 in interval of 2 99

LIST OF TABLES

Table Page

2.1 Estimated significance levels (in %) of the Brillinger test for 1000 replications of the model in Eq. (1.1) with a constant $S(t)$ and $E(t)$ in form of $(1-\phi_1 B)E(t) = a(t)$, where $a(t)$ is a $N(0,1)$ Gaussian white noise 9

2.2 Brillinger's test statistic, average of $\sqrt{2\pi \hat{f}_{EE}(0) \sum_{t=1}^{T}[c(t)]^2}$ and standard error of $L = \sum_{t=1}^{T} c(t)Y(t)$ for the 500 simulated time series sample of the model $Y(t)$ with a constant signal term $S(t)$ and an AR(1) residual $(1-0.95B)E(t) = a(t)$, where $a(t)$ is a $N(0,1)$ white noise series..... 13

2.3 Estimated power (in %) for the three proposed bootstrap-based procedures (parametric bootstrap) for different record lengths and different forms of trends. 22

2.4 Estimated significance level (in %) for simulations. 25

3.1 The 24 possible arrangements of the component lifetime in a 4-component series-parallel III system 30

3.2 Simulated standard errors the MDE_S and the averaged standard error estimates based on the theoretical results from Basu et al. (1998) ($\widehat{SE}_A$), based on observed Fisher information matrix ($\widehat{SE}_F$), and based on bootstrap method ($\widehat{SE}_B$) with bootstrap size $B = 250$ 81

3.3 Simulated coverage probabilities (in %) and average widths of confidence intervals of the scale parameter computed based on MLE and MDE_S with different values of α under the longer-life and shorter-life contamination models for System I 84

3.4 Simulated coverage probabilities and average widths of confidence intervals of the shape parameter computed based on MLE and MDE_S with different values of α under the longer-life and shorter-life contamination models for System I 85

3.5 Simulated coverage probabilities and average widths of confidence intervals of the scale parameter computed based on MLE and MDE_S with different values of α under the longer-life and shorter-life contamination models for System II 86

3.6 Simulated coverage probabilities and average widths of confidence intervals of the shape parameter computed based on MLE and MDE_S with different values of α under the longer-life and shorter-life contamination models for System II 87

3.7 Simulated system lifetimes with system signature $\boldsymbol{s} = (1/4, 1/4, 1/2, 0)$ with component lifetime distribution $Weibull(3, 2)$ 88

3.8 Simulated system lifetimes with system signature $\boldsymbol{s} = (1/4, 1/4, 1/2, 0)$ with component lifetime distribution of $Weibull(3, 2)$ and one contaminated observation from $Weibull(9, 2)$ 88

3.9 Point and interval estimates for Weibull scale parameter for the data set presented in Table 3.7 90

3.10 Point and interval estimates for Weibull shape parameter for the data set presented in Table 3.7 91

3.11 Point and interval estimates for Weibull scale parameter for the data set presented in Table 3.8 92

3.12 Point and interval estimates for Weibull shape parameter for the data set presented in Table 3.8 93

I dedicate this dissertation to my family - Bo, Maddie, Jacey and Wolfram

Chapter 1

Introduction

The time dimension is an essential part in academic research. There are tremendous observations along the time domain in many fields of studies, such as economics, climatology, physics, chemistry, medical science and social sciences etc. When we analyze measurements at each time points along a time line, we are dealing with time series data. On the other hand, when we consider the time from an origin to an event that occurs, we are dealing with time-to-event (lifetime/reliability/survival) data. We accordingly study the two fields related to time - time series analysis and time-to-event data analysis - in this dissertation.

In the analysis of time series data, one of the fundamental questions of interest is whether there is a trend in the time series. The study of trends in times series is important in many applications, such as in the scientific study of climate (Cohn and Lins, 2005; Woodward and Gray, 1993), in temperature and precipitation (Feidas et al., 2004; Xu et al., 2002), in meteorology (Bonaccorso et al., 2005), and in economics. Detecting trends in a time series has been discussed in the literature for linear trends (Bloomfield and Nychka, 1992; Cochrane and Orcutt, 1949; Sun and Pantula, 1999; Woodward and Gray, 1993, 1995; Woodward et al., 1997), for quadratic trends (Woodward and Gray, 1995; Woodward, 2003) and for monotonic trends (Balakrishnan et al., 2016; Brillinger, 1989; Hofmann and Balakrishnan, 2006). For example, for temperature data, if there is indeed an underlying trend in the data, it is typically either linear or quadratic. In the first part of this dissertation, we focus on the general case of detecting monotonic trends.

In the second part, statistical analysis of system lifetime data with known system structure is considered. System lifetime data are commonly encountered in industrial or engineering settings where n components form a system and only the failure time of the system can be observed. Methods for estimating parameters of component lifetime distributions based on observed system lifetime data have been discussed in the literature (Balakrishnan et al., 2011a; Balakrishnan et al., 2011b; Ng et al., 2012; Yang et al., 2016; Zhang et al., 2015). However, these classical estimation methods may perform poorly in estimating component reliability when there are contaminations and/or outliers in the observed system lifetime data. To resolve this, we propose a robust parametric estimation for component lifetime distribution using the minimum density divergence method (Basu et al., 1998) based on system lifetime data.

1.1. Introduction of Improved Test for Monotonic Trend in Time Series Data

In the study of tests for monotonic trends, we consider a general form of trend in which the time series $Y(t)$, $t = 1, 2, \ldots, T$, is decomposed as

$$Y(t) = S(t) + E(t), \tag{1.1}$$

where $S(t)$ is a signal series and $E(t)$ is a stationary zero-mean noise series. The noise series $E(t)$ could be a stationary white noise process, or a stationary zero-mean autoregressive process. The hypothesis of interest is whether $S(t)$ has no trend or a monotonic trend.

To test the hypothesis that $S(t)$ has no trend or a monotonic trend, Brillinger (Brillinger, 1989) proposed a test statistic based on a linear combination of the time series

$$L = \sum_{t=1}^{T} c(t)Y(t), \tag{1.2}$$

where the coefficient $c(t)$ is defined as

$$c(t) = \left[t\left(1 - \frac{t}{T}\right)\right]^{1/2} - \left[(t+1)\left(1 - \frac{t+1}{T}\right)\right]^{1/2}.$$

If the noise series $E(t)$ is independent and identically distributed (i.i.d.) white noise, i.e., $N(0, \sigma^2)$, then the mean and variance of L are respectively $\sum_{t=1}^{T} c(t)S(t)$ and $\sigma[\sum_{t=1}^{T} c(t)]^2$, and we can use the test statistic in the form of $\sum_{t=1}^{T} c(t)S(t)/\sigma[\sum_{t=1}^{T} c(t)]^2$. However, when the noise series is a zero-mean autocorrelated process, while the mean of L is still $\sum_{t=1}^{T} c(t)S(t)$, the variance of L is no longer $\sigma[\sum_{t=1}^{T} c(t)]^2$. Brillinger (Brillinger, 1989) assumed that the cumulant function of the noise series $E(t)$ is finite and the signal series $S(t)$ is square integrable and has finite Lipshitz integral modulus of continuity. Under these assumptions, the variance of L can be obtained as $2\pi f_{EE}(0) \sum_{t=1}^{T}[c(t)]^2$, with $f_{EE}(0)$ being the power spectrum of the noise series $E(t)$ at frequency of 0. In our study, we consider time series with an autocorrelated noise series $E(t)$ satisfying $\phi(B)E(t) = a(t)$, where $\phi(B) = 1 - \phi_1 B - \cdots - \phi_p B^p$, B is the back-shift operator such that $B^k E(t) = E(t-k)$, and $a(t)$, $t = 1, 2, \ldots, T$ are i.i.d. normally distributed, denoted as $a(t) \sim N(0, \sigma_a^2)$. For a large T (i.e., a long record length), the distribution of L is proved to be asymptotically normal (Brillinger, 1989).

Under the null hypothesis of a constant signal $S(t)$, the distribution of L becomes asymptotically normal with mean 0 and variance $2\pi f_{EE}(0) \sum_{t=1}^{T}[c(t)]^2$. The test statistic proposed by Brillinger (Brillinger, 1989),

$$T_1 = \frac{\sum_{t=1}^{T} c(t)Y(t)}{\{2\pi f_{EE}(0) \sum_{t=1}^{T}[c(t)]^2\}^{\frac{1}{2}}}, \tag{1.3}$$

is asymptotically distributed as standard normal. We refer to the test statistics T_1 in Eq. (1.3) as Brillinger's test statistic hereafter. In practice, $2\pi \hat{f}_{EE}(0) \sum_{t=1}^{T} [c(t)]^2$ is used to estimate the variance of L, where $\hat{f}_{EE}(0)$ is a smoothed periodogram spectral estimate.

When testing a linear trend in time series, several testing procedures, such as the Cochran-Orcutt (CO) procedure (Cochrane and Orcutt, 1949), the maximum likelihood procedure, and the Bloomfield and Nychka (BN) procedure (Bloomfield and Nychka, 1992), tend to have a significance level higher than the nominal level when the time series is strongly auto-correlated and/or with short to moderate record lengths (Park and Michell, 1980; Woodward and Gray, 1993; Woodward et al., 1997). To solve the inflated-significance problem, Woodward et al. (1997) proposed an improved test for linear trends using the empirical distribution of the test statistic of the CO procedure from bootstrap samples.

In our study, it is found that the Brillinger test statistic also has the inflated-significance problem when the time series is strongly auto-correlated. We will provide further detailed discussions of this inflated-significance problem in Chapter 2. In the sequel, we propose improved tests for monotonic trends using the Brillinger test statistic, by adopting the bootstrap idea from Woodward et al. (1997).

1.2. Introduction of Robust Parameter Estimation Based on System Lifetime Data

We first formally describe a system with n components, where only the failure time of the system can be observed. Suppose the n component' lifetimes, $X_1, X_2, ..., X_n$, are i.i.d. with probability density function (p.d.f.) $f_X(t;\theta)$, cumulative distribution function (c.d.f.) $F_X(t;\theta)$, and survival function (s.f.) $\bar{F}_X(t;\theta)$. The ordered component lifetimes are $X_{1:n} < X_{2:n} ... < X_{n:n}$, where $X_{i:n}$ is the i-th ordered component lifetime. The failure of the whole system, measured by the system lifetime T, depends on the order of failure time of the n components. Accordingly, we define a system signature as an n-element probability vector $\boldsymbol{s} = (s_1, s_2, ..., s_n)$, where s_i is the probability that the i-th ordered component failure causes the failure of the system, i.e., $s_i = Pr(T = X_{i:n}), i = 1, 2, ..., n$ (Samaniego, 2007).

Note that the system signature depends on the system structrue only, and is distribution free. With a known system signature, the p.d.f. and s.f. of the system lifetime T for an n-component system can be expressed respectively as (Kochar et al., 1999):

$$f_T(t;\theta) = \sum_{i=1}^{n} s_i \binom{n}{i} i f_X(t;\theta) \left[F_X(t;\theta)\right]^{i-1} \left[\bar{F}_X(t;\theta)\right]^{n-i}, \tag{1.4}$$

and

$$\bar{F}_T(t;\theta) = \sum_{i=1}^{n} s_i \sum_{j=0}^{i-1} \left[F_X(t;\theta)\right]^{j} \left[\bar{F}_X(t;\theta)\right]^{n-j}. \tag{1.5}$$

Based on the p.d.f. and s.f. of the system lifetime T, statistical inference of the component lifetime distribution based on system lifetime data with a known system signature has been discussed extensively in the literature. For example, Balakrishnan et al. (2011a) developed an exact nonparametric inference for population quantiles and tolerance limits of the component lifetime distribution in a system. Balakrishnan et al. (2011b) derived the best linear unbiased estimator (BLUE) for the component lifetime of reliability systems with known signatures. Ng et al. (2012) discussed the method of moments, the maximum likelihood method and the least squares method for system lifetime data based on a proportional hazard rate model. Chahkandi et al. (2014) proposed nonparametric methods to construct prediction intervals for the lifetime of a system with known signature. Zhang et al. (2015) proposed a regression-based method for model parameters of the component lifetime in a censored system failure data with known signature. Yang et al. (2016) proposed a stochastic expectation-maximization (SEM) algorithm for obtaining the maximum likelihood estimates of the parameters in component lifetime distribution based on system lifetimes. More recently, Yang et al. (2019) developed the expectation maximization algorithm to obtain the maximum likelihood estimates (MLEs) of the parameters in component lifetime distribution based on system lifetime data when the system structure is unknown.

In industrial experiments on systems, there are many situations in which the underlying system is removed from experimentation before the occurrence of a failure of the system. Two common reasons for such pre-planned censoring are saving the time on

test and reducing the cost associated with the experiment because failure implies the destruction of a system, which can be costly (Cohen, 1991; Meeker and Escobar, 1998). In this dissertation, we consider a Type-II right censoring scheme in which the number of observed failures is pre-specified as r and the experiment is terminated as soon as a r-th ordered system failure is observed. Several studies on the Type-II censored system lifetime data with system signature have been conducted (Balakrishnan et al., 2011b; Ng et al., 2012; Yang et al., 2016, 2019; Zhang et al., 2015).

Finally, when there are contaminations or outliers in observed lifetime data, the performance of the maximum likelihood or other classical estimation methods may be affected, resulting in poor estimates of the component reliability characteristics. Basu et al. (1998) developed a family of density-based divergences measure with a single power parameter α that controls the trade-off between robustness and efficiency, and proposed a procedure for estimating model parameters based on minimizing the density divergence. Base et al. (2006) further extended the minimum density divergence procedure to censored survival data with and without contamination, and found that the minimum density divergence estimator (MDE) is superior than the MLE when there is contamination in the censored survival data.

In our study, we propose to use the MDE for parameter estimation of component reliability based on system lifetime data with and without contamination. For lifetime data, since censoring is a common feature as a result of time or budget constraints, we consider Type-II censoring in this study (Cohen, 1991; Meeker and Escobar, 1998), and evaluate the performance of the MDE with and without the Type-II censoring.

1.3. Scope of The Dissertation

In Chapter 2, we investigate the-inflated-significance-level problem in the Brillinger test for testing monotonic trends. As mentioned, the Brillinger test can have an inflated significance level, especially when the autoregressive process is strong in time series. This could be caused by the differences between the empirical distribution of the Brillinger

test statistic and the asymptotic normal distribution of the Brillinger test statistic. We propose three different bootstrap testing procedures for testing monotonic trends, based on the Brillinger test statistic. In order to evaluate the performance of the three proposed bootstrap-based procedures, we then carry out a Monte Carlo simulation study under different settings. The observed significance level and the power of proposed bootstrap-based procedures are further investigated and compared with the Brillinger test procedure. Moreover, the proposed bootstrap-based procedures are also compared with four other trend testing procedures in the literature.

In Chapter 3, we discuss robust parameter estimation of the component lifetime distribution based on system lifetime data. In the literature, parametric and nonparametric estimation of the component lifetime distribution based on system lifetime data have been developed. However, some methods have poor performance when there are contaminations in the data. To resolve this issue, we adopt the minimum density divergence estimator to system lifetime data to make statistical inference of component lifetime distribution, and propose three procedures based on the minimum density divergence estimator. In addition, we conduct a Monte Carlo simulation to evaluate the performance of the proposed minimum density divergence estimation procedures, and provide an illustrative example to illustrate the proposed estimation methods for component lifetime distribution based on system lifetime data.

Finally, in Chapter 4, we present some concluding remarks with some recommendations on the two studies, testing for monotonic trends and robust parameter estimation of component lifetime based on system lifetime data. We also provide some possible future research directions based on these two studies.

Chapter 2

Improved Test for Monotonic Trend in Time Series Based on Resampling Method

In this chapter, we present the improved monotonic trend test based on the Brillinger test statistic. In Section 2.1, we illustrate the issue of inflated significance level of the Brillinger test and analyze the possible reasons for this issue. By adopting the resampling method, three different bootstrap testing procedures based on Brillinger's test statistic are proposed in Section 2.2. In Section 2.3, a Monte Carlo simulation study is used to evaluate the performance of the proposed bootstrap-based procedures in terms of their significance levels and power values under different settings. In Section 2.4, the proposed procedures are compared with four other trend testing procedures and are further discussed on their performance under different scenarios. In Section 2.5, the proposed methodologies are illustrated by testing for trend in the annual global mean temperature anomaly from 1880 to 2016.

2.1. The Issue of Inflated Significance Levels

When there are highly correlated residuals or short record lengths, Brillinger's test procedure tends to have a significance level much higher than the nominal level. To illustrate this inflated-significance issue in the Brillinger test procedure, we first conduct a preliminary Monte Carlo simulation study. In the simulation study, we generate time series based on the model in Eq. (1.1), assuming a constant $S(t)$ and a noise series $E(t)$ with a first-order autoregressive (AR(1)) structure (i.e., $\phi(B) = 1 - \phi_1 B$). We consider eight record lengths, $T = 100$, 500, 1000, 5000, 10000, 15000, 20000 and 25000, and two

autoregressive coefficients $\phi_1 = 0.8$ and 0.95. For each setting, 1000 replications are used to estimate the significance level of the Brillinger test.

The estimated significance levels of the Brillinger test under different settings are presented in Table 2.1. We can see that with an autoregressive coefficient of 0.95, the estimated significance level for testing monotonic trends is 76% for a record length of 100, and reaches 4.9% only when the record length becomes 25000. With a smaller autoregressive coefficient ($\phi_1 = 0.8$), the inflated-significance problem is less severe; however, the estimated significance levels are still higher than 8% for record lengths $T = 100$, 500 and 1000, indicating the existence of an inflated-significance problem in the Brillinger test procedure when the autocorrelation is strong and/or when the record length is short. In the sequel of this section, we refer to small sample size as $T \leq 200$, moderate sample size as $200 < T \leq 1000$, and large sample size as $T > 1000$ for convenience.

One plausible reason for the inflated-significance-level problem is that the actual small-sample sampling distribution of the test statistic cannot be well approximated by a normal distribution. In order to study the sampling distribution of Brillinger's test statistic, we simulate time series from the model in Eq. (1.1) with a constant signal series $S(t)$ and an AR(1) residual series, $(1 - \phi_1 B)E(t) = a(t)$, where $a(t)$ is an i.i.d. $N(0, 1)$ Gaussian white noise series. Fixing the autocorrelation coefficient ϕ_1 to be 0.95, we set the record length T to be 100, 500, 1000 and 10000. For each simulated time series with a certain record length, we estimate the autoregressive coefficients ϕ_1, denoted as $\hat{\phi}_1$, for the noise series by assuming a constant signal term $S(t)$. With the estimated coefficient $\hat{\phi}_1$, we

Table 2.1: Estimated significance levels (in %) of the Brillinger test for 1000 replications of the model in Eq. (1.1) with a constant $S(t)$ and $E(t)$ in form of $(1 - \phi_1 B)E(t) = a(t)$, where $a(t)$ is a $N(0, 1)$ Gaussian white noise

Record length (T)	100	500	1000	5000	10000	15000	20000	25000
$\phi_1 = 0.95$	76.0	50.0	32.6	14.0	8.9	7.9	5.9	4.9
$\phi_1 = 0.80$	45.8	11.3	8.4	4.3	3.7	3.5	3.7	2.7

then generate 500 bootstrap samples ($N_b = 500$) from the associated AR(1) time series and calculate Brillinger's test statistic for each bootstrap sample. To illustrate the observations from the simulation study, the histograms and the estimated density curves (blue curves) for Brillinger's test statistics of the 500 simulated samples are compared with the asymptotic normal distribution (red curves) in Figure 2.1 for one of the simulations.

Figure 2.1 demonstrates that there are substantial discrepancies between the empirical distribution of Brillinger's test statistic, T_1, and the standard normal distribution, especially for short record length and large autoregressive coefficient ϕ_1. For example, with a record length of 100, both empirical distribution and standard normal distribution are centered at 0, but the empirical distribution of T_1 has a much fatter tail compared to the standard normal distribution (Figure 2.1a). As a result, the absolute values of the critical values for rejecting the null hypothesis based on the empirical distribution of T_1 (blue dashed lines in Figure 2.1a) are larger than those critical values based on the standard normal distribution (red dashed lines in Figure 2.1a). Hence, for example, with the value of the test statistic T_1 being 14.78 (black dashed line in Figure 2.1a), we fail to reject the null hypothesis based on the empirical distribution of T_1, but reject the null hypothesis based on the standard normal distribution.

We also observe that when the record length increases, the discrepancies between the empirical distribution of T_1 and the standard normal distribution become smaller, as is to be expected. When the record length increases to 500 and 1000, the empirical distributions of Brillinger's test statistics become closer to the standard normal distribution, but they still have relatively heavier tails compared to the standard normal distribution (Figures 2.1b and 2.1c). When the record length reaches 10000, the empirical distribution of Brillinger's test statistic shows a bell shape similar to the standard normal distribution (Figure 2.1d). These observations suggest that the asymptotic normal approximation works well for long record lengths, which verifies the results in Brillinger (1989).

In order to further investigate the reason for inflated significance level, we study the accuracy of the variance estimate of the linear combination L in Eq. (1.2) using Monte

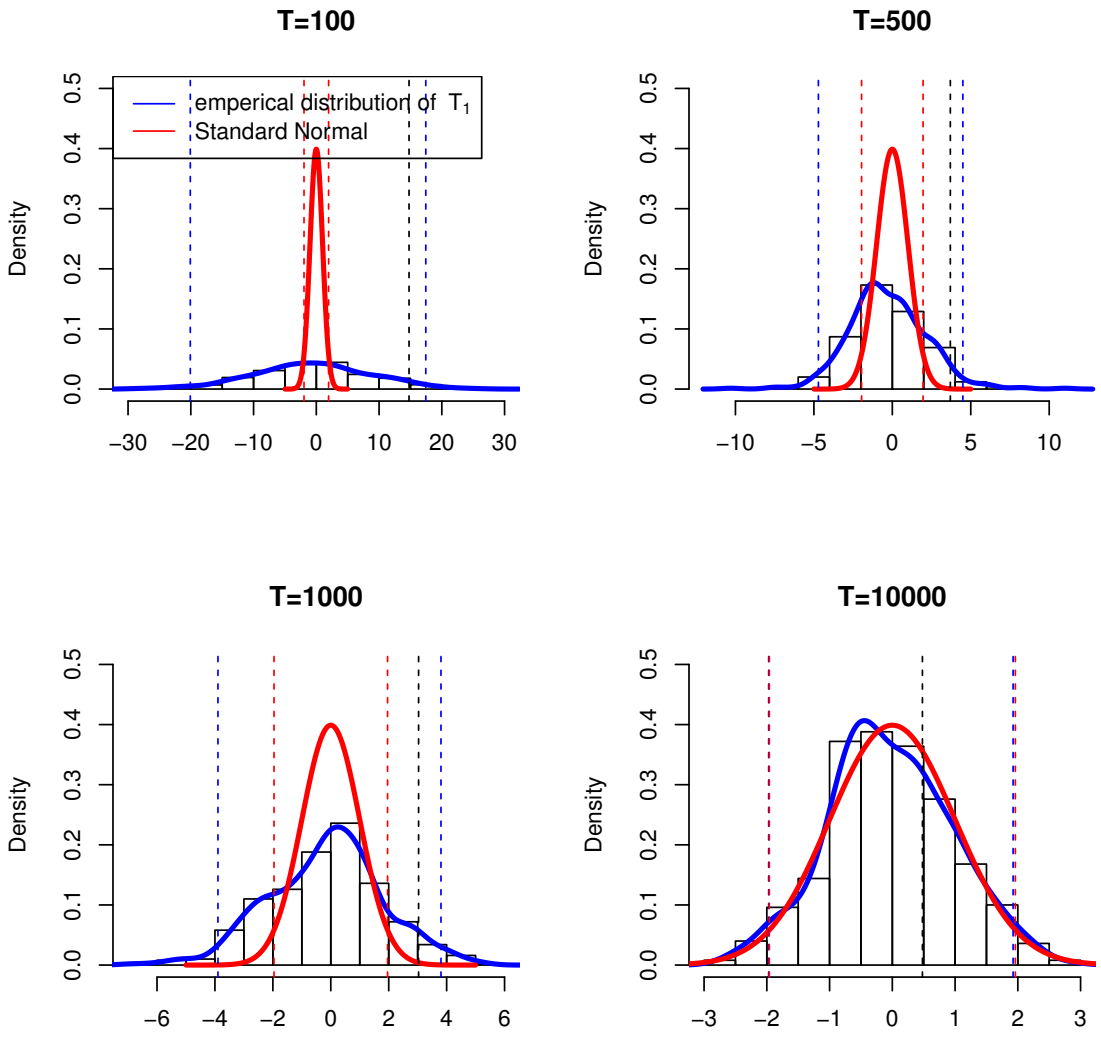

Figure 2.1: The empirical distributions of Brillinger's test statistic (blue solid curves) and the standard normal distributions (red solid curves) with different record lengths. (a) $T = 100$, (b) $T = 500$, (c) $T = 1000$ and (d) $T = 10000$. The black dash lines demonstrate the observed test statistic, the blue dash lines are the critical values for rejecting the null hypothesis based on the empirical distributions, the red dash lines are the critical value for rejecting the null hypothesis based on the asymptotic standard normal.

Carlo simulation. In Brillinger's test procedure, the standard deviation of L is estimated as

$$\sqrt{2\pi \hat{f}_{EE}(0) \sum_{t=1}^{T} [c(t)]^2}.$$

In the preliminary simulation study, we obtain the standard error of L for the 500 bootstrap samples and compare it with the average value of $\sqrt{2\pi \hat{f}_{EE}(0) \sum_{t=1}^{T} [c(t)]^2}$ based on the 500 bootstrap samples (Table 2.2). With a record length of 100, the standard error of L is about 10 times larger than the average of $\sqrt{2\pi \hat{f}_{EE}(0) \sum_{t=1}^{T} [c(t)]^2}$. We observe that the discrepancy between the standard error of L and the average of $\sqrt{2\pi \hat{f}_{EE}(0) \sum_{t=1}^{T} [c(t)]^2}$ becomes smaller when the record length increases. When the record length reaches 10000, the standard error of L is close to the average of $\sqrt{2\pi \hat{f}_{EE}(0) \sum_{t=1}^{T} [c(t)]^2}$. This indicates that the variance of L is well estimated by $2\pi \hat{f}_{EE}(0) \sum_{t=1}^{T} [c(t)]^2$ for realizations with long record lengths, but not for those with short to moderate record lengths.

2.2. Test Procedures Based on Bootstrap Methods

In the literature, Woodward et al. (1997) found the inflated significance level problem in the Cochrane-Orcutt (CO) procedure for testing a linear trend and proposed an improved bootstrap-based procedure based on the CO procedure. By adopting the bootstrap method, based on the investigations in the previous section, we first propose a bootstrap-based procedure, namely Procedure 1, by using empirical distribution of the Brillinger's test statistic T_1 from bootstrap samples. In Procedure 1, based on the observed time series $Y(t)$, we first estimate an autoregressive process under the null hypothesis that $S(t)$ is a constant. We use the Burg estimate for the estimated autocorrelation coefficients for the autoregressive process, denoted as $\hat{\phi}(B)$. Burg estimates for the autoregressive coefficients (Burg, 1975) uses the Durbin-Levinson algorithm to minimize the forward and backward sum of squares (FBSS) of the $AR(p)$ model:

Table 2.2: Brillinger's test statistic, average of $\sqrt{2\pi \hat{f}_{EE}(0) \sum_{t=1}^{T}[c(t)]^2}$ and standard error of $L = \sum_{t=1}^{T} c(t)Y(t)$ for the 500 simulated time series sample of the model $Y(t)$ with a constant signal term $S(t)$ and an AR(1) residual $(1 - 0.95B)E(t) = a(t)$, where $a(t)$ is a $N(0, 1)$ white noise series.

Record length (T)	100	500	1000	10000
Brillinger's test statistic	14.78	3.69	3.03	0.48
Average of $\sqrt{(2\pi \hat{f}_{EE}(0) \sum_{t=1}^{T}[c(t)]^2)}$	2.43	9.27	15.70	32.36
SE($\sum_{t=1}^{T} c(t)Y(t)$)	21.95	21.80	30.24	31.72

$$FBSS = \sum_{t=p+1}^{T} (Y(t) - \hat{\phi}_1 Y(t-1) \ldots - \hat{\phi}_p Y(t-p))^2 + \sum_{t=1}^{T-p} (Y(t) - \hat{\phi}_1 Y(t+1) \ldots - \hat{\phi}_p Y(t+p))^2$$

and always produce a stationary model. Then, the estimated residual, denoted as a $\hat{a}(t)$, is obtained as $Y(t) - \hat{\phi}_1 Y(t-1) \ldots - \hat{\phi}_p Y(t-p)$, with variance $\hat{\sigma}_a^2 = \frac{1}{T-1} \sum_{t=1}^{T} [\hat{a}(t) - \bar{a}]^2$, where $\bar{a} = \sum_{t=1}^{T} \hat{a}(t)/T$.

Note that when fitting the time series $Y(t)$ under the null hypothesis, the order of the autoregressive process $\hat{\phi}(B) = 1 - \hat{\phi}_1 B - \hat{\phi}_2 B^2 - \cdots - \hat{\phi}_p B^p$ (i.e., the value of p) best fitting the observed series is not specified. We use the Akaike Information Criterion (AIC) model selection criteria to determine the value of p that gives the best fitting stationary autoregressive process and we let the order p vary from 0 to 12. Then, based on the estimated autoregressive coefficients $\hat{\phi}(B)$, we generate N_b bootstrap samples of the time series, denoted as $Y_n(t)$ as follows:

$$\hat{\phi}(B) Y_n(t) = a(t), n = 1, 2, \ldots, N_b.$$

We consider both the parametric and nonparametric bootstrap for generating the bootstrap samples (Efron and Tibshirani, 1993). For the parametric bootstrap, we generate the residuals $a(t)$, $t = 1, 2, \ldots, T$ in model (1.1) for each bootstrap sample from a normal distribution with mean zero and variance $\hat{\sigma}_a^2$. For the nonparametric bootstrap, we treat the residuals from the original time series, $\hat{a}(t)$, $t = 1, 2, \ldots, T$, as the sampling pool and obtain a sample of size T with replacement from the sampling pool.

For each bootstrap sample, we obtain the Brillinger's test statistic T_1. Then, we sort the N_b values of T_1 in ascending order to obtain $\hat{T}_1^{(1)} < \hat{T}_1^{(2)} < \cdots < \hat{T}_1^{(N_b)}$, which gives the empirical distribution of the Brillinger test statistic T_1. Let the value of Brillinger's test statistic T_1 based on the observed time series $Y(t)$ be $T_{1,obs}$, then for a two-sided α level test for the hypothesis, we reject the null hypothesis if $T_{1,obs} < \hat{T}_1^{[\alpha n/2]}$ or $T_{1,obs} > \hat{T}_1^{[(1-\alpha/2)n]}$, where $[a]$ is the integer part of a.

The second bootstrap procedure, namely Procedure 2, is based on the bootstrap estimate of the standard error of L defined in Eq. (2). In Procedure 2, we first estimate the variance of L based on the bootstrap samples $Y_n(t)$, $n = 1, 2, \ldots, N_b$. Specifically, using the same bootstrap method described in the Procedure 1, we compute the linear combination $L_n = \sum_{t=1}^{T} c(t) Y_n(t)$ given in Eq. (1.2) for the n-th bootstrap sample and then estimate the standard error of the linear combination $\sum_{t=1}^{T} c(t) Y(t)$ as

$$s_L = \sqrt{\frac{1}{N_b} \sum_{n=1}^{N_b} (L_n - \bar{L})^2},$$

where $\bar{L} = \sum_{n=1}^{N_b} L_n / N_b$. The test statistic for Procedure 2 is

$$T_2 = \frac{\sum_{t=1}^{T} c(t) Y(t)}{s_L}, \tag{2.1}$$

in which the standard error of $\sum_{t=1}^{T} c(t)Y(t)$ is estimated by the bootstrap method. Based on the results of Bloomfield and Nychka (1992), the asymptotic distribution of the test statistic T_2 can be approximated by a standard normal distribution and hence, we reject the null hypothesis at α level if $|T_2| > z_{\alpha/2}$, where z_q is the q-th upper percentile of the standard normal distribution.

The third bootstrap procedure, namely Procedure 3, is based on the linear combination of the time series L. Similar to the bootstrap procedure in the Procedure 1, based on the estimated autoregressive coefficients $\hat{\phi}(B)$, we generate N_b bootstrap samples of the time series (denote as $Y_n(t)$, $n = 1, 2, \ldots, N_b$). We obtain the test statistic

$$T_3 = L = \sum_{t=1}^{T} c(t)Y(t) \tag{2.2}$$

for each bootstrap sample and we sort the N_b values of T_3 in ascending order to obtain $\hat{T}_3^{(1)} < \hat{T}_3^{(2)} < \cdots < \hat{T}_3^{(N_b)}$. Then, for a two-sided α level test, we reject the null hypothesis if $T_{3,obs} < \hat{T}_3^{[\alpha n/2]}$ or $T_{3,obs} > \hat{T}_3^{[(1-\alpha/2)n]}$, where $T_{3,obs}$ is the test statistic T_3 of the observed time series $Y(t)$.

2.3. Performance of the Proposed Procedures

A Monte Carlo simulation study is conducted to evaluate the performance and properties of the proposed bootstrap procedures for testing a monotonic trend. Significance levels of all test procedures are estimated through Monte Carlo simulations under the null hypothesis that $S(t)$ is a constant, i.e., there is no trend, while power of all test procedures are evaluated with Monte Carlo simulations under the alternative hypothesis that $S(t)$ has a monotonic trend, i.e., $S(t) = \ln(t), \sqrt{t}$ and $at + b$. Then, the significance level is estimated as the percentage of correctly identified constant signal series, and the power is estimated as the percentage of correctly identified a monotonic trend. When constructing the realization of $Y(t)$, we assume an AR(1) noise term (i.e., $(1 - \phi_1 B)E(t) = a(t)$) with

autoregressive coefficients ϕ_1 of 0.8 and 0.95. We evaluate the proposed procedures with three different record lengths, i.e., $T = 100, 500$ and 1000. We use 1000 replications for each setting.

Moreover, we consider different values of the ratio of the variance of the signal series $S(t)$ (denoted as σ_S^2)to the variance of the noise series $E(t)$(denoted as σ_E^2). Specifically, we consider the signal-to-noise (S/N) ratio σ_S^2/σ_E^2 to be $0.25, 1$ and 4. In order to construct the time series $Y(t)$ with a specified S/N ratio, we generate $S(t)$ from a specific form of signal and generate $E(t)$ from an autoregressive process separately. Then, we standardize the generated series $S(t)$ and $E(t)$, and multiply standardized $S(t)$ by a constant that reflect the S/N ratio. After that, we add the two series together to get the time series $Y(t)$.

For the size of the bootstrap samples in the bootstrap-based procedure, we conduct an additional simulation with different sizes of bootstrap samples, i.e., $N_b = 50$, 100, 200, 400, 500, 700 and 1000. Then, the variance of the estimated significance levels and estimated power values are evaluated to decide a proper size of bootstrap samples. There are three record lengths being considered, which are $T = 100, 500$ and 1000. From the simulation results, we observe that the smaller the record length, the larger the variances of estimated significance levels and observed power values (Figure 2.2). However, for all three record lengths, the variances of the estimated significance levels and estimated power values are relatively flat after bootstrap size reaches 200. Moreover, all three proposed procedures show similar performance regarding the bootstrap sizes. Hence, we use 200 bootstrap samples ($N_b = 200$) in our bootstrap-based procedures.

2.3.1. Significance Level

Comparing with the estimated significance level of the Brillinger's test (Table 2.1), we see that the estimated significance levels of the three proposed bootstrap-based procedures are greatly improved. When the record length is 100, for highly correlated residuals ($\phi_1 = 0.95$), the estimated significance level in the proposed procedures is around 10%, while the estimated significance level of the Brillinger's test is around 76%. Moreover,

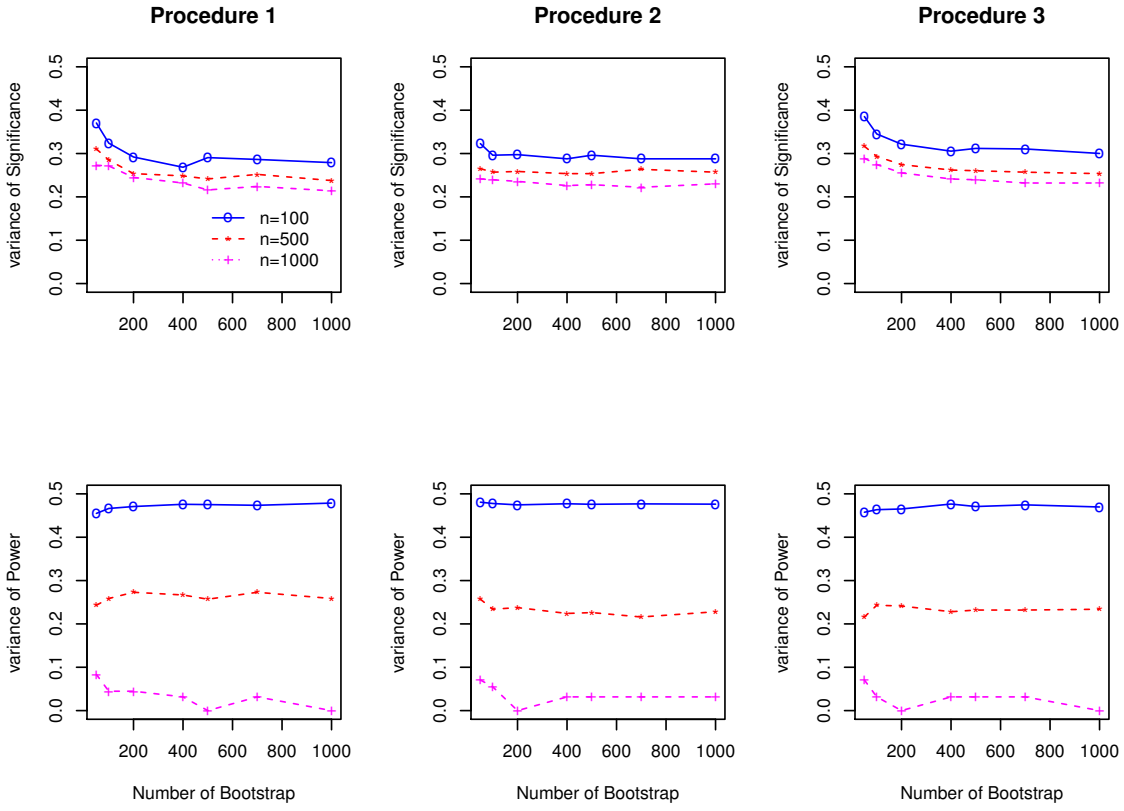

Figure 2.2: The variance of estimated significance and observed power for Procedure 1, Procedure 2, and Procedure 3 with different record lengths. The blue circle lines are for $T = 100$, the red star lines are for $T = 500$, and the purple cross lines are for $T = 1000$.

when the record length increases from 100 to 1000, the estimated significance levels of all the procedures considered here becomes closer to the 5% nominal level. However, the three proposed test procedures have significance levels much closer to the nominal level when the record length is large. This indicates that all the three bootstrap-based procedures better control the significance level compare to the original Brillinger test procedure.

In Figure 2.3, the estimated significance levels of the three proposed procedures are presented. To take the Monte Carlo errors into account, we plot the standard errors of the simulated significance levels as the error bars. When comparing the three proposed bootstrap-based procedures, Procedure 2 gives significance levels closer to the 5% level in most cases. For example, for the parametric bootstrap with ϕ_1 of 0.95 (Figure 2.3a), the significance levels for the Procedure 2 (blue dots) are 9%, 6.3% and 5.6% for record length of 100, 500 and 1000 respectively, which are the closest to the 5% level among all three procedures. For the nonparametric bootstrap with ϕ_1 of 0.95 (Figure 2.3c), Procedure 2 also controls the significance levels well, with significance level of 9.6%, 5.2% and 5.4% for record length of 100, 500 and 1000, respectively. However, overlaps of the Monte Carlo errors among all three proposed procedures indicate that there is no distinct difference among the three procedures.

We also observe that the performances of parametric (upper panel in Figure 2.3) and nonparametric bootstrap methods (lower panel in Figure 2.3) are similar in terms of controlling the significance level. For example, when ϕ_1 is 0.95 with record length T of 100, the estimated significance levels for the proposed procedures with parametric bootstrap method are around 9% (Figure 2.3a), while those with nonparametric bootstrap method are around 10% (Figure 2.3c). When the Monte Carlo error is taken into account, there is no distinct difference between the parametric bootstrap and the nonparametric bootstrap in all three bootstrap-based procedures.

In addition, the estimated significance levels are well controlled in both strong autocorrelated residuals (left panel in Figure 2.3) and weaker autocorrelated residuals (right

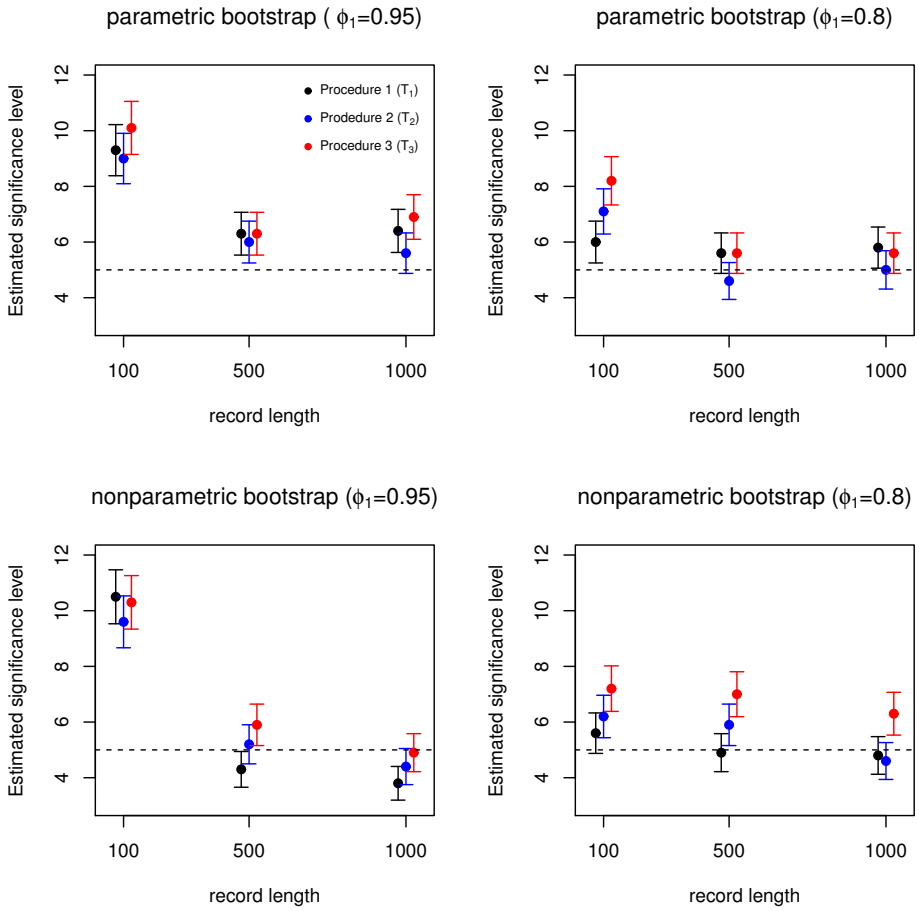

Figure 2.3: Estimated significance levels of the three proposed bootstrap-based procedures (black for Procedure 1, blue for Procedure 2 and red for Procedure 3) with parametric and nonparametric bootstrap methods, different record lengths and autocorrelation coefficients. The dots represent the values of the estimated significance levels and the error bars represent the Monte Carlo error.

panel in Figure 2.3). For short record length, i.e., $T = 100$, the significance level is larger than the nominal level when ϕ_1 is 0.95, compared to the case when ϕ_1 is 0.8. However, when the record length increases, all three procedures have well controlled significance level around 5% for both $\phi_1 = 0.95$ and $\phi_1 = 0.8$.

2.3.2. Power

It has been shown in the literature that the power values of tests for the linear trend decrease when the autocorrelation of the time series increases (Woodward et al., 1997). Hence, in this section, we only present the estimated power for settings with strong correlated noise series, i.e., $\phi_1 = 0.95$.

In Figure 2.4a, we present the estimated power values of the three bootstrap-based procedures based on both parametric and nonparametric bootstrap methods for $S(t) = \sqrt{t}$ with different record lengths. As we expected, the power values of the test procedures increase when the record length increases. We observe from Figure 2.4a that the power values of the proposed procedures based on the parametric bootstrap method are higher than those based on the nonparametric bootstrap method, especially when the record length is larger than 500. This may be related to the assumption of Gaussian white noise in simulating $a(t)$.

In addition, we present the power values of the three proposed test procedures based on parametric bootstrap method with signal-to-noise ratio (S/N) of 0.25 and 4.0 in Figure 2.4b. It is shown that the larger the signal-to-noise ratio, the larger the power of the three proposed test procedures. In the strong noise scenario (S/N of 0.25), the power of all three proposed procedures have no distinct differences while the Monte Carlo error is taken into account. However, in the strong signal scenario (S/N of 2), Procedure 1 has weaker power than the other two proposed procedures when the record length is small, i.e., $T = 100$.

It is also interesting to study whether the performance of all three proposed procedures is sensitive to the form of the signal. Hence, we present the estimated power of the three

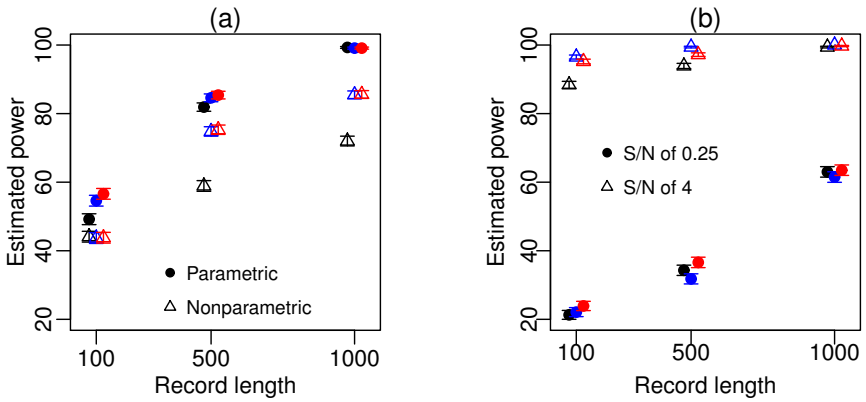

Figure 2.4: (a) Estimated power of the three proposed bootstrap-based procedures (black for Procedure 1, blue for Procedure 2 and red for Procedure 3) for $S(t) = \sqrt{t}$ and signal-to-noise ratio of 1, with parametric (dots) and nonparametric (triangles)bootstrap methods. (b) Estimated power values of the three proposed bootstrap-based procedures (black for Procedure 1, blue for Procedure 2 and red for Procedure 3) for $S(t) = \sqrt{t}$ and parametric bootstrap method, with signal-to-noise ratios(S/N) of 0.25 (dots) and 4.0 (triangles). The dots and triangles represent the values of estimated power and the error bars represent the Monte Carlo error.

proposed procedures for simulated $Y(t)$ with different forms of $S(t)$ in Table 2.3. In order to focus on the aspect of forms of the signal, we fix the signal-to-noise ratio to be 2 and use parametric bootstrap for generating bootstrap samples. Among all the record lengths, the power of the three proposed procedures are higher when the signal term is in the form of $\ln(t)$. However, as the record length increases, the power of the three proposed procedures becomes less sensitive to the forms of signal.

2.4. Comparison with Other Trend Tests

In addition to comparing the three proposed bootstrap-based procedures to Brillinger's original test, we consider three nonparametric trend test procedures in the literature and compare their performances with the proposed test procedures. The three trend tests are the Mann-Kendall test (MK) (Ken, 1955; Mann, 1945), a generalized nonparametric trend test proposed by Hofmann and Balakrishnan (HB) (Hofmann and Balakrishnan, 2006), and a modified Mann-Kendall test proposed by Hamed and Rao (HR) (Hamed and Rao, 1998). The MK test statistic is

$$MK = \sum_{1<i<j<T} sgn(Y_j - Y_i), \tag{2.3}$$

Table 2.3: Estimated power (in %) for the three proposed bootstrap-based procedures (parametric bootstrap) for different record lengths and different forms of trends.

	$T = 100$			$T = 500$			$T = 1000$		
$S(t)$	$\ln(t)$	$\sqrt{t}$	$at + b$	$\ln(t)$	$\sqrt{t}$	$at + b$	$\ln(t)$	$\sqrt{t}$	$at + b$
Procedure 1	64.9	49.2	42.3	92.8	81.9	74.9	99.8	99.3	97.7
Procedure 2	63.7	54.6	44.7	94.7	84.6	78.8	99.9	99.1	98.0
Procedure 3	66.2	56.6	47.7	94.4	85.4	80.9	99.9	99.1	97.9

where $sgn(x)$ is the signum function. It has been shown that the MK test statistic is asymptotic normally distributed with mean of 0 and variance of

$$\left[T(T-1)(2T+5) - \sum_{j=1}^{j=m} d_j(d_j-1)(2d_j+5)\right]/18,$$

where m is the number of tied groups in the time series and d_j is the number of observation in the j-th tied group. The HB test statistic proposed by Hofmann and Balakrishnan (2006) is constructed based on initial ranks:

$$HB = \left[\ln\left(\frac{1+a^*}{1-a^*}\right)\right]^{-1} \sum_{k=1}^{k=T}(k-1)^3 \left[\ln\left(\frac{1+a^*\gamma_k}{1-a^*\gamma_k}\right) - \ln\left(\frac{1+a^*\gamma_k^*}{1-a^*\gamma_k^*}\right)\right], \tag{2.4}$$

where γ_k and γ_k^* are the standardized initial ranks, i.e.,

$$\gamma_1 = \gamma_1^* = 0,$$

$$\gamma_k = \left[\rho_k - (k+1)/2\right]/\left[(k-1)/2\right]$$

and

$$\gamma_k^* = \left[\rho_k^* - (k+1)/2\right]/\left[(k-1)/2\right],$$

in which ρ_k and ρ_k^* are the initial ranks with ρ_k be the number of $X_i \leq X_k, 1 \leq i \leq k$ and ρ_{n+1-k} be the number of $X_i \leq X_k, k \leq i \leq n$. The value of a^* is set to be 0.999 as suggested in Hofmann and Balakrishnan (2006) and the critical values of the test are obtained from Table 4 of Hofmann and Balakrishnan (2006) for $T = 100$ and from 10000 Monte Carlo simulations for $T = 500$ and 1000 under the null hypothesis that the time series has no trend and is i.i.d.. Hamed and Rao (1998) proposed a trend test for autocorrelated data which is a modification of the Mann-Kendall test. The form of the HR test is the same as the MK test statistic, but the variance of the test statistic is modified as

$$\frac{T(T-1)(2T+5)}{18}\frac{T}{T^*}, \tag{2.5}$$

where T^* is effective number of observations after accounting autocorrelation. Here, T/T^* is calculated as $1 + 2/[T(T-1)(T-2)] + \sum_{i=1}^{T-1}(T-i)(T-i-1)(T-i-2)\rho(i)$, where $\rho(i)$ is autocorrelation of the ranks of observation.

Together with the Brillinger test procedure (BR) and the three bootstrap-based procedures proposed in Section 2.3, seven trend test procedures are compared in terms of their significance levels and power values via a Monte Carlo simulation study. For the significance levels, 1000 replications of time series $Y(t)$ with record length $T = 100$, 500 and 1000 and correlated noise series $a(t) = (1 - 0.95B)E(t)$ are simulated under the null hypothesis that there is no trend. The seven test procedures are used to test for trend for each simulated time series and the significance level of each test procedure is estimated by the rejection rate of the null hypothesis. The estimated significance levels for the seven test procedures are presented in Table 2.4.

From Table 2.4, we observe that the three proposed bootstrap-based procedures have significance levels closer to the nominal 5% level, especially when the record length is $T = 1000$. In contrast, the other four test procedures existed in the literature have seriously inflated significance levels. Specifically, for short record length ($T = 100$), the MK procedure and the HB procedure have simulated significance levels 71.3% and 73.3%, respectively. For the HR procedure, although it has taken the autocorrelation in the time series into account, the estimated significance level only reduces to 41.9%. Although the simulated significance levels of the BR, MK, HB and HR procedures are getting closer to the nominal 5% level, the simulated significance levels are still higher than 30%.

Note that the noise series in our Monte Carlo simulation study is assumed to have an autoregressive structure. If the noise series is i.i.d., the significance levels of the MK, HB and HR procedures are well controlled around 5%. If the noise series is highly

correlated, the proposed procedures are recommended for testing the monotonic trend as the significance levels of those procedures are better controlled.

2.5. Illustrative Example

In this section, we illustrate the proposed bootstrap-based procedures by applying them to the annual atmospheric temperature series from 1880 to 2016 presented in Figure 2.5. We first decomposed the temperature time series $Y(t)$ (black solid line in the top figure of Figure 2.5) into the signal term $S(t)$, which is estimated as a fifteen years running mean (blue solid line in Figure 2.5) and the noise term $E(t)$ as the residuals.

If the noise series $E(t)$ is an independent series, the test statistic

$$\sum_{t=1}^{T} c(t)Y(t) / \left[\sigma^2 \sum_{t=1}^{T} c(t)\right]^{1/2} \tag{2.6}$$

can be used to test for monotonic trend (Brillinger, 1989). Therefore, we first examine the sample autocorrelations and carry out the Ljung-Box test for white noise for the noise series $E(t)$. The sample autocorrelation for $E(t)$ shows several significant lag autocorrelations and the Ljung-Box test statistic is 43.18 (degrees of freedom is 24) with p-value of 0.009. Both significant lag autocorrelation and significant Ljung-Box test statistic suggest that the noise series $E(t)$ is not white noise and has some autocorrelation structure. Hence, autocorrelation in noise series needs to be considered for trend test.

To test the hypotheses that no trend as null hypothesis and monotonic trend as alternative hypothesis, the value obtained for the Brillinger's test statistic is 18.42, with corre-

Table 2.4: Estimated significance level (in %) for simulations.

	BR	MK	HB	HR	$Procedure1$	$Procedure2$	$Procedure3$
$T = 100$	79.0	71.3	73.3	41.9	9.3	9.0	10.1
$T = 500$	50.0	73.0	75.0	29.1	6.3	6.0	6.3
$T = 1000$	32.6	73.3	75.0	30.2	6.4	5.6	6.9

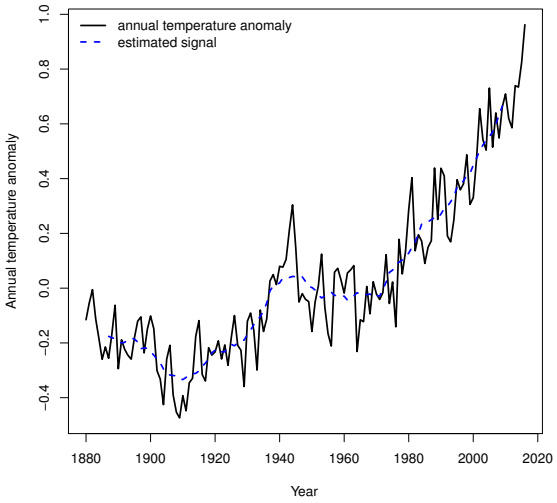

Figure 2.5: Global annual temperature anomaly (black solid line) from 1880 to 2016 with fifteen years running mean of annual data (blue dash line)

sponding p-value less than 0.001 based on normal approximation. Based on Procedure 1, the test statistic is also 18.42 but the p-value is 0.002. The test statistic obtained by the Procedure 2 is 2.103, with corresponding p-value of 0.018, while the test statistic obtained by Procedure 3 is 4.26 with p-value of 0.004. All the bootstrap-based procedures and the original Brillinger's test reject the null hypothesis that there is no trend in the annual temperature anomaly from 1880 to 2016. It is noteworthy that although all the test procedures studied here reach the same conclusion in testing the hypotheses of no trend versus monotonic trend, the Brillinger's test based on normal approximation does not well control the type-I error rate.

Chapter 3

Robust Parameter Estimation of Component Lifetime Distribution based on System Lifetime with Known Signature

In this chapter, we study the robust minimum density divergence estimation method and apply it to the system lifetime with and without contamination. The system lifetime with known signature is described in Section 3.1. In Section 3.2, we introduce three proposed parametric estimation procedure based on the minimum density power divergence for system lifetime data with known system signature. We also discuss the estimation of the standard error and confidence interval coverage of the estimate in section 3.2. In Section 3.3, a Monte Carlo simulation study is presented to evaluate the proposed procedures in terms of their point estimates, as well as their standard error estimation and confidence interval coverage. In Section 3.4, a numerical example is used to illustrate the proposed minimum density power divergence estimators.

3.1. System Lifetime Data

Based on the notation for n-component system and system signature described in Section 1.2, we consider the coherent system in which every component is relevant and the system has a monotone structure function (Boland and Samaniego, 2004). In a coherent system consists of n i.i.d. components, the system structure can be described by the system signature defined as an n-element probability vector $\boldsymbol{s} = (s_1, s_2, \ldots, s_n)$,

where the i-th element is the probability that the i-th ordered component failure causes the failure of the system (Samaniego, 2007), i.e.,

$$s_i = \Pr(T = X_{i:n}), i = 1, 2, \ldots, n.$$

To further illustrate the idea of system signature, we consider the 4-component series-parallel III system with system lifetime $T = \min\{X_1, \max\{X_2, X_3, X_4\}\}$ presented in Figure 3.1a. For the 4-component series-parallel III system, there are 24 possible arrangements of the component lifetimes, The 24 arrangements and their corresponding system lifetimes are presented in Table 3.1. From Table 3.1, we can obtain

$$\begin{aligned} s_1 &= \Pr(T = X_{1:4}) = 6/24 = 1/4, \\ s_2 &= \Pr(T = X_{2:4}) = 6/24 = 1/4, \\ s_3 &= \Pr(T = X_{3:4}) = 12/24 = 1/2, \\ s_4 &= \Pr(T = X_{4:4}) = 0. \end{aligned}$$

Hence, the system signature of the 4-component series-parallel III system in Figure 3.1a is $\boldsymbol{s} = (1/4, 1/4, 1/2, 0)$. Similarly, for the 4-component mixed parallel I system presented in Figure 3.1b, the system signature is $\boldsymbol{s} = (0, 1/2, 1/4, 1/4)$.

As mentioned in Section 1.2, in industrial experiments on systems, there are many situations in which systems are removed from experimentation before the occurrence of the failure of the system. Moreover, when there is contamination and/or outliers exist in observed lifetime data, the performance of the maximum likelihood method or other classical estimation methods may be affected and poor estimates of the component reliability characteristics may be yielded. Based on the minimum density divergence estimators (MDEs) studied in Basu et al. (1998) and Base et al. (2006), in this study, we consider the robust minimum density divergence estimation method for the system lifetime data with

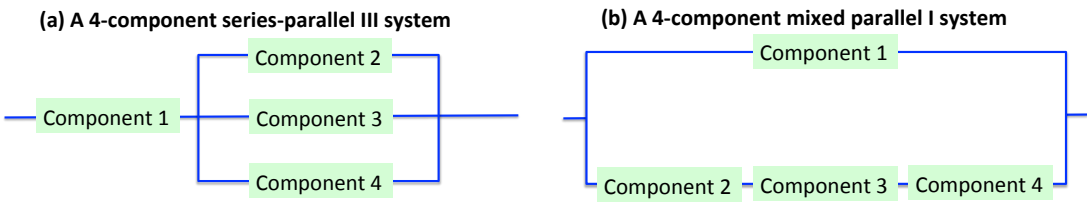

Figure 3.1: (a) a 4-component series-parallel III system ($\boldsymbol{s} = (1/4, 1/4, 1/2, 0)$, referred to as *system I*) and (b) a 4-component mixed parallel I system ($\boldsymbol{s} = (0, 1/2, 1/4, 1/4)$), referred to as *System II*

and without contamination.

3.2. Minimum Density Divergence Estimator for System Lifetime Data

3.2.1. Minimum Density Divergence Estimator

The density power divergence, proposed by Basu et al. (1998), describes a family of density-based divergence measures between two probability density functions $g(t)$ and $f(t)$ with a single parameter α. Consider that $f(t;\boldsymbol{\theta})$ is a parametric p.d.f. of the fitted model with parameter vector $\boldsymbol{\theta}$ and $g(t)$ is the target density function, the density power divergence between $f(t;\boldsymbol{\theta})$ and $g(t)$ is defined as

$$d_\alpha(g,f) = \int \left[f^{1+\alpha}(t;\boldsymbol{\theta}) - \left(1+\frac{1}{\alpha}\right) g(t) f^{\alpha}(t;\boldsymbol{\theta}) + \frac{1}{\alpha} g^{1+\alpha}(t) \right] dt, \quad \alpha > 0 \tag{3.1}$$

and

$$d_0(g,f) = \lim_{\alpha \to 0} d_\alpha(g,f) = \int g(t) \ln \left[\frac{g(t)}{f(t;\boldsymbol{\theta})} \right] dt. \tag{3.2}$$

It is obvious that the density power divergence is zero when $f(t;\boldsymbol{\theta}) = g(t)$. The MDE of the parameter vector $\boldsymbol{\theta}$ can be obtained by minimizing the density power divergence

Table 3.1: The 24 possible arrangements of the component lifetime in a 4-component series-parallel III system

Arrangement	System lifetime T	Arrangement	System lifetime T
$X_1 < X_2 < X_3 < X_4$	$X_{1:4}$	$X_3 < X_1 < X_4 < X_2$	$X_{2:4}$
$X_1 < X_2 < X_4 < X_4$	$X_{1:4}$	$X_3 < X_4 < X_1 < X_2$	$X_{3:4}$
$X_1 < X_4 < X_2 < X_3$	$X_{1:4}$	$X_3 < X_1 < X_2 < X_4$	$X_{2:4}$
$X_1 < X_4 < X_3 < X_2$	$X_{1:4}$	$X_3 < X_4 < X_1 < X_2$	$X_{3:4}$
$X_1 < X_3 < X_2 < X_4$	$X_{1:4}$	$X_3 < X_2 < X_1 < X_4$	$X_{3:4}$
$X_1 < X_3 < X_4 < X_2$	$X_{1:4}$	$X_3 < X_2 < X_4 < X_1$	$X_{3:4}$
$X_2 < X_1 < X_3 < X_4$	$X_{2:4}$	$X_4 < X_1 < X_2 < X_3$	$X_{2:4}$
$X_2 < X_1 < X_4 < X_3$	$X_{2:4}$	$X_4 < X_1 < X_3 < X_2$	$X_{2:4}$
$X_2 < X_3 < X_1 < X_4$	$X_{3:4}$	$X_4 < X_2 < X_1 < X_3$	$X_{3:4}$
$X_2 < X_3 < X_4 < X_1$	$X_{3:4}$	$X_4 < X_2 < X_1 < X_1$	$X_{3:4}$
$X_2 < X_4 < X_1 < X_3$	$X_{3:4}$	$X_4 < X_3 < X_1 < X_2$	$X_{3:4}$
$X_2 < X_3 < X_3 < X_1$	$X_{3:4}$	$X_4 < X_3 < X_2 < X_1$	$X_{3:4}$

between $f(t;\boldsymbol{\theta})$ and $g(t)$ with respect to (w.r.t.) $\boldsymbol{\theta}$. Notice that the term $\int [(1/\alpha)g^{1+\alpha}(t)]\, dt$ in Eq.(3.1) does not depend on the parameter vector $\boldsymbol{\theta}$. Therefore, the MDE of $\boldsymbol{\theta}$ can be obtained by minimizing the term

$$\int \left[f^{1+\alpha}(t;\boldsymbol{\theta}) - \left(1 + \frac{1}{\alpha}\right) g(t) f^{\alpha}(t;\boldsymbol{\theta}) \right] dt \tag{3.3}$$

w.r.t. $\boldsymbol{\theta}$.

The density power divergence reduces to the Kullack-Leibler divergence (Kullback and Leibler, 1951) when $\alpha = 0$, and is the mean squared error when $\alpha = 1$. Hence, the minimum density power divergence procedure is degenerated into the maximum likelihood method when $\alpha = 0$, and becomes the minimization of the mean squared error when $\alpha = 1$. The parameter α in Eq. (3.1) controls the trade-off between robustness and efficiency of the MDE (Basu et al., 1998; Base et al., 2006). It has been shown that the typical value of α is in between 0 and 1 and the estimation procedure becomes less efficient as α increases (Basu et al., 1998). Hence, in our study, we consider the value of α

in between 0 and 1.

Base et al. (2006) proposed a method that uses the empirical distribution function $\hat{G}_n$ to estimate the target distribution G. Based on this method, we have

$$\begin{aligned} & \int \left[f^{1+\alpha}(t;\boldsymbol{\theta}) - (1+1/\alpha)g(t)f^{\alpha}(t;\boldsymbol{\theta})\right] dt \\ = & \int f^{1+\alpha}(t;\boldsymbol{\theta})dt - \int (1+1/\alpha)f^{\alpha}(t;\boldsymbol{\theta})dG(t) \\ \approx & \int f^{1+\alpha}(t;\boldsymbol{\theta})dt - \int (1+1/\alpha)f^{\alpha}(t;\boldsymbol{\theta})d\hat{G}(t). \end{aligned}$$

Suppose that in a life testing experiment with m independent n-component systems and a Type-II censored system lifetime data $T_{1:m} < T_{2:m} < \ldots < T_{r:m}$ $(r < m)$ is observed, the empirical distribution function of the system lifetime, $\hat{G}_T(t)$, can be obtained by using the Kaplan-Meier (K-M) estimator of the survival function $\hat{S}_T(t) = 1 - \hat{G}_T(t)$ (Kaplan and Meier, 1958) based on the Type-II censored system lifetime data. Then, the MDE of $\boldsymbol{\theta}$ can be obtained at the system level by minimizing

$$\hat{d}_{\alpha}(g,f) = \int f_T^{1+\alpha}(t;\boldsymbol{\theta})dt - \int \left(1+\frac{1}{\alpha}\right) f_T^{\alpha}(t;\boldsymbol{\theta})d\hat{G}_T(t) \tag{3.4}$$

w.r.t. $\boldsymbol{\theta}$. As this minimization is carried out at the system lifetime level, this estimator is named as the MDE at system lifetime level, denoted as MDE_S.

In addition to the MDE at system lifetime level, the MDE can be considered at the component level. Based on the K-M estimator of the survival function of the system lifetime $\hat{S}_T(t)$, a nonparametric empirical distribution of the component lifetime distribution $\hat{G}_X(t)$ can be obtained based on the relationship between the c.d.f. of system life time and the c.d.f. of component lifetime in Eq. (1.5) as

$$\hat{S}_T(t) = \sum_{i=1}^{n} s_i \sum_{j=0}^{i-1} \left[\hat{G}_X(t)\right]^j \left[1-\hat{G}_X(t)\right]^{n-j}.$$

Then, the model parameter $\boldsymbol{\theta}$ can be estimated by minimizing the density power divergence based on component lifetime distribution

$$\hat{d}_\alpha(g, f) = \int f_X^{1+\alpha}(t; \boldsymbol{\theta}) dt - \int \left(1 + \frac{1}{\alpha}\right) f_X^{\alpha}(t; \boldsymbol{\theta}) d\hat{G}_X(t). \tag{3.5}$$

Since the MDE is obtained based on component lifetime distribution, we refer to the estimator obtained by minimizing Eq. (3.5) as the MDE at component lifetime level, denoted as MDE_C.

Instead of estimating the c.d.f. nonparametrically, we consider the nonparametric kernel density estimator to estimate the density function $g(t)$ (Sheather and Jones, 1991). With the observed Type-II censored system lifetime data, the p.d.f. of system lifetime can be estimated using the Gaussian kernel density estimator, denoted as $\hat{g}_T(t)$. Then, the density power divergence function can be expressed as

$$\hat{d}_\alpha(g, f) = \int f_T^{1+\alpha}(t; \boldsymbol{\theta}) dt - \int \left(1 + \frac{1}{\alpha}\right) f_T^{\alpha}(t; \boldsymbol{\theta}) \hat{g}_T(t) dt. \tag{3.6}$$

A MDE of $\boldsymbol{\theta}$ can be obtained by minimizing the density power divergence in Eq. (3.6) with the estimated kernel density $\hat{g}_T(t)$ w.r.t. $\boldsymbol{\theta}$. We name the MDE obtained by minimizing Eq. (3.6) as the MDE with estimated p.d.f., denoted as MDE_P.

For comparative purposes, we also consider the maximum likelihood estimator (MLE) based on Type-II censored system lifetime data $T_{1:m} < T_{2:m} < \ldots, T_{r:m}$. The log-likelihood function based on the observed Type-II censored system lifetime data $t_{1:m} < t_{2:m} < \ldots, t_{r:m}$ is

$$\ln L(\boldsymbol{\theta} | t_{1:m}, t_{2:m} \ldots t_{r:m}) = \sum_{k=1}^{r} \ln f_T(t_{k:m}; \boldsymbol{\theta}) + (m - r) \ln \bar{F}_T(t_{r:m}; \boldsymbol{\theta}), \tag{3.7}$$

where $r \leq m$ is the number of observed system lifetime and m is the total number of systems on test. The MLE of $\boldsymbol{\theta}$ can be obtained by maximizing the log-likelihood function in Eq. (3.7) w.r.t. $\boldsymbol{\theta}$.

3.2.2. Standard Error Estimation and Confidence Intervals

3.2.2.1. Based on The Theoretical Results from Basu et al. (1998)

For the MDE, Theorem 2.2 in Basu et al. (1998) proved that under some regularity conditions, the MDE of the parameter $\boldsymbol{\theta}$ (denoted as $\hat{\boldsymbol{\theta}}$) is a consistent estimator for $\boldsymbol{\theta}$, and $n^{1/2}(\hat{\boldsymbol{\theta}} - \boldsymbol{\theta})$ is asymptotically multivariate normally distributed with zero mean and variance-covariance matrix $J^{-1}KJ^{-1}$, where

$$\begin{aligned} J &= \int \boldsymbol{u}_\theta(t)\boldsymbol{u}_\theta^T(t) f^{1+\alpha}(t,\boldsymbol{\theta})dt \\ &\quad + \int \left[\boldsymbol{i}_\theta(t) - \alpha \boldsymbol{u}_\theta(t)\boldsymbol{u}_\theta^T(t)\right]\left[g(t) - f(t;\boldsymbol{\theta})\right] f^\alpha(t;\boldsymbol{\theta})dt \end{aligned} \tag{3.8}$$

and

$$\begin{aligned} K &= \int \boldsymbol{u}_\theta(t)\boldsymbol{u}_\theta^T(t) f^{2\alpha}(t;\boldsymbol{\theta})g(t)dt \\ &\quad - \left[\int \boldsymbol{u}_\theta f^\alpha(t;\boldsymbol{\theta})g(t)dt\right]\left[\int \boldsymbol{u}_\theta f^\alpha(t;\boldsymbol{\theta})g(t)dt\right]^T \end{aligned} \tag{3.9}$$

with $\boldsymbol{u}_\theta(t) = \partial \ln f(t;\boldsymbol{\theta})/\partial\boldsymbol{\theta}$, and $\boldsymbol{i}_\theta(t) = -\partial \boldsymbol{u}_\theta(t)/\partial\boldsymbol{\theta}$. Base et al. (2006) further proved that the asymptotic property of the MDE holds for censored survival data as well. Based on these results, the variance of the MDE estimator can be approximated by discretizing the integrals in Eqs. (3.8) and (3.9) with the nonparametric estimated target distribution $\hat{G}(t)$ or the nonparametric estimated density $\hat{g}(t)$. Consider the MDE estimator MDE_S, $\boldsymbol{\theta}_S$, the standard error of the MDE_S estimator can be approximated as

$$\widehat{SE}_A(\boldsymbol{\theta}_S) = \sqrt{\hat{J}_S^{-1}\hat{K}_S\hat{J}_S^{-1}/n}, \tag{3.10}$$

where

$$\begin{aligned}\hat{J}_S &= \int \left[(1+\alpha)\boldsymbol{u}_{\hat{\theta}_S}(t)\boldsymbol{u}_{\hat{\theta}_S}^T(t) - \boldsymbol{i}_{\hat{\theta}_S}(t)\right] f_T^{1+\alpha}(t,\hat{\boldsymbol{\theta}}_S)dt \\ &\quad + \int \left[i_{\hat{\theta}_S}(t) - \alpha\boldsymbol{u}_{\hat{\theta}_S}(t)\boldsymbol{u}_{\hat{\theta}_S}^T(t)\right] f_T^{\alpha}(t;\hat{\boldsymbol{\theta}}_S)d\hat{G}_T(t)\end{aligned}$$

and

$$\begin{aligned}\hat{K}_S &= \int \boldsymbol{u}_{\hat{\theta}_S}(t)\boldsymbol{u}_{\hat{\theta}_S}^T(t) f_T^{2\alpha}(t;\hat{\boldsymbol{\theta}}_S)d\hat{G}_T(t) \\ &\quad - \left[\int \boldsymbol{u}_{\hat{\theta}_S}(t) f_T^{\alpha}(t;\hat{\boldsymbol{\theta}}_S)d\hat{G}_T(t)\right]\left[\int \boldsymbol{u}_{\hat{\theta}_S} f_T^{\alpha}(t;\hat{\boldsymbol{\theta}}_S)d\hat{G}_T(t)\right]^T,\end{aligned}$$

with

$$\boldsymbol{u}_{\hat{\theta}_S}(t) = \frac{1}{f_T(t;\boldsymbol{\theta})}\frac{\partial f_T(t;\boldsymbol{\theta})}{\partial\boldsymbol{\theta}}\bigg|_{\boldsymbol{\theta}=\hat{\boldsymbol{\theta}}_S}$$

and

$$\boldsymbol{i}_{\hat{\theta}_S}(t) = -\frac{\partial\boldsymbol{u}_{\theta}(t)}{\partial\boldsymbol{\theta}}\bigg|_{\boldsymbol{\theta}=\hat{\boldsymbol{\theta}}_S}.$$

The variance-covariance matrices of the MDE estimators MDE_C and MDE_P, $\hat{\boldsymbol{\theta}}_C$ and $\hat{\boldsymbol{\theta}}_P$, can be obtained in a similar manner. For the MDE_C, the matrices J and K can be approximated as

$$\begin{aligned}\hat{J}_C &= \int \left[(1+\alpha)\boldsymbol{u}_{\hat{\theta}_C}(t)\boldsymbol{u}_{\hat{\theta}_C}^T(t) - \boldsymbol{i}_{\theta_C}(t)\right] f_X^{1+\alpha}(t,\hat{\boldsymbol{\theta}}_C)dt \\ &\quad + \int \left[\boldsymbol{i}_{\hat{\theta}_C}(t) - \alpha\boldsymbol{u}_{\hat{\theta}_C}(t)\boldsymbol{u}_{\hat{\theta}_C}^T(t)\right] f_X^{\alpha}(t;\hat{\boldsymbol{\theta}}_C)d\hat{G}_X(t)\end{aligned}$$

and

$$\begin{aligned}\hat{K}_C &= \int \boldsymbol{u}_{\hat{\theta}_C}(t)\boldsymbol{u}_{\hat{\theta}_C}^T(t) f_X^{2\alpha}(t;\hat{\boldsymbol{\theta}}_C)d\hat{G}_X(t) \\ &\quad - \left[\int \boldsymbol{u}_{\hat{\theta}_C}(t) f_X^{\alpha}(t;\hat{\boldsymbol{\theta}}_C)d\hat{G}_X(t)\right]\left[\int \boldsymbol{u}_{\hat{\theta}_C} f_X^{\alpha}(t;\hat{\boldsymbol{\theta}}_C)d\hat{G}_X(t)\right]^T,\end{aligned}$$

where

$$\boldsymbol{u}_{\hat{\theta}_C}(t) = \frac{1}{f_X(t;\boldsymbol{\theta})}\frac{\partial f_X(t;\boldsymbol{\theta})}{\partial\boldsymbol{\theta}}\bigg|_{\boldsymbol{\theta}=\hat{\boldsymbol{\theta}}_C}$$

and

$$\boldsymbol{i}_{\hat{\theta}_C}(t) = -\frac{\partial\boldsymbol{u}_{\theta}(t)}{\partial\boldsymbol{\theta}}\bigg|_{\boldsymbol{\theta}=\hat{\boldsymbol{\theta}}_C}.$$

With the approximated matrices $\hat{J}_C$ and $\hat{K}_C$, the variance-covariance matrix of $\hat{\boldsymbol{\theta}}_C$ can be approximated as $\hat{J}_C^{-1}\hat{K}_C\hat{J}_C^{-1}/n$.

Similarly, for MDE_P, the matrices J and K can be approximated with $\hat{\boldsymbol{\theta}}_P$ from the MDE_P procedure. The estimates of J and K can be obtained as

$$\begin{aligned}\hat{J}_P &= \int \left[(1+\alpha)\boldsymbol{u}_{\hat{\theta}_P}(t)\boldsymbol{u}_{\hat{\theta}_P}^T(t) - \boldsymbol{i}_{\theta_P}(t)\right] f_T^{1+\alpha}(t,\hat{\boldsymbol{\theta}}_P)dt \\ &\quad + \int \left[\boldsymbol{i}_{\hat{\theta}_P}(t) - \alpha\boldsymbol{u}_{\hat{\theta}_P}(t)\boldsymbol{u}_{\hat{\theta}_P}^T(t)\right] f_T^{\alpha}(t;\hat{\boldsymbol{\theta}}_P)\hat{g}_T(t)dt\end{aligned}$$

and

$$\begin{aligned}\hat{K}_P &= \int \boldsymbol{u}_{\hat{\theta}_P}(t)\boldsymbol{u}_{\hat{\theta}_P}^T(t) f_T^{2\alpha}(t;\hat{\boldsymbol{\theta}}_P)\hat{g}_T(t)dt \\ &\quad - \left[\int \boldsymbol{u}_{\hat{\theta}_P}(t) f_T^{\alpha}(t;\hat{\boldsymbol{\theta}}_P)\hat{g}_T(t)dt\right]\left[\int \boldsymbol{u}_{\hat{\theta}_P} f_T^{\alpha}(t;\hat{\boldsymbol{\theta}}_P)\hat{g}_T(t)dt\right]^T,\end{aligned}$$

with

$$\boldsymbol{u}_{\hat{\theta}_P}(t) = \frac{1}{f_X(t;\boldsymbol{\theta})}\frac{\partial f_X(t;\boldsymbol{\theta})}{\partial \boldsymbol{\theta}}\bigg|_{\boldsymbol{\theta}=\hat{\boldsymbol{\theta}}_P}$$

and

$$\boldsymbol{i}_{\hat{\theta}_P}(t) = -\frac{\partial \boldsymbol{u}_{\theta}(t)}{\partial \boldsymbol{\theta}}\bigg|_{\boldsymbol{\theta}=\hat{\boldsymbol{\theta}}_P}.$$

With the approximated matrices $\hat{J}_P$ and $\hat{K}_P$, the variance-covariance matrix of $\hat{\boldsymbol{\theta}}_P$ can be approximated as $\hat{J}_P^{-1}\hat{K}_P\hat{J}_P^{-1}/n$.

3.2.2.2. Based on The Observed Fisher Information Matrix

From our preliminary study (results are not presented here), we found that when the sample size is not large enough, the standard error estimation based on the theoretical results for the MDE provide estimates that are seriously underestimating the simulated standard errors of the estimators. Therefore, we consider different ways to approximate the standard error of the MDE proposed in this paper. Based on our observations in the preliminary study, the standard error of the MLE and the standard error of the MDE are in the same order of magnitude, especially when the value of α is close to 0. Hence, we consider a standard error estimation method based the Fisher information matrix similar to using the observed Fisher information matrix in estimating the standard error of MLE. For the MLE of $\boldsymbol{\theta}$, the asymptotic variance-covariance matrix of the MLE can be approximated by the inverse of the observed Fisher information matrix, i.e.,

$$\widehat{SE}_F(\hat{\boldsymbol{\theta}}) = \left[-\frac{\partial^2 \ln L(\boldsymbol{\theta})}{\partial \boldsymbol{\theta}\partial \boldsymbol{\theta}'}\bigg|_{\boldsymbol{\theta}=\hat{\boldsymbol{\theta}}}\right]^{-1/2}.$$

According to the asymptotic theory of the MLE, the sampling distribution of $n^{1/2}(\hat{\boldsymbol{\theta}} - \boldsymbol{\theta})$ is asymptotically multivariate normally distributed with mean zero and variance $Var(\hat{\boldsymbol{\theta}})$. When $\alpha = 0$, the MDE is equivalent to the MLE. Here, we propose to approximate the standard error of the MDE by inverting the observed Fisher information with the estimated parameters from the MDE.

3.2.2.3. Based on The Bootstrap Method

As we expected, when the power parameter α in the MDE method is far from zero, the performance of the approximation of standard error based on Fisher information matrix may not fulfill the expectations. Therefore, we also consider approximating the standard error of the MDE based on the bootstrap method. Given the estimated parameters, parametric bootstrap samples of system lifetimes are generated with the corresponding censoring proportion. For each bootstrap sample, the MDE method is applied to estimate the parameter and a bootstrap estimate is obtained. Based on B bootstrap MDE estimates, we compute the standard error of those bootstrap MDE estimates as an approximation of the standard error of the MDE. For instance, consider the MDE based on system-level data, suppose we have B bootstrap samples and obtained B estimates $\hat{\boldsymbol{\theta}}_S^{(1)}$, $\hat{\boldsymbol{\theta}}_S^{(2)}$, ..., $\hat{\boldsymbol{\theta}}_S^{(B)}$, the standard error of the estimator $\hat{\boldsymbol{\theta}}_S$ can be approximated as

$$\widehat{SE}_B(\hat{\boldsymbol{\theta}}_S) = \sqrt{\frac{1}{B}\sum_{b=1}^{B}(\hat{\boldsymbol{\theta}}_S^{(b)} - \bar{\hat{\boldsymbol{\theta}}}_S)^2}, \tag{3.11}$$

where $\bar{\hat{\boldsymbol{\theta}}}_S = \sum_{b=1}^{B} \hat{\boldsymbol{\theta}}_S^{(b)}/B$. The size of bootstrap samples needed will be discussed in Section 3.3 based on a Monte Carlo simulation study.

After obtaining the standard error estimates based on the above three methods, consider the asymptotic distribution of MLE and the proposed MDE, a two-sided $100(1-\alpha)\%$

normal approximated confidence interval of the k-th element of the parameter vector $\boldsymbol{\theta}$ can be obtained as

$$[\theta_{kl}, \theta_{ku}] = \left[\hat{\theta}_k - z_{1-\alpha/2}\widehat{SE}(\hat{\theta}_k), \hat{\theta}_k + z_{1-\alpha/2}\widehat{SE}(\hat{\theta}_k)\right],$$

where z_q is the q-th upper percentile of the standard normal distribution. The performance of the standard error estimation methods and the corresponding confidence intervals will be evaluated via a Monte Carlo simulation study in Section 3.3.

3.3. Monte Carlo Simulation Studies

In this section, a Monte Carlo simulation study is used to evaluate the performance of the proposed estimation method for different systems, different sample sizes with different censoring rates, different underlying distributions and different values of α in the MDE and different contamination proportions. Since similar observations are obtained based on different sample sizes, different system structures and different distributions, for the sake of simplicity, we only present the simulation results for the 4-component series-parallel III system (namely System I) and the 4-component mixed parallel I system (namely System II) in Figures 3.1 for sample size $m = 50$ (with different censoring rate) and the component lifetime X follows the two-parameter Weibull distribution with p.d.f.

$$f_X(x; a, b) = \frac{b}{a}\left(\frac{x}{a}\right)^{b-1} \exp^{-(x/a)^b}, x > 0,$$

where a is the scale parameter and b is the shape parameter (denoted as $Weibull(a, b)$).

In the simulation, we consider the scale parameters $a = 3$ or $a = 9$ and the shape parameter to be 2 ($b = 2$). For the case that the contaminates have longer lifetime than the true distribution on average (namely the longer-life contamination model), the $Weibull(3, 2)$ distribution with mean lifetime 2.6587 is the true distribution and the $Weibull(9, 2)$ distribution with mean lifetime 7.9760 is the contaminated distribution. Similarly, for the case that the contaminates have shorter lifetime than the true distribution on

average (namely the shorter-life contamination model), the $Weibull(9, 2)$ distribution is the true distribution and the $Weibull(3, 2)$ distribution is the contaminated distribution.

In the simulation study, the contamination proportion is set to be $0\%, 5\%, 10\%$ and 15%, the Type-II censoring rate $(1 - r/m)$ is set to be 0% and 5% (i.e., no censoring and $r = 0.95m$, respectively). The power parameter α in the MDE method is set to be $0.01, 0.1, 0.25, 0.5, 0.75$ and 0.9.

3.3.1. Results for Estimation of Scale and Shape Parameters

3.3.1.1. Results for The MDE_S Procedure

At first, the proposed MDE_S method is compared with the MLE for different contamination models and censoring schemes with the two system structures considered here. Boxplots of the estimates of scale and shape parameters for different settings are presented in Figures 3.2 - 3.9. From Figures 3.2 - 3.9, we observe that when the power parameter is small, i.e. $\alpha = 0.01$, the MDE_S estimates show similar results as the MLE. Moreover, when the contamination rate is 0, the MLE method tends to have estimates closer to the true value than the MDE_S method. However, when the contamination rate increases, the MLE deviates form the true parameter, but the MDE_S with larger power parameter still gives estimates closer to the true parameter. These results are consistent among different censoring schemes, different contamination models as well as different systems.

Moreover, it is noticed that the sampling distributions of the MLE and the MDE_S tend to be symmetric or slightly skew to the right. A possible reason for this slightly right skewness is that the scale and shaper parameter are positive parameters for the Weibull distribution. Despite the right skewness, the overall sampling distributions of the MLE and the MDE_S are symmetric about the mean. Hence, it is reasonable to use the asymptotic normal approximation to construct confidence intervals for the model parameters.

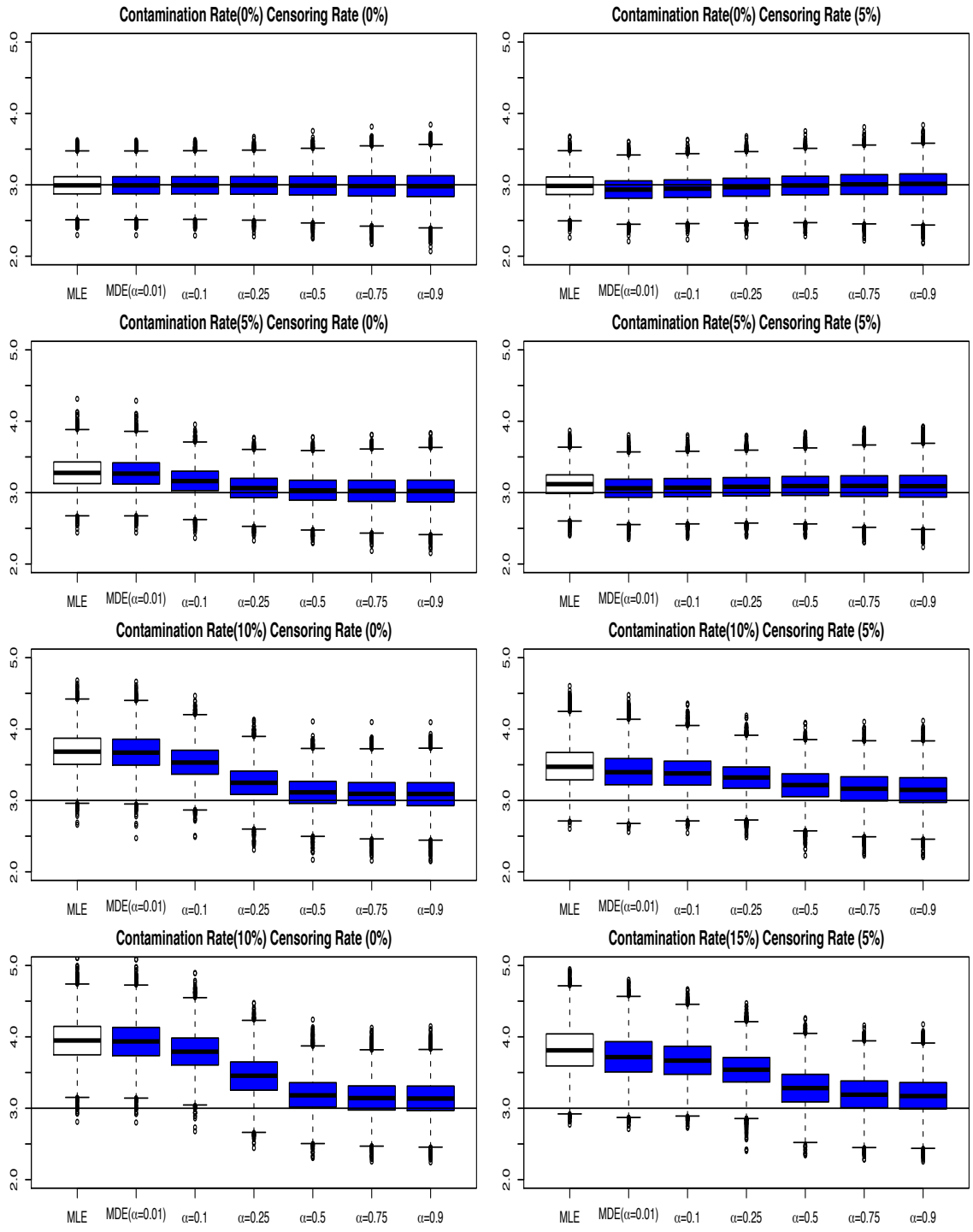

Figure 3.2: Boxplot of 10000 estimates of scale parameters by the MDE_S procedure for the System I with the longer-life contamination model

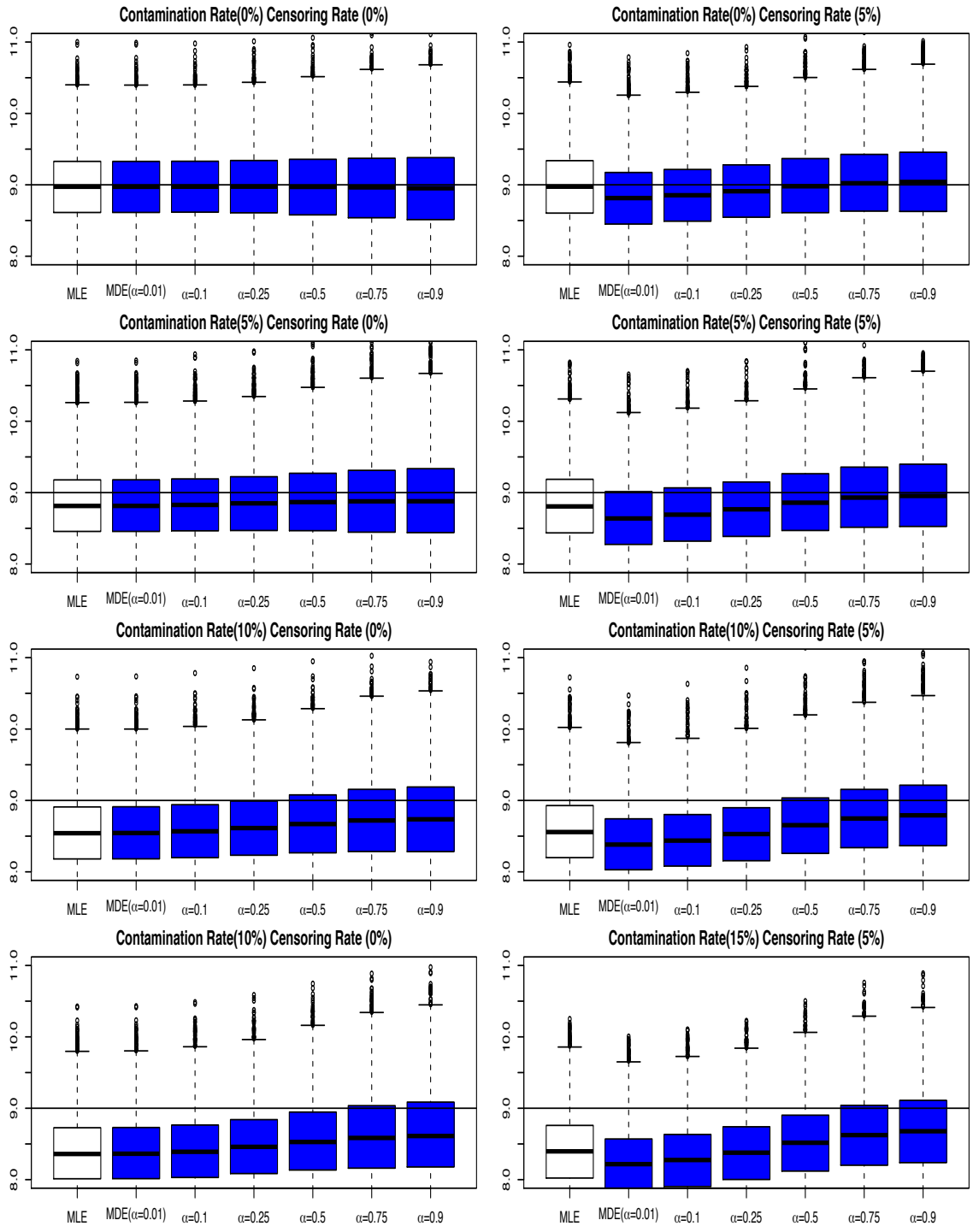

Figure 3.3: Boxplot of 10000 estimates of scale parameters by the MDE_S procedure for the System I with the shorter-life contamination model

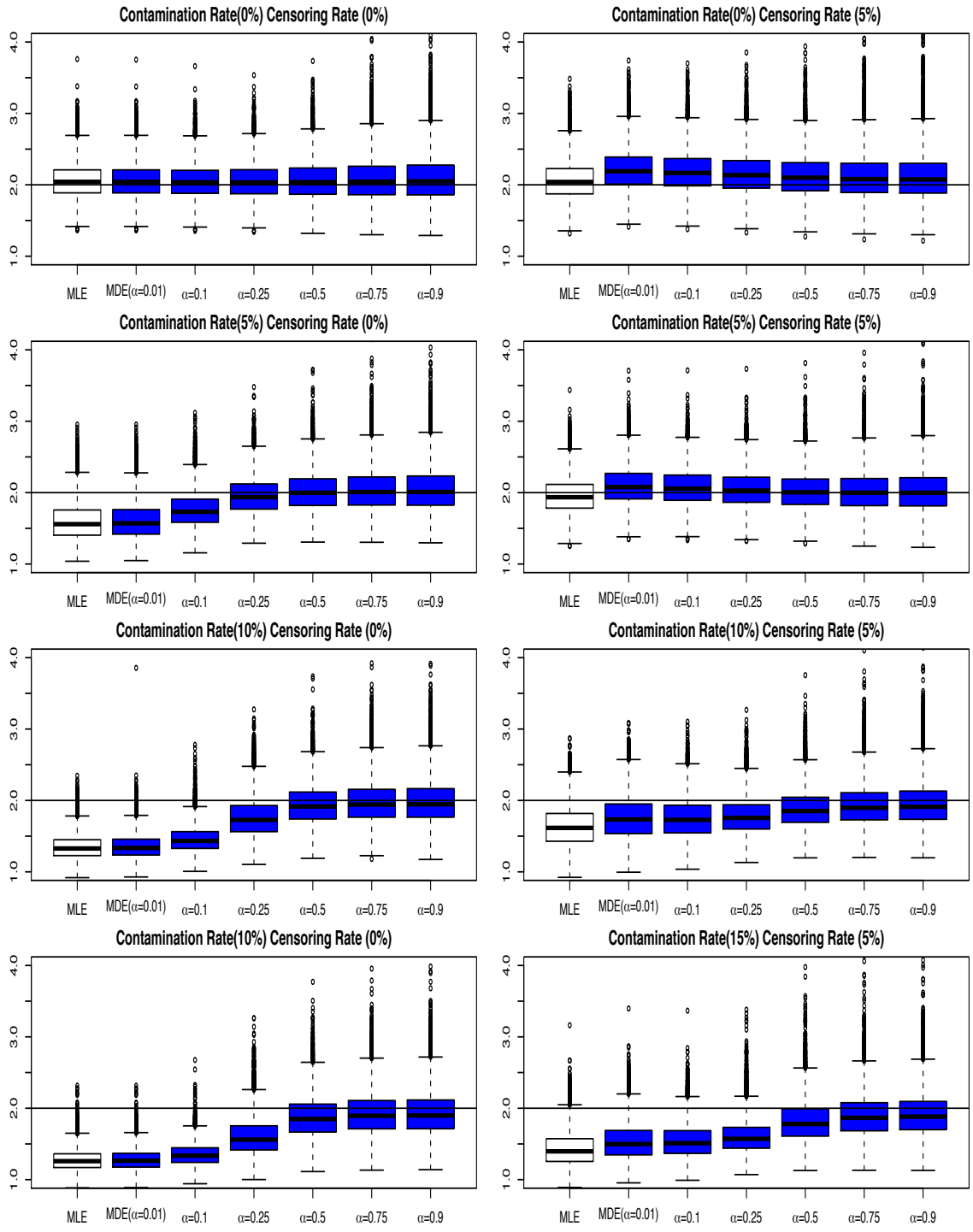

Figure 3.4: Boxplot of 10000 estimates of shape parameters by the MDE_S procedure for the System I with the longer-life contamination model

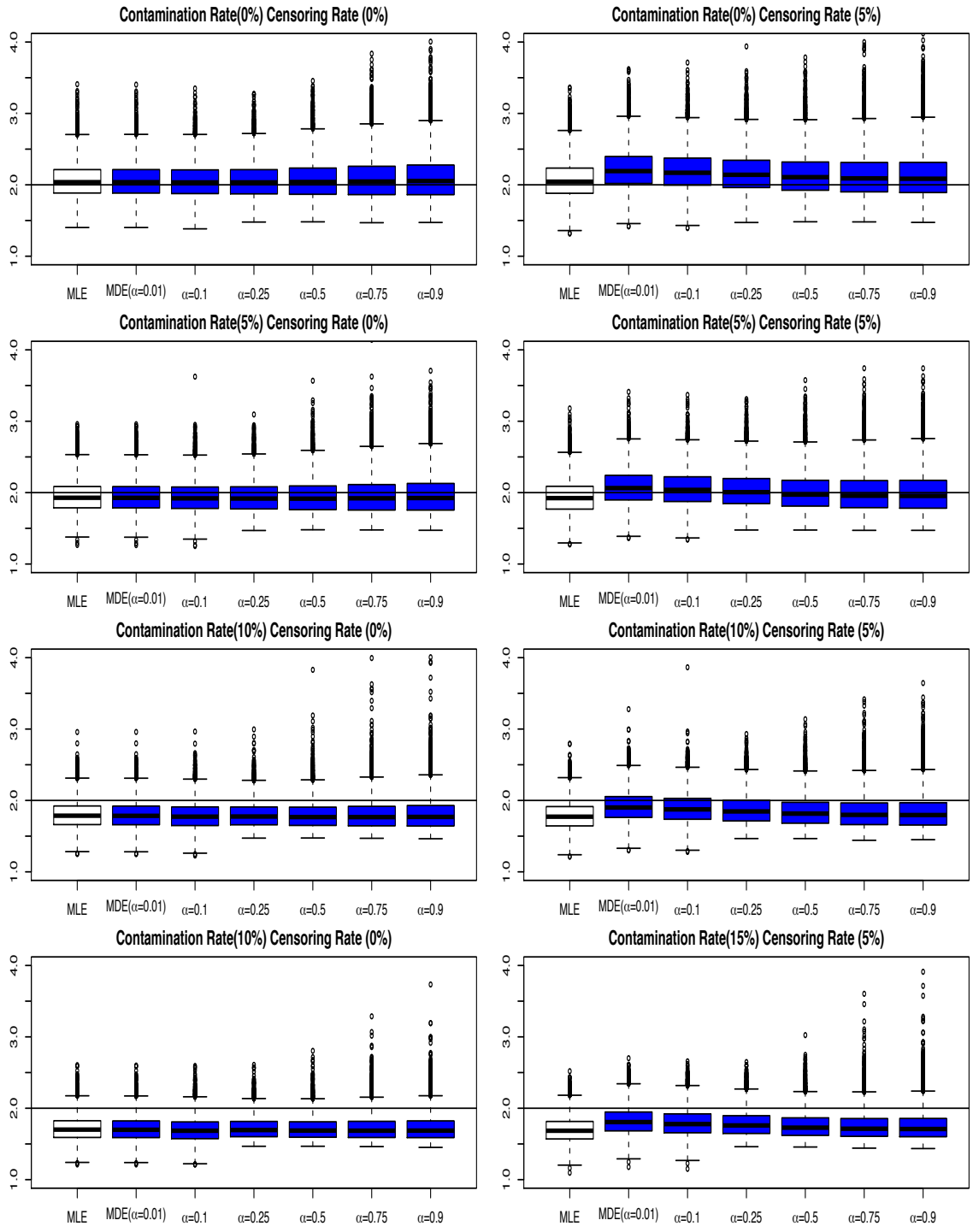

Figure 3.5: Boxplot of 10000 estimates of shape parameters by the MDE_S procedure for the System I with the shorter-life contamination model

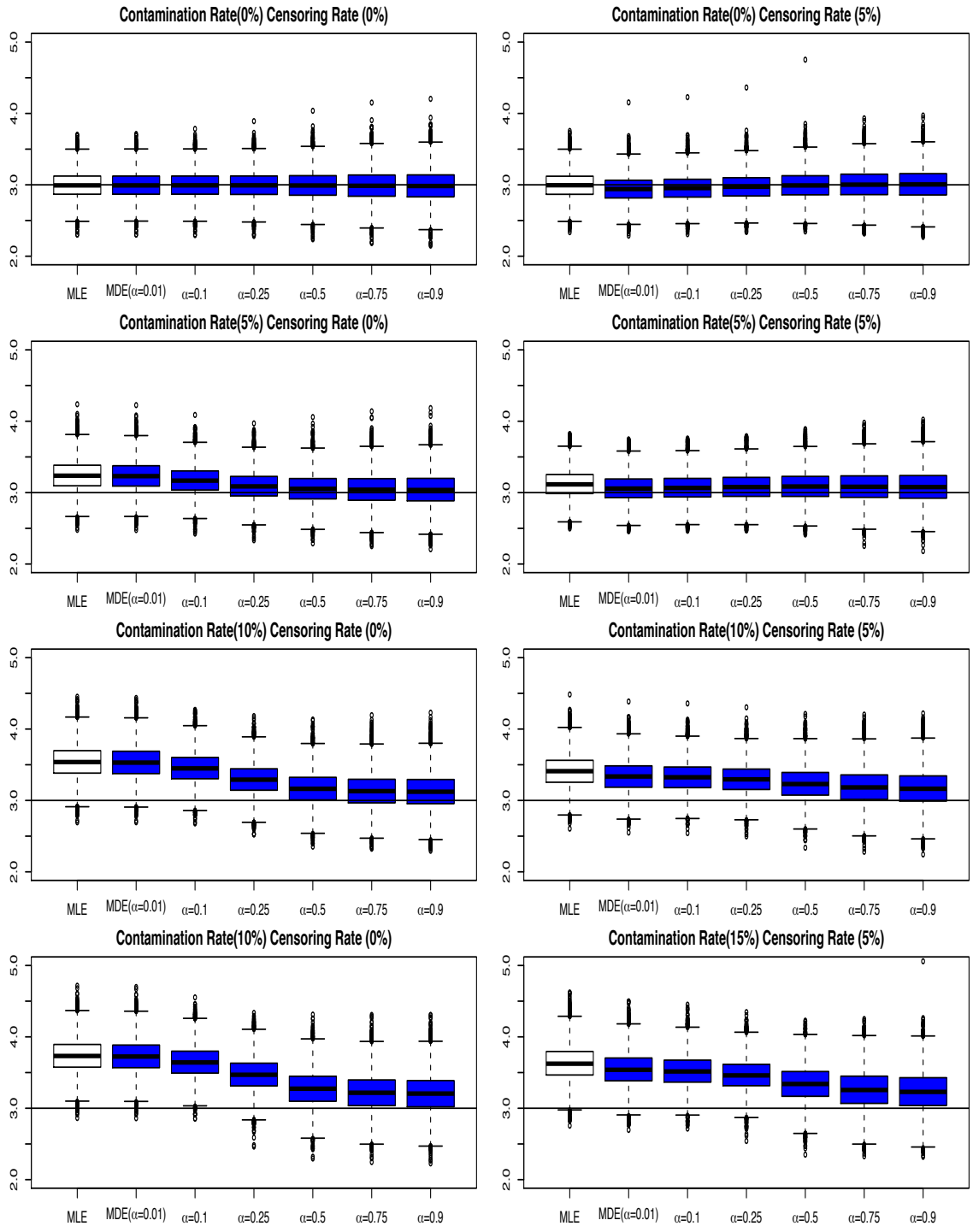

Figure 3.6: Boxplot of 10000 estimates of scale parameters by the MDE_S procedure for the System II with the longer-life contamination model

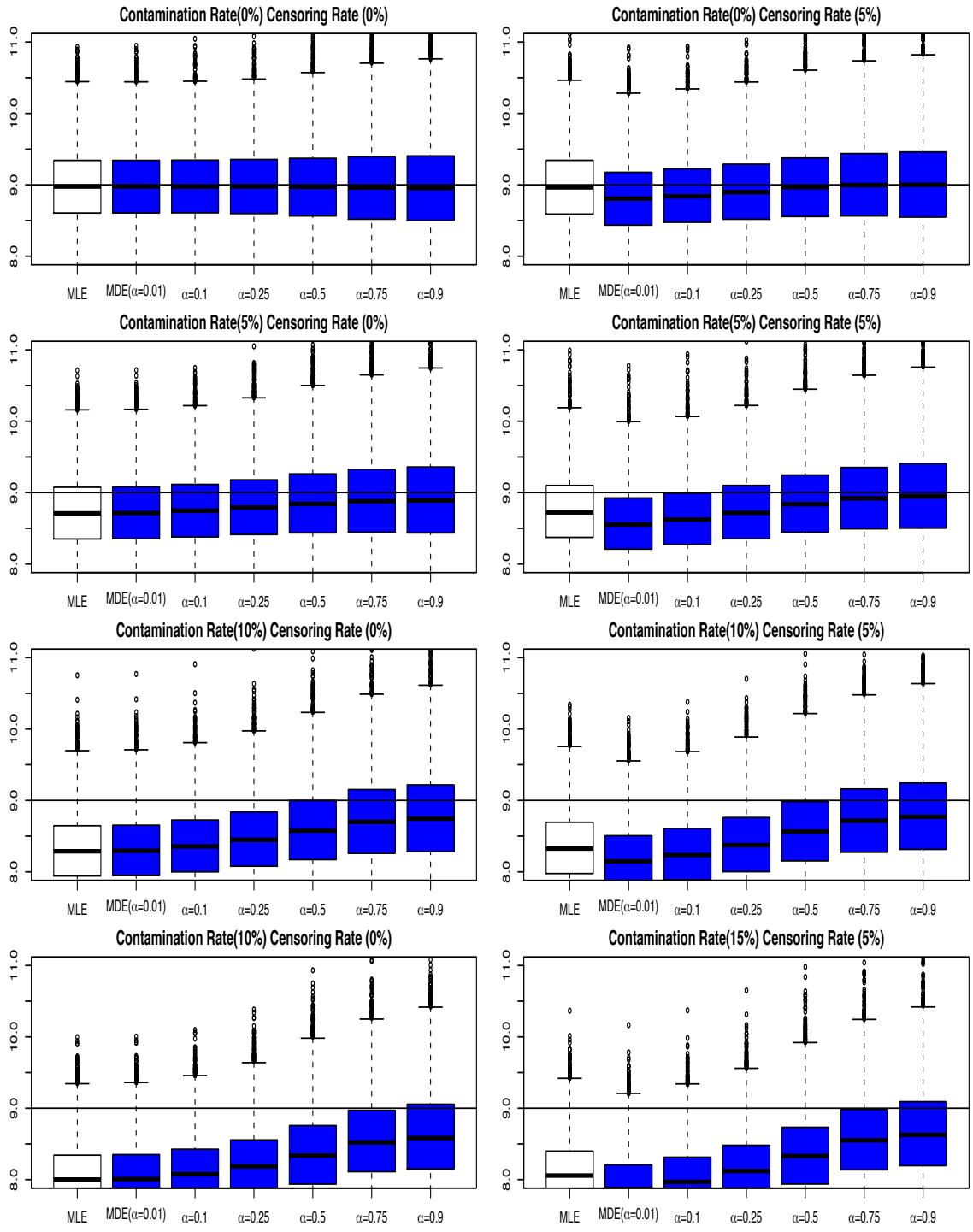

Figure 3.7: Boxplot of 10000 estimates of scale parameters by the MDE_S procedure for the System II with the shorter-life contamination model

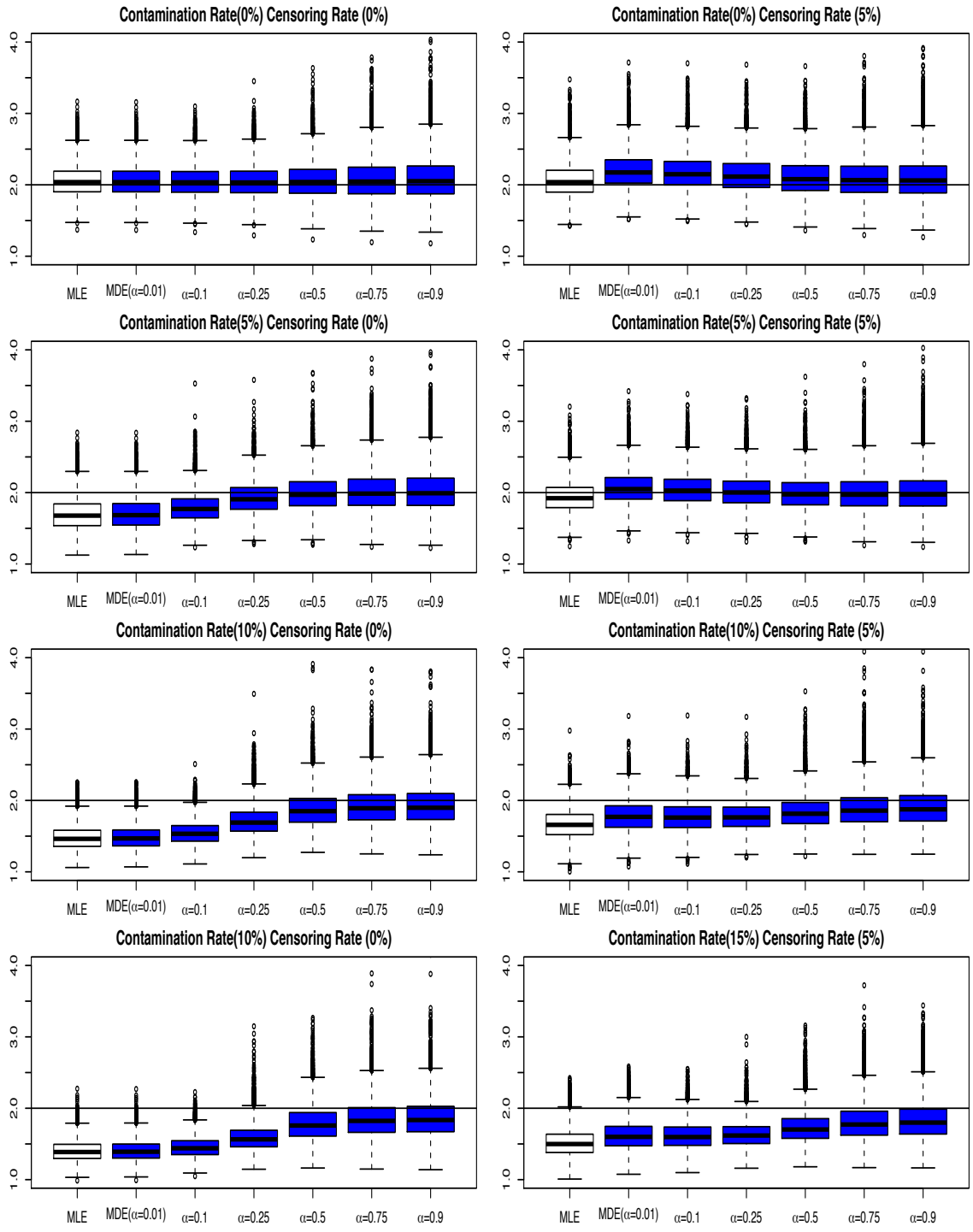

Figure 3.8: Boxplot of 10000 estimates of shape parameters by the MDE_S procedure for the System II with the longer-life contamination model

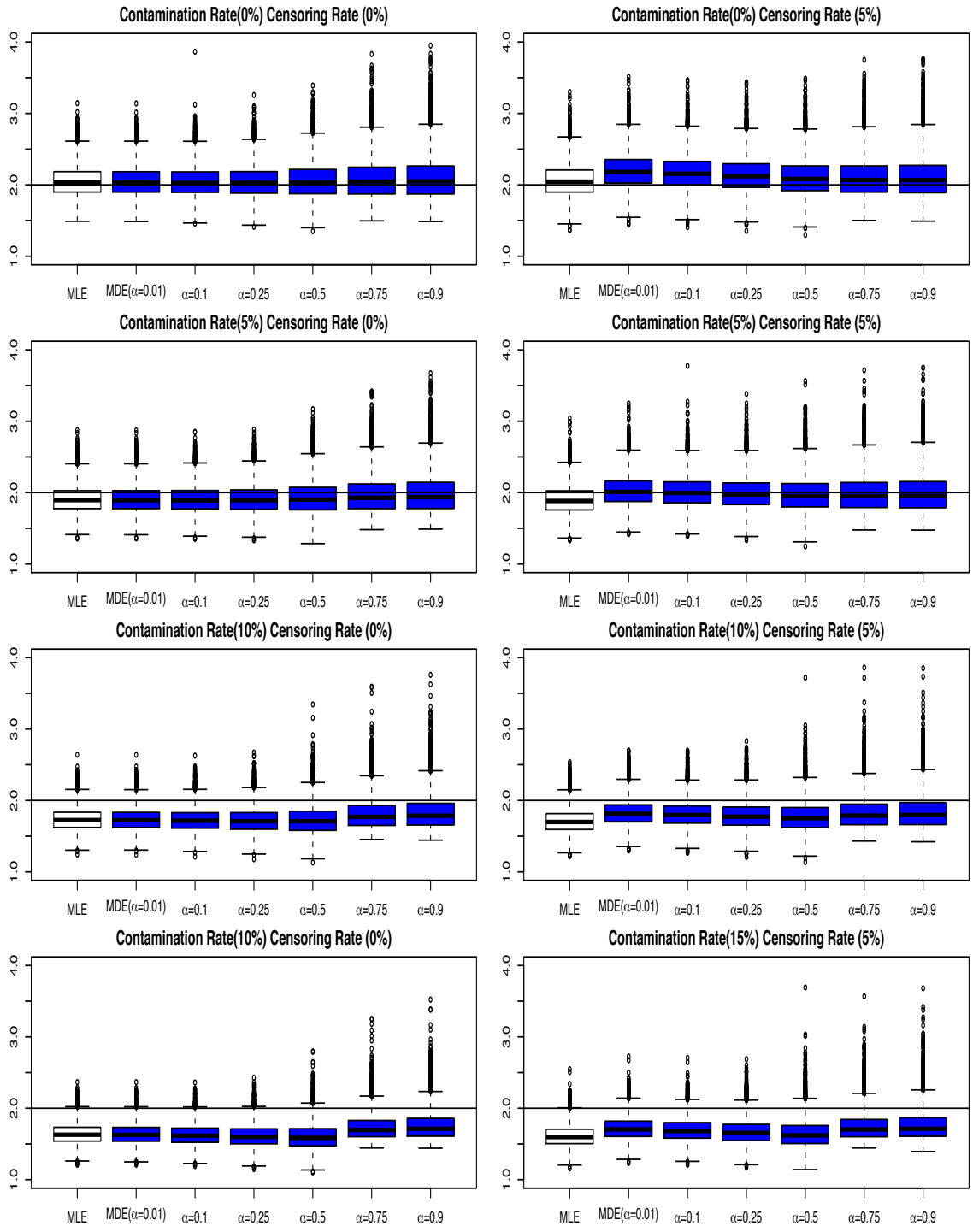

Figure 3.9: Boxplot of 10000 estimates of shape parameters by the MDE_S procedure for the System II with the shorter-life contamination model

To quantitatively evaluate the performance, the MDE_S is compared with the MLE in terms of their mean squared errors (MSE). The relative efficiency, defined in Base et al. (2006), is the ratio of mean squared errors of the MDE method to the MLE as follows:

$$RE_{MDE_S} = \frac{MSE(MLE)}{MSE(MDE_S)}.$$

The value of relative efficiency greater than 1 indicates that the performance of the MDE_S procedure is better than the MLE as the mean squared error of the MDE_S is smaller. The relative efficiencies are plotted in Figures 3.10 - 3.13 for different contamination models and different censoring schemes in the system I and system II.

From Figures 3.10 - 3.13, we observe that when there is contamination in the data, the MDE_S gives smaller mean squared errors compared to the MLE. The larger the contamination rate, the better the performance of the MDE_S comparing to the MLE. For example, with power parameter $\alpha = 0.9$, the relative efficiency for scale parameter in longer-life contamination model with 15% contamination proportion is about 3 (Figure 3.10). This means that in this setting, the MDE_S with power parameter $\alpha = 0.9$ has mean squared error three times smaller than the MLE.

When comparing the two contamination models, we observe that the MDE_S method performs better in the longer-life contamination model as the relative efficiency is large. For example, when there is no censoring in the data, the relative efficiency for the estimates of shape parameter can reach 2.25 in the longer-life contamination model (Figure 3.11a), but the largest value of relative efficiency is 1.05 in the shorter-life contamination model (Figure 3.11c). Nevertheless, in both contamination models, the MDE_S consistently performs better than the MLE when the contamination rate is high.

It is interesting to notice that when censoring is involved, for the same contamination proportion, the relative efficiency decreases in the longer-life contamination model, while the relative efficiency increases in the shorter-life contamination model. A possible reason is that the censoring scheme in this study is a Type-II censoring. In the longer-life contam-

ination model, the contaminated data tends to be larger than the data from the true model on average. Consider that the experiment is terminated when a certain number of failures are observed in the Type-II censoring scheme, the number of contaminated observations is smaller in the censored sample since those contaminated observations are censored in the Type-II censoring scheme in the longer-life contamination model. As a result, when the Type-II censoring is considered, the actual contamination proportion in the longer-life contamination model is likely to be smaller than the preset value and hence, the relative efficiency could be lower.

Moreover, these results are consistent in both system I (Figures 3.10 and 3.11) and system II (Figures 3.12 and 3.13). This indicates that the MDE_S can perform better than the MLE when there is contamination in the data regardless of the system structures.

3.3.1.2. Results for The MDE_C Procedure

Similar to the MDE_S, the MDE_C is compared with the MLE by using boxplots of parameter estimates and relative efficiencies under different settings. It is also observed for the MDE_C that the sampling distribution of the MDE_C tends to be symmetric about the mean or slightly right skewed. Moreover, the comparison between MLE and MDE_C also shows that when the contamination proportion is 0, the MLE gives estimates closer to the true parameter. When the contamination proportion is large, the MDE_C with larger power parameter α could give estimates closer to the true parameter (Figures 3.14 - 3.21). However, in most cases, the MDE_C with small power parameter α gives estimates far away from the true parameter. Only when the power parameter α is large, the MDE_C could become closer to the true parameter.

In addition, the performance of the MDE_C method could be different in the two contamination models. For example, when the contamination proportion is high in the longer-life contamination model for System I, the MDE_C of scale parameter overestimates the true parameter (Figure 3.14). However, for the shorter life contamination model under the same setting, the MDE_C of scale parameter underestimates the true parameter (Figure

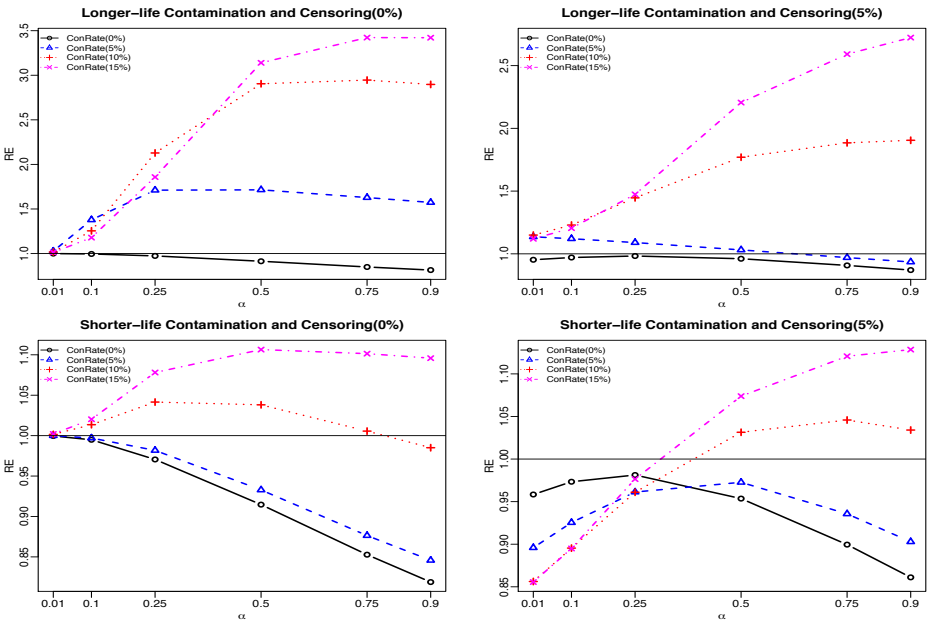

Figure 3.10: Relative efficiencies of estimated scale parameter by the MDE_S procedure for the System I

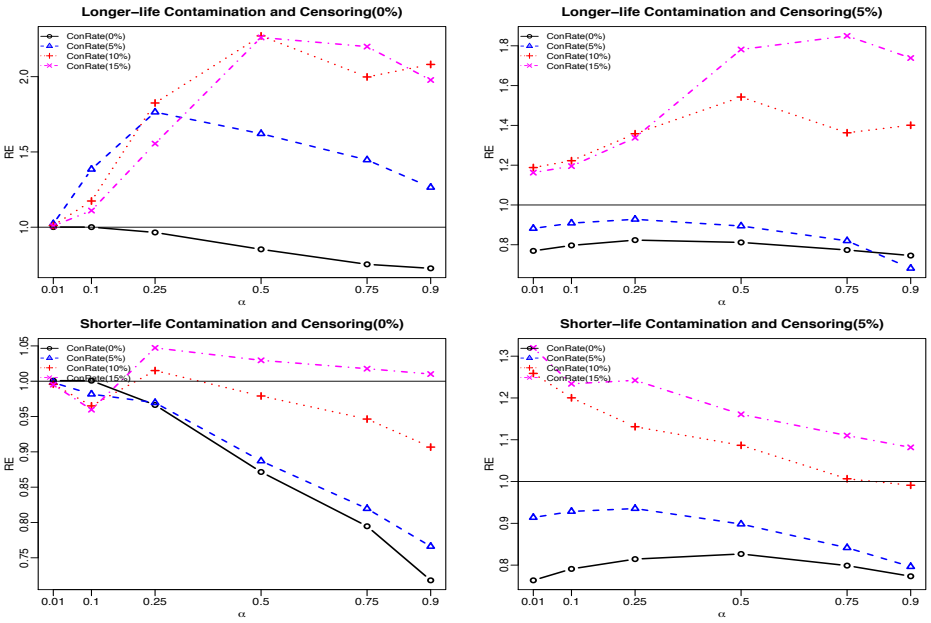

Figure 3.11: Relative efficiencies of estimated shape parameter by the MDE_S procedure for the System I

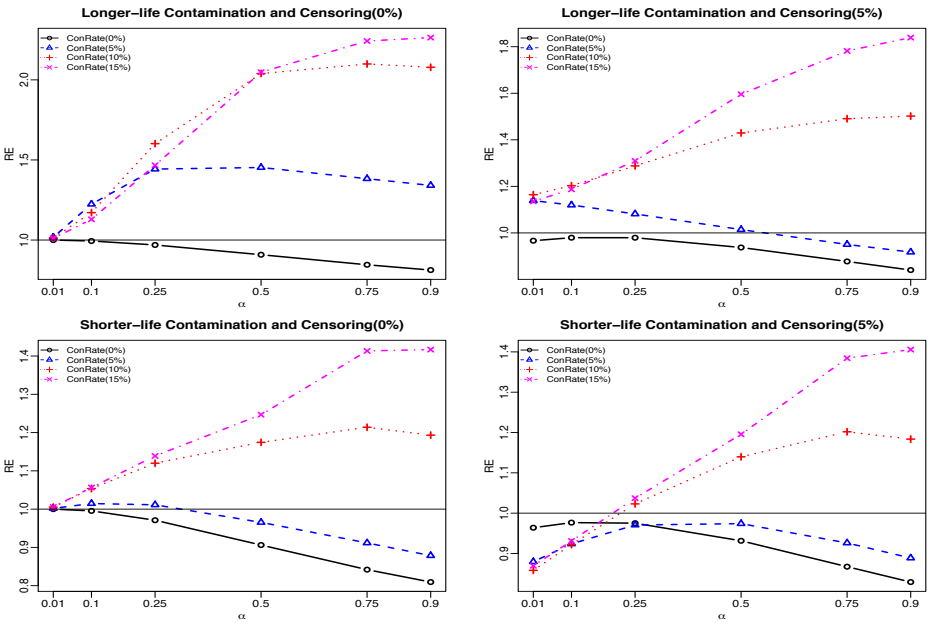

Figure 3.12: Relative efficiencies of estimated scale parameter by the MDE_S procedure for the System II

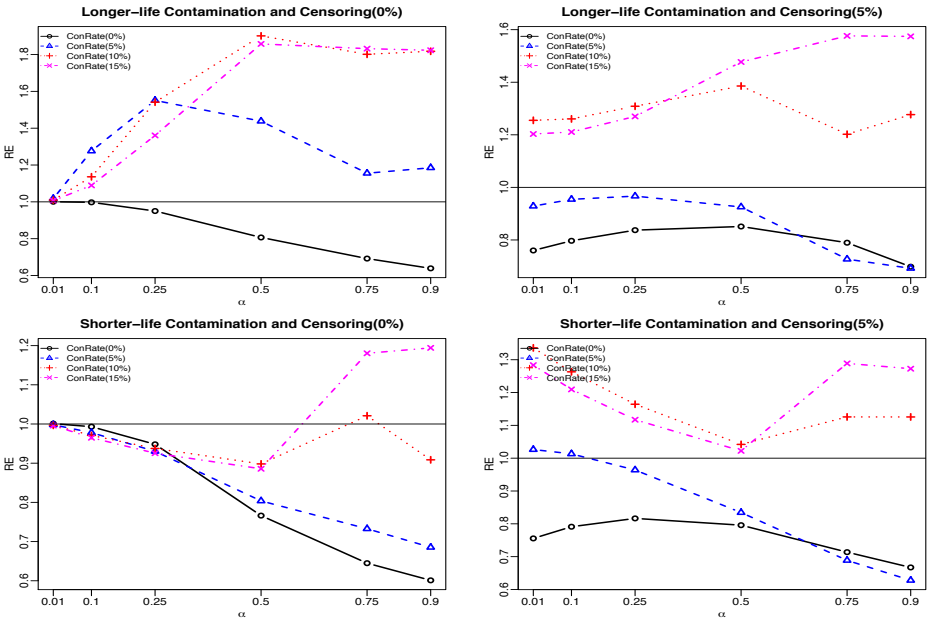

Figure 3.13: Relative efficiencies of estimated shape parameter by the MDE_S procedure for the System II

3.15).

Moreover, the performance of the MDE_C method could be different in the two systems in some situations. For example, in the shorter-life contamination model, the MDE_C of scale parameter underestimates the true parameter in System I (Figure 3.15), but overestimates the true parameter in System II (Figure 3.19). This indicates that the MDE_C may be not stable as it is sensitive to the underlying contamination models and system structures.

To compare the performance of the MDE_C and the MLE, the relative efficiencies under different settings are presented in Figures 3.22 - 3.25. Compared to the MLE, the MDE_C does not show a significant improvement in estimating scale and shape parameters in the Weibull distrbution. In most cases, the MLE has smaller MSE than the MDE_C, i.e., relative efficiency less than 1. There are only a few cases that the MDE_C gives smaller MSE compared to the MLE. For example, when the contamination proportion is large in the longer life contamination model with System I, the relative efficiencies of MDE_C are larger than 1 for the scale parameter (Figure 3.22) and the shape parameter (Figure 3.23). Moreover, the relative efficiencies of MDE_C further support that the performance of MDE_C depends on the underlying contamination model and the system structure.

3.3.1.3. Results for The MDE_P Procedure

Once again, the performance of MDE_P is compared with the MLE by using boxplots of the parameter estimates and relative efficiencies under different settings. The boxplots of the MDE_P presented in Figures 3.26 - 3.33 show that the sampling distribution of the MDE_P is similar to that of the MDE_S, which is symmetric about the mean or slightly skewed to the right. Also, for the point estimation, when the contamination proportion is 0, the MLE provides closer estimates to the true parameter. However, when the contamination proportion increases, the MDE_P with larger power parameter α provides estimates closer to the true parameter.

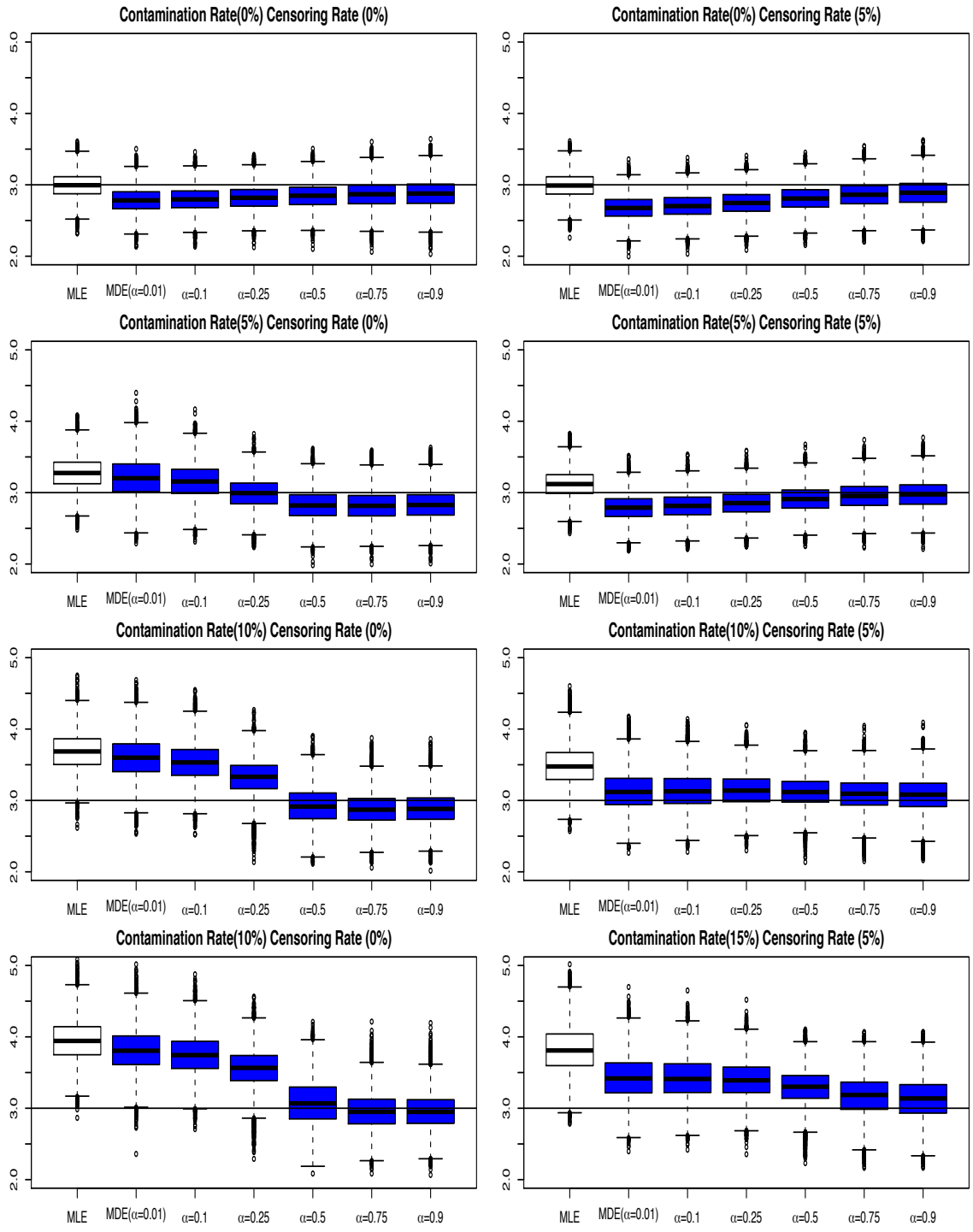

Figure 3.14: Boxplot of 10000 estimates of scale parameters by the MDE_C procedure for the System I with the longer-life contamination model

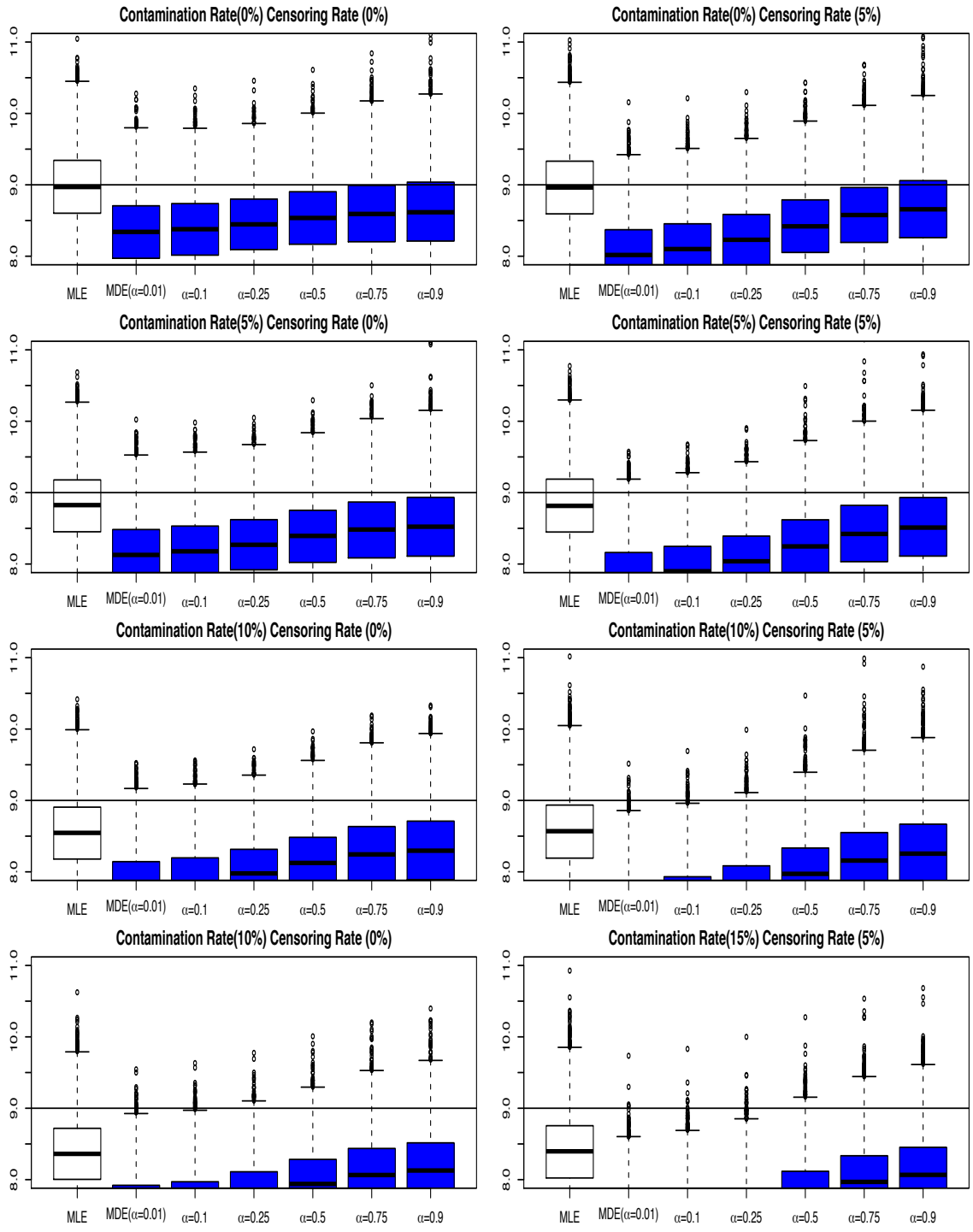

Figure 3.15: Boxplot of 10000 estimates of scale parameters by the MDE_C procedure for the System I with the shorter-life contamination model

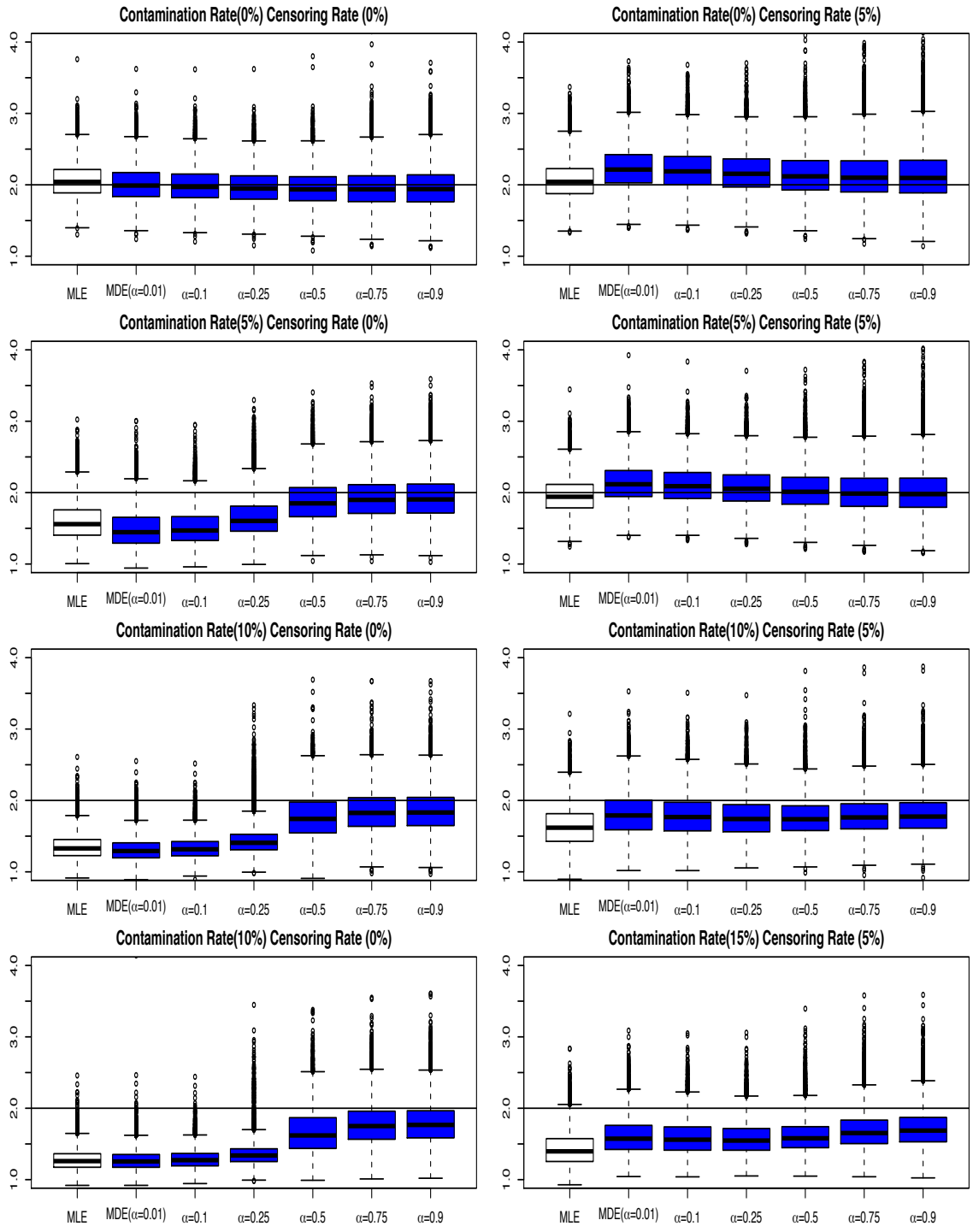

Figure 3.16: Boxplot of 10000 estimates of shape parameters by the MDE_C procedure for the System I with the longer-life contamination model

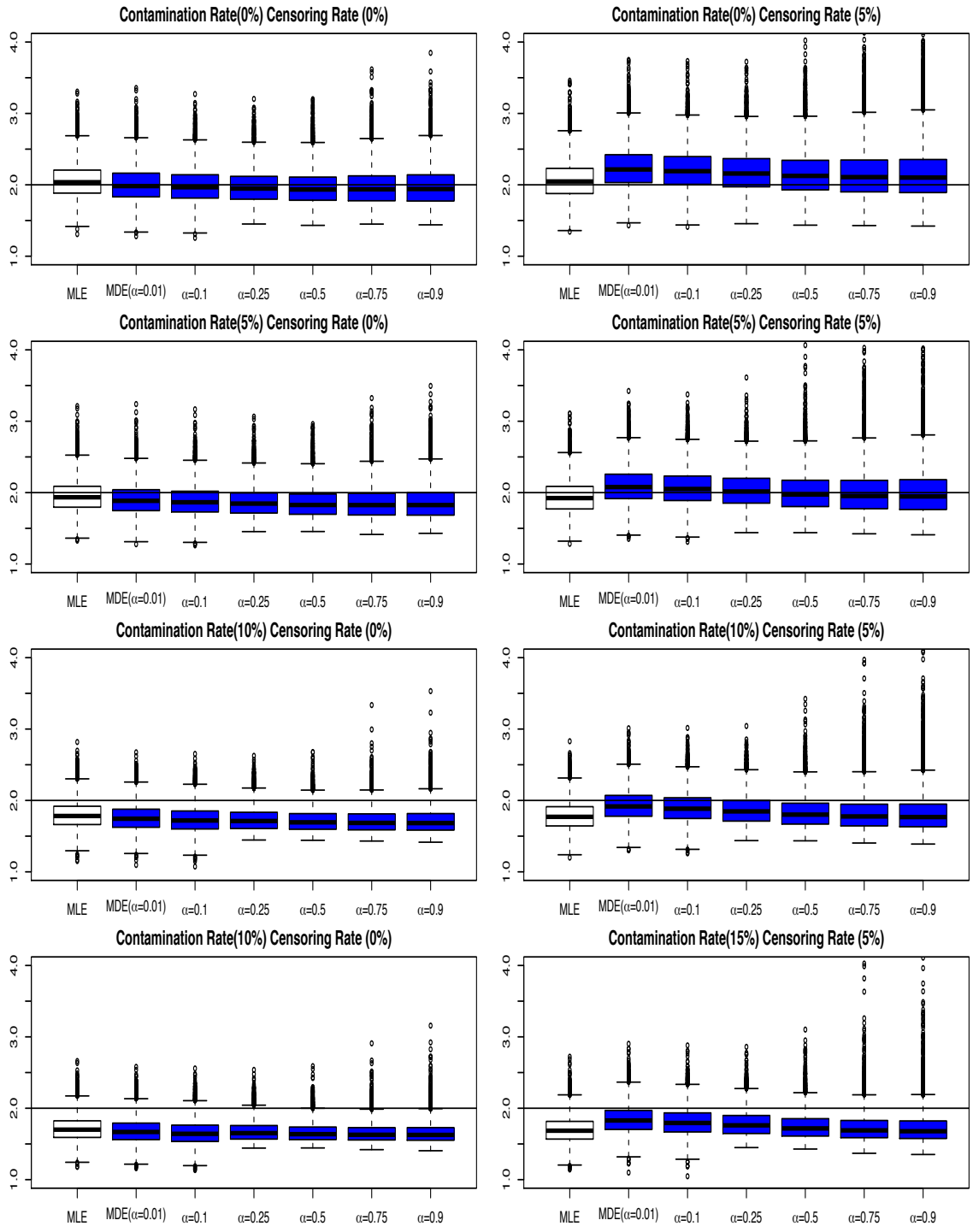

Figure 3.17: Boxplot of 10000 estimates of shape parameters by the MDE_C procedure for the System I with the shorter-life contamination model

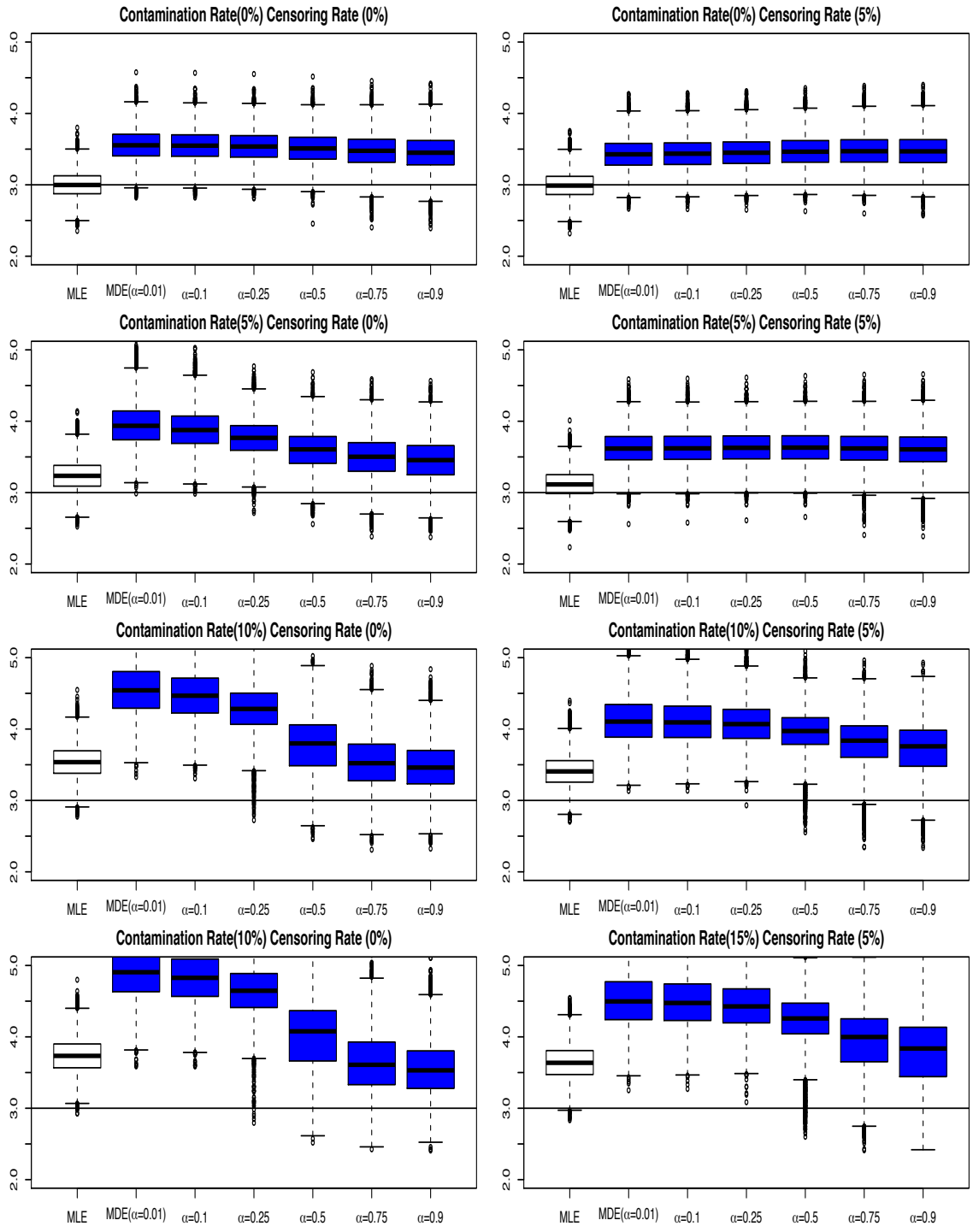

Figure 3.18: Boxplot of 10000 estimates of scale parameters by the MDE_C procedure for the System II with the longer-life contamination model

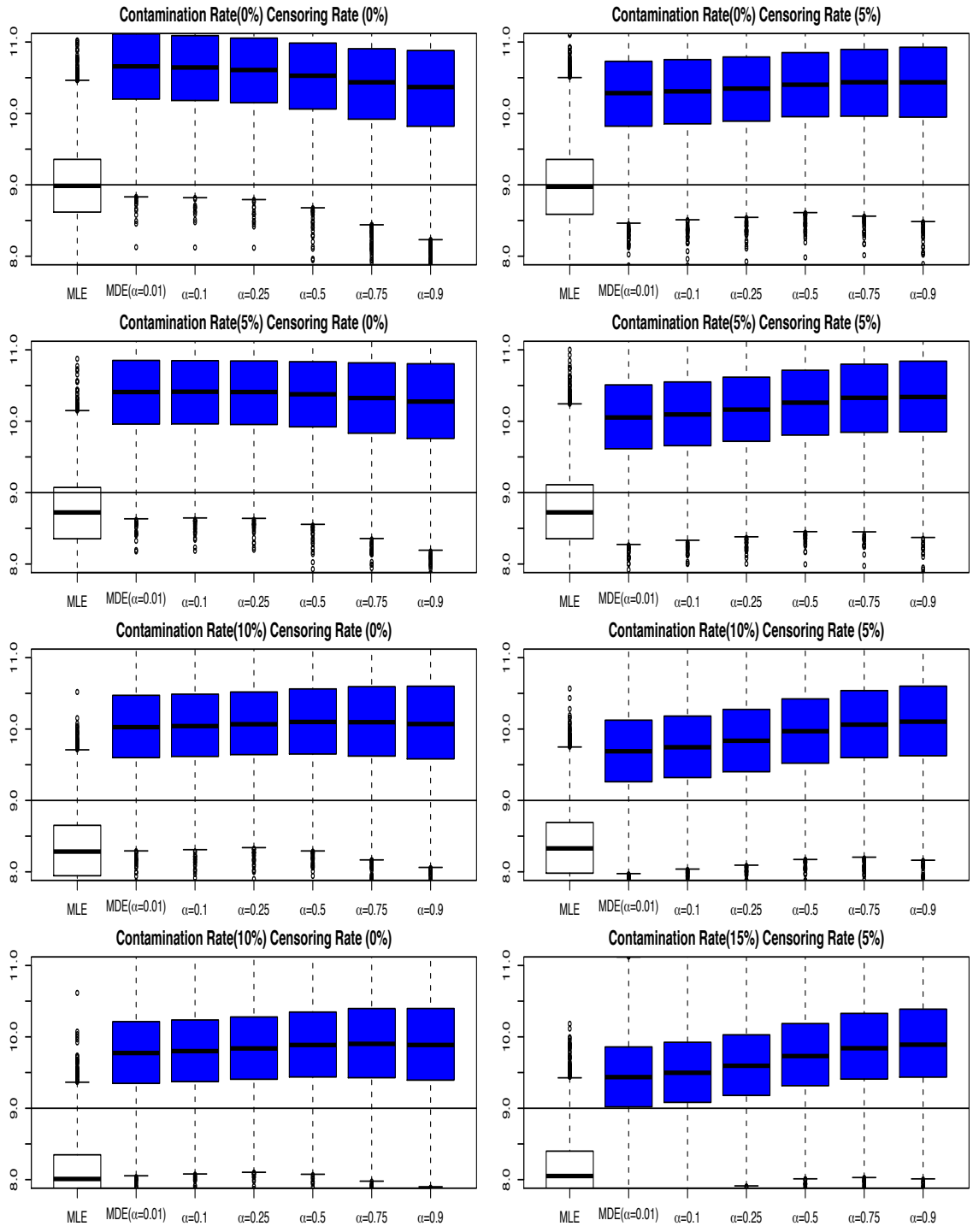

Figure 3.19: Boxplot of 10000 estimates of scale parameters by the MDE_C procedure for the System II with the shorter-life contamination model

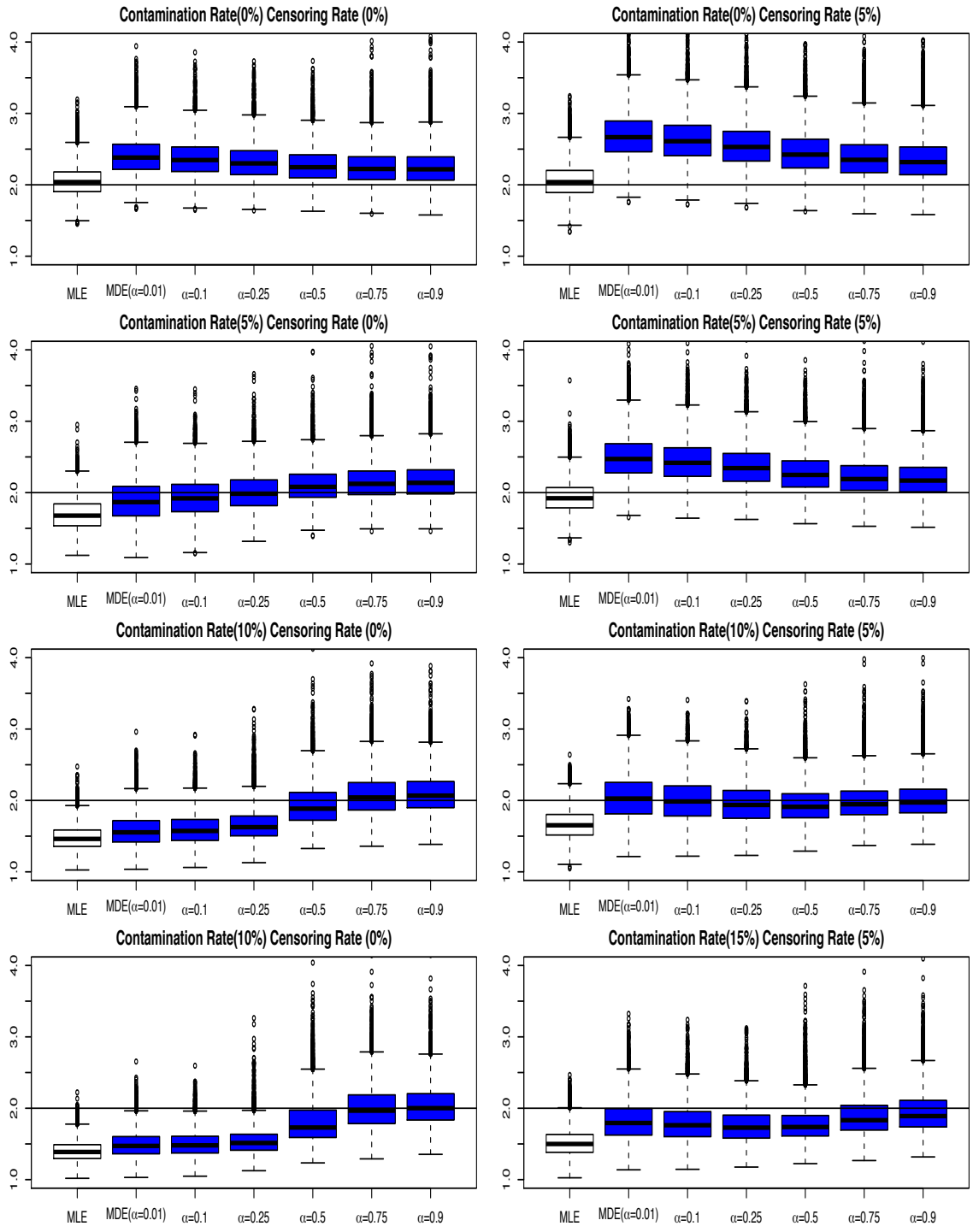

Figure 3.20: Boxplot of 10000 estimates of shape parameters by the MDE_C procedure for the System II with the longer-life contamination model

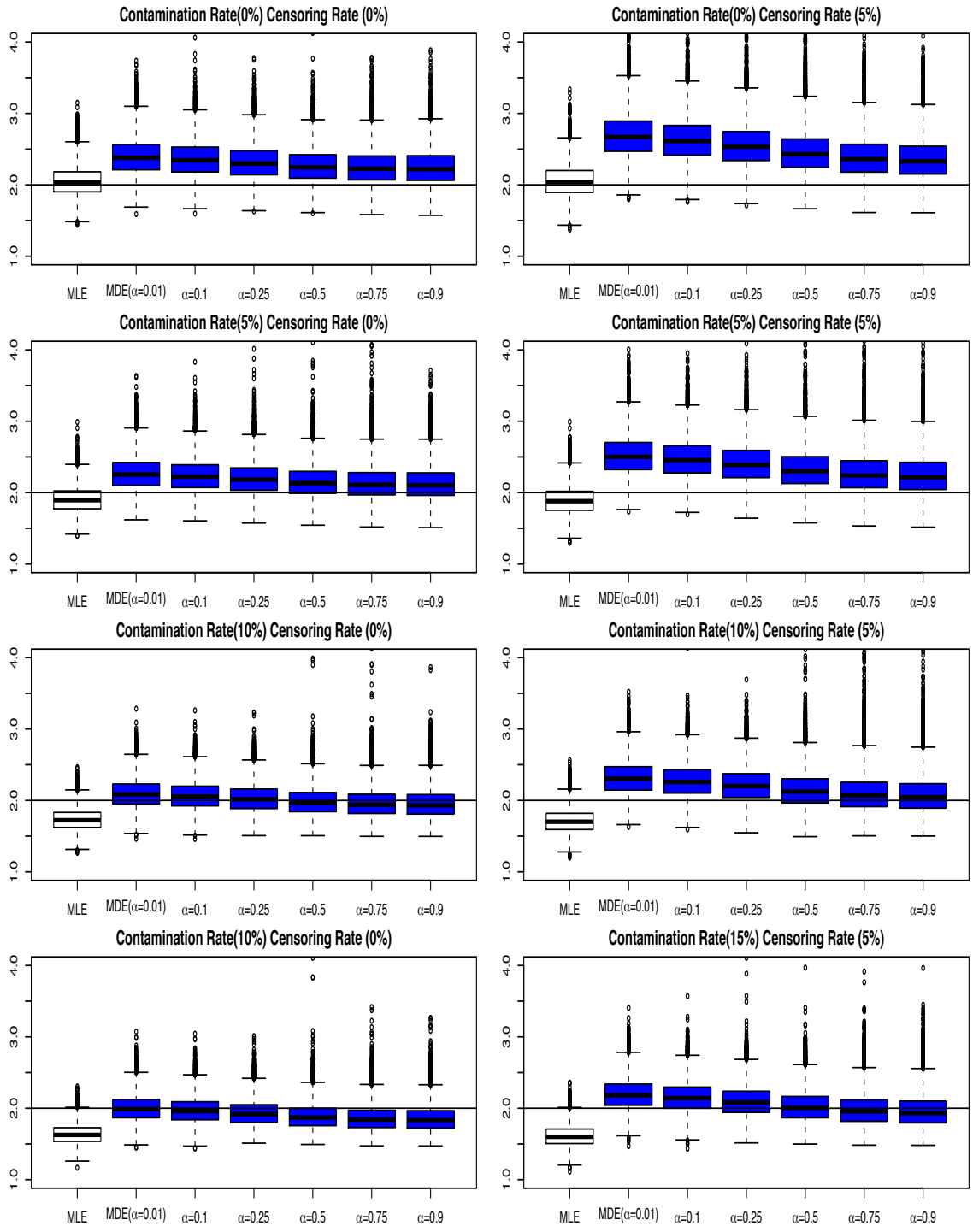

Figure 3.21: Boxplot of 10000 estimates of shape parameters by the MDE_C procedure for the System II with the shorter-life contamination model

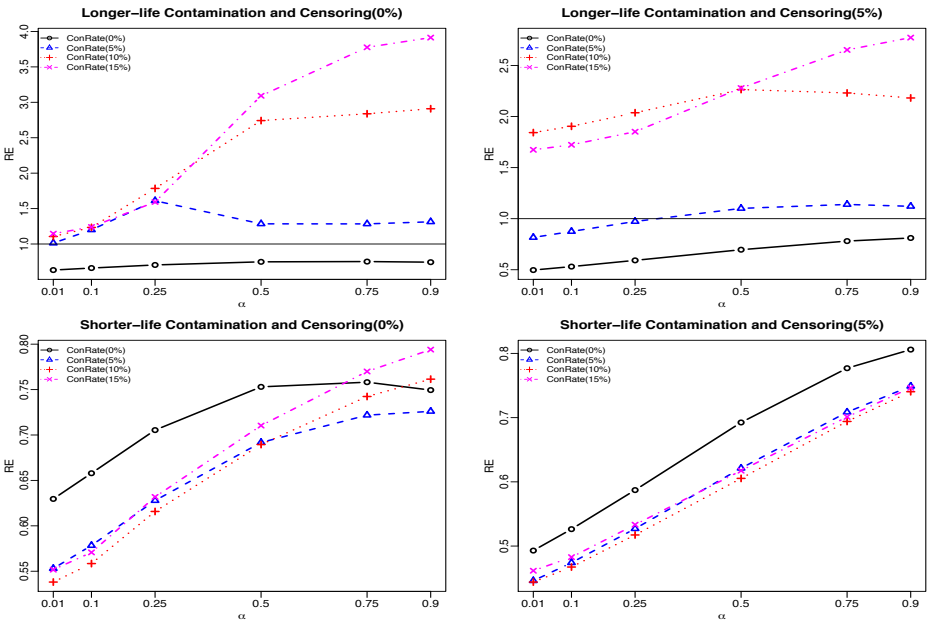

Figure 3.22: Relative efficiencies of estimated scale parameter by the MDE_C procedure for the System I

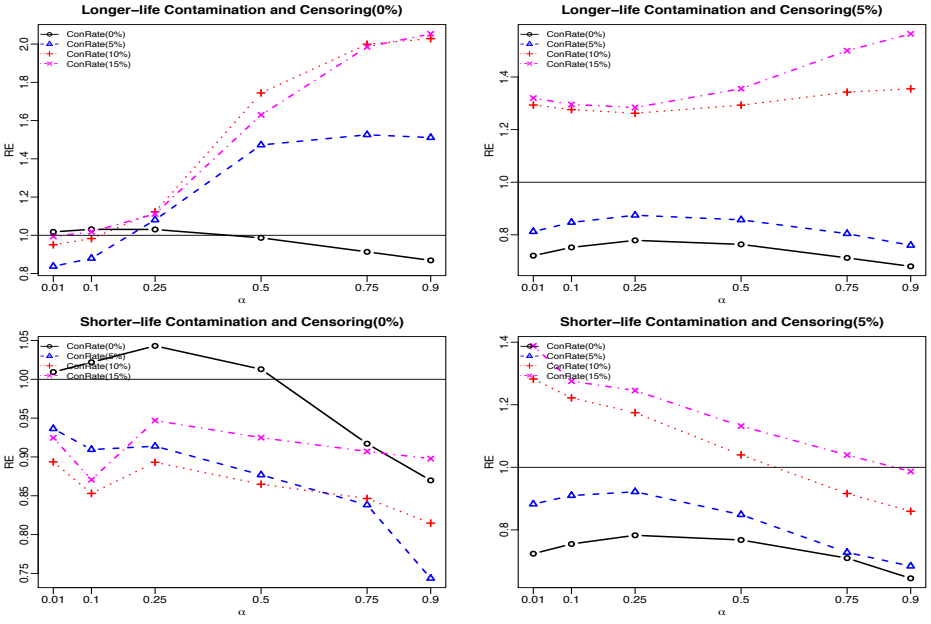

Figure 3.23: Relative efficiencies of estimated shape parameter by the MDE_C procedure for the System I

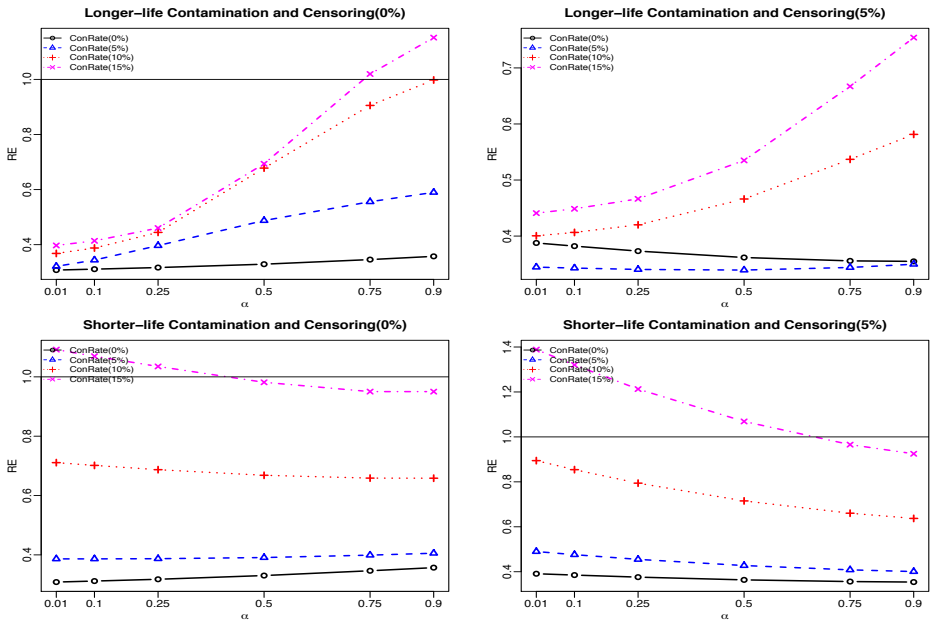

Figure 3.24: Relative efficiencies of estimated scale parameter by the MDE_C procedure for the System II

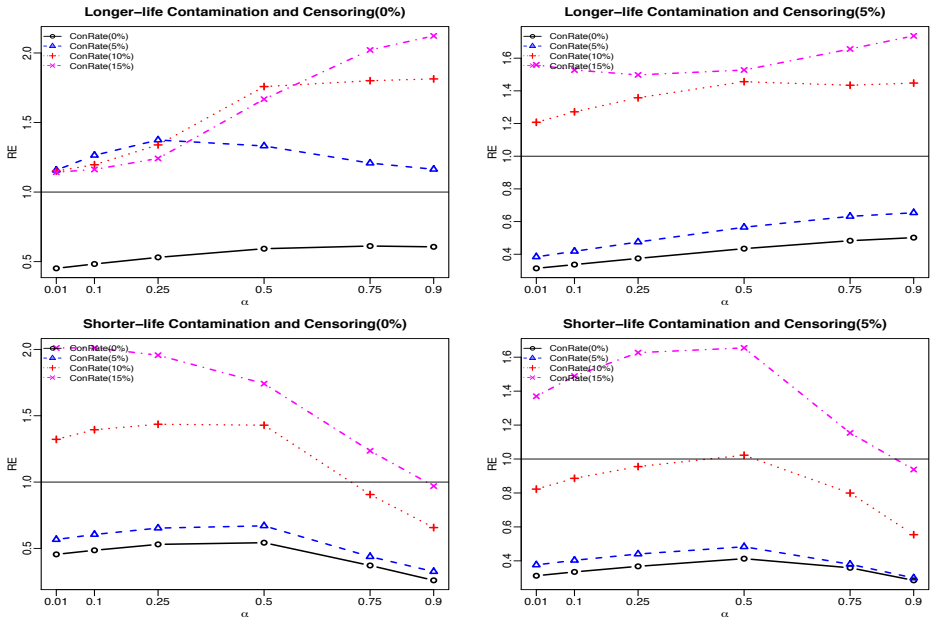

Figure 3.25: Relative efficiencies of estimated shape parameter by the MDE_C procedure for the System II

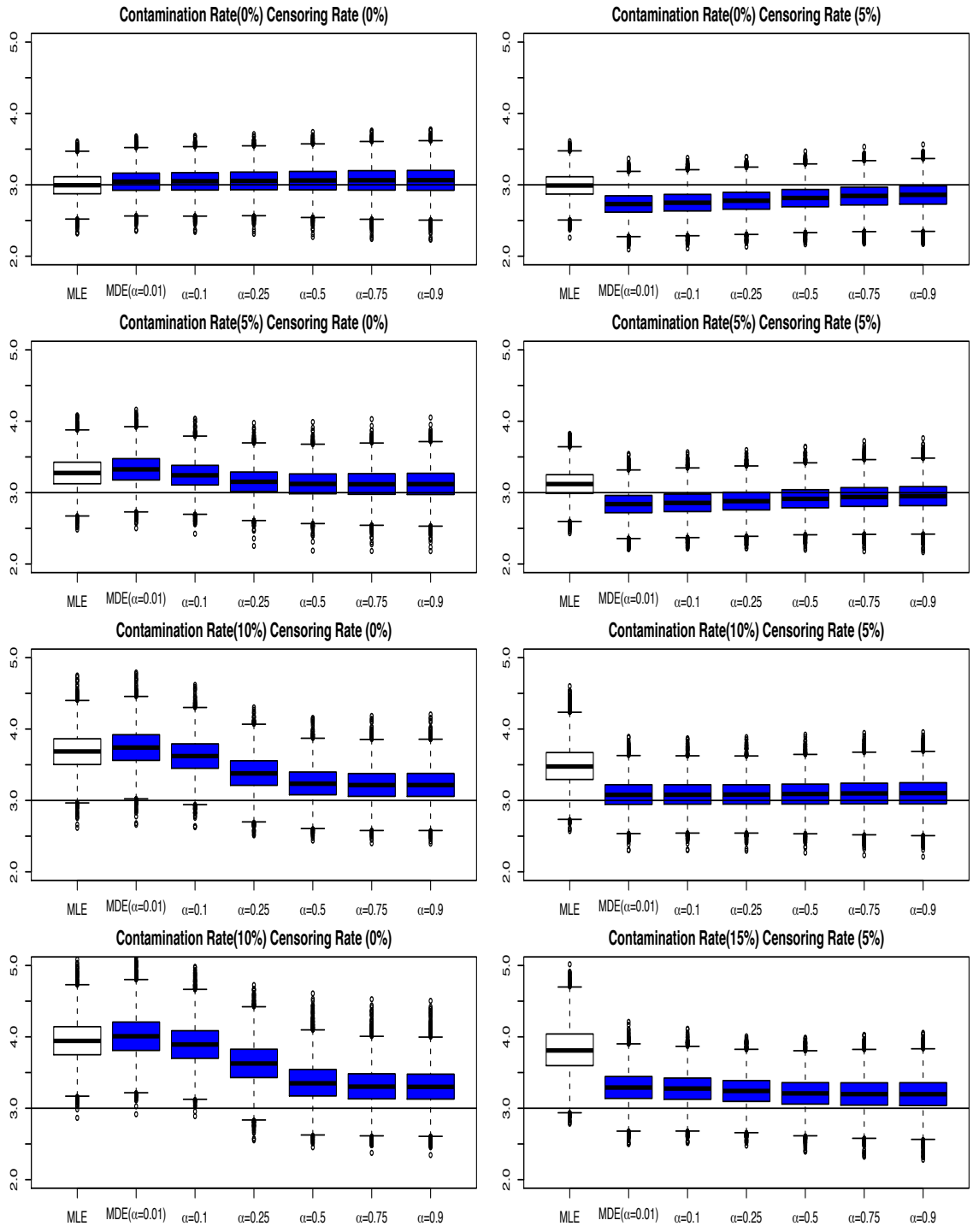

Figure 3.26: Boxplot of 10000 estimates of scale parameters by the MDE_P procedure for the System I with the longer-life contamination model

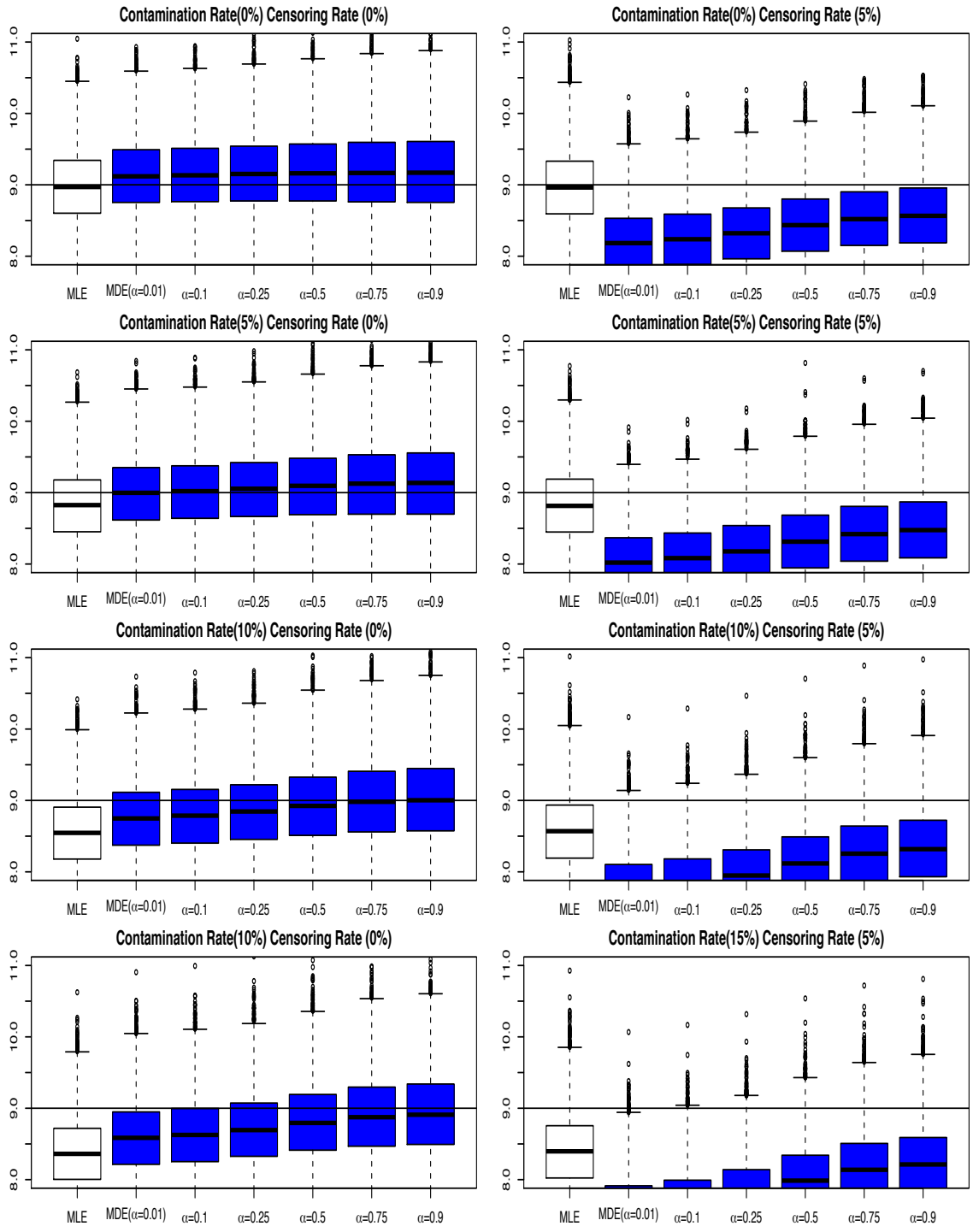

Figure 3.27: Boxplot of 10000 estimates of scale parameters by the MDE_P procedure for the System I with the shorter-life contamination model

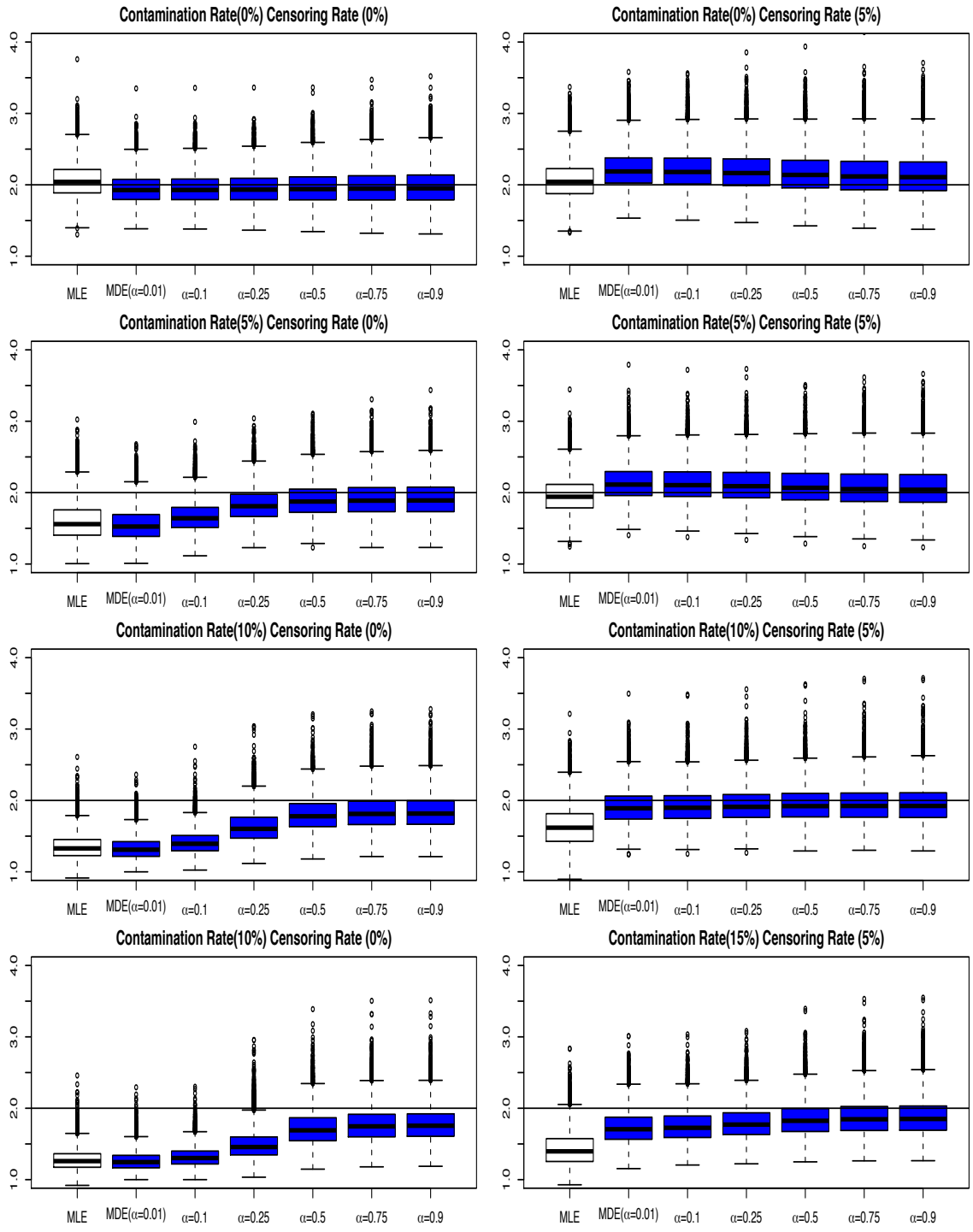

Figure 3.28: Boxplot of 10000 estimates of shape parameters by the MDE_P procedure for the System I with the longer-life contamination model

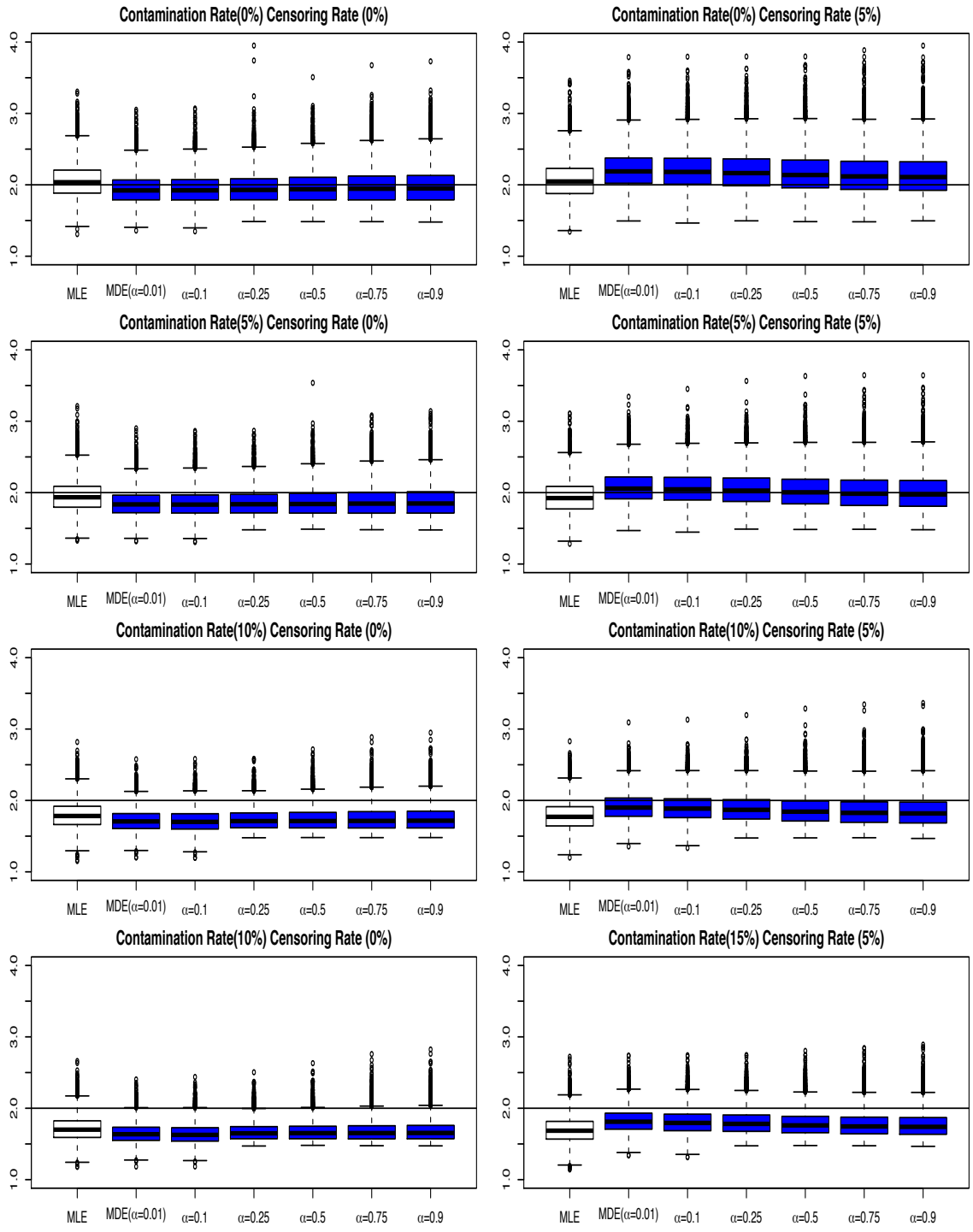

Figure 3.29: Boxplot of 10000 estimates of shape parameters by the MDE_P procedure for the System I with the shorter-life contamination model

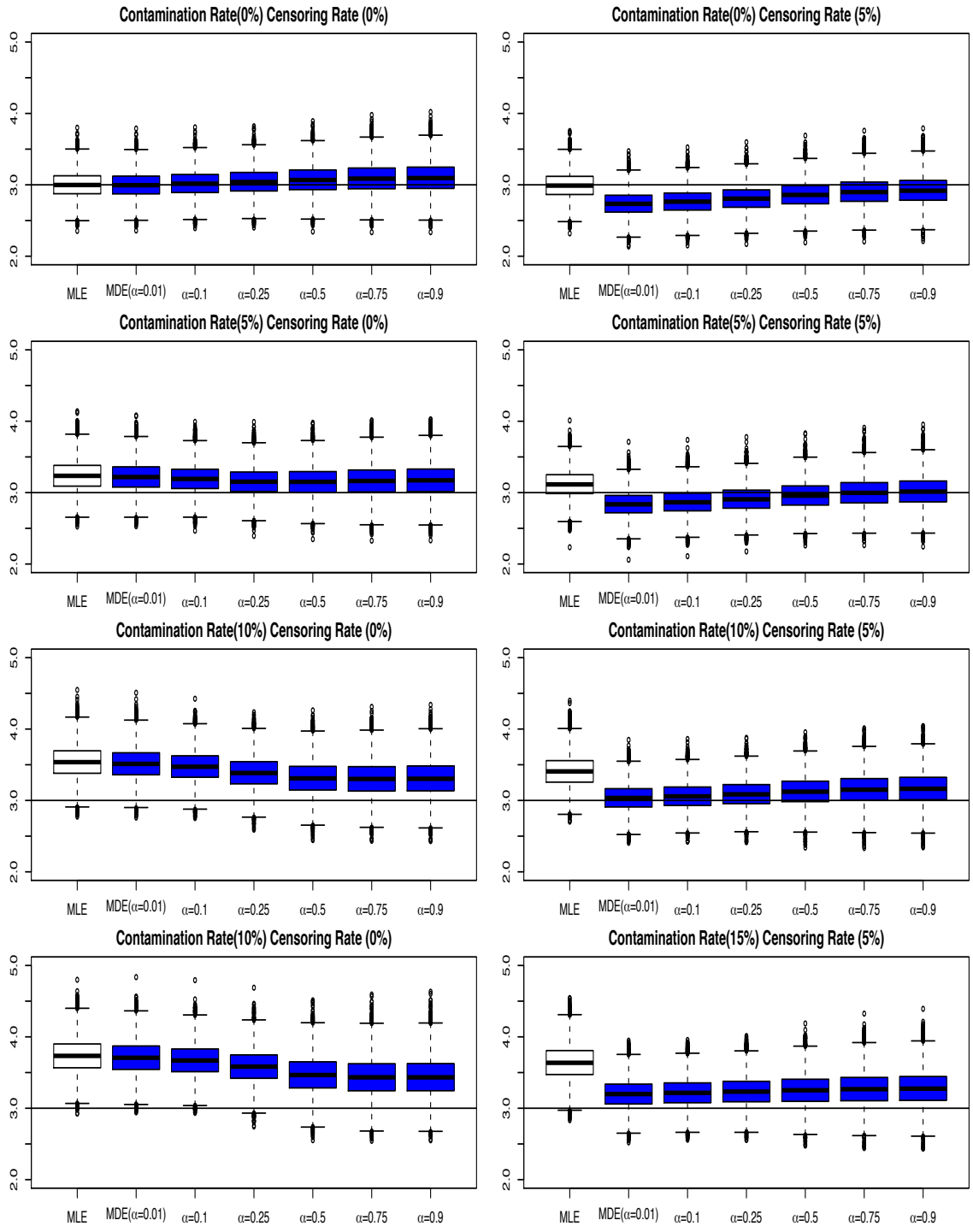

Figure 3.30: Boxplot of 10000 estimates of scale parameters by the MDE_P procedure for the System II with the longer-life contamination model

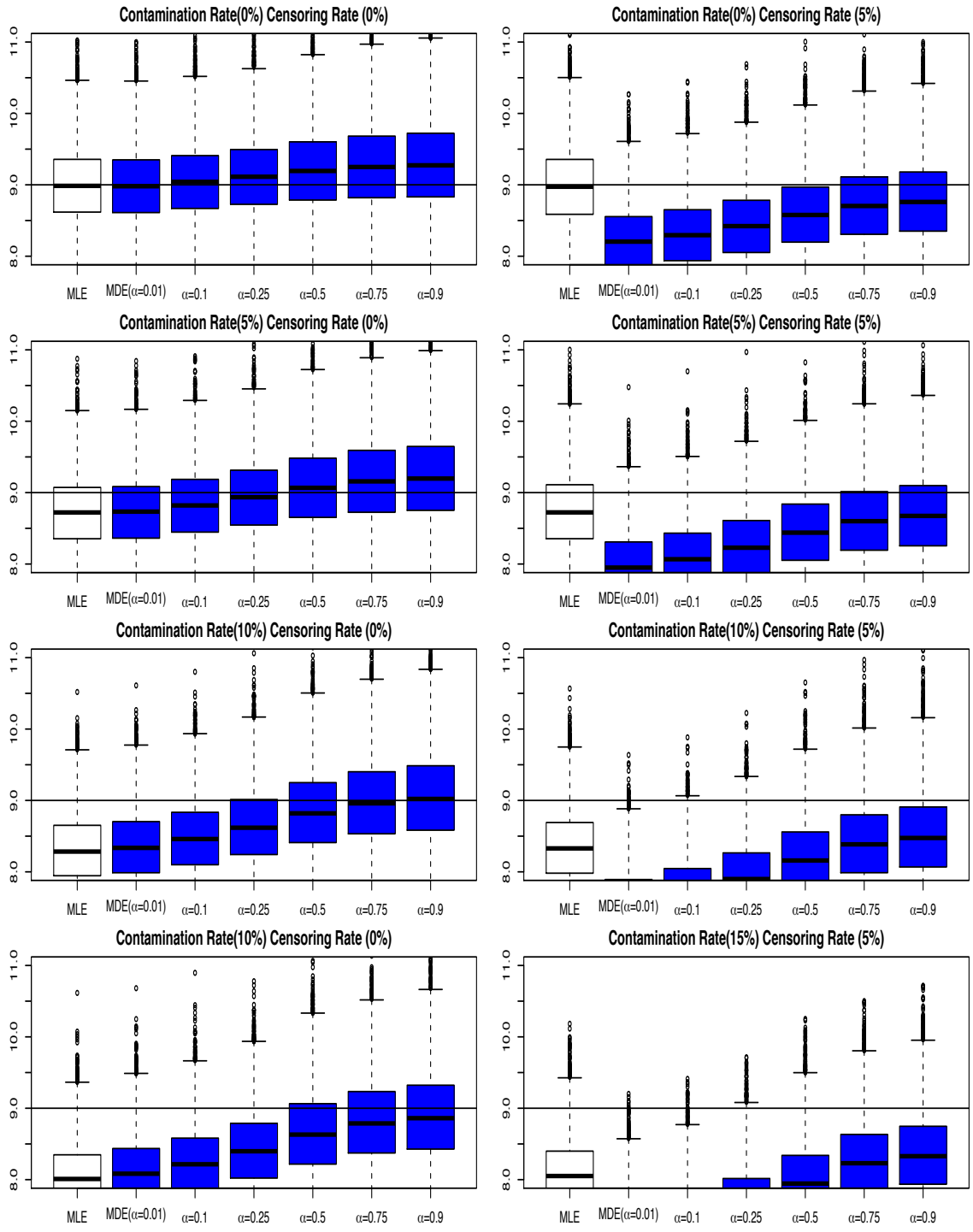

Figure 3.31: Boxplot of 10000 estimates of scale parameters by the MDE_P procedure for the System II with the shorter-life contamination model

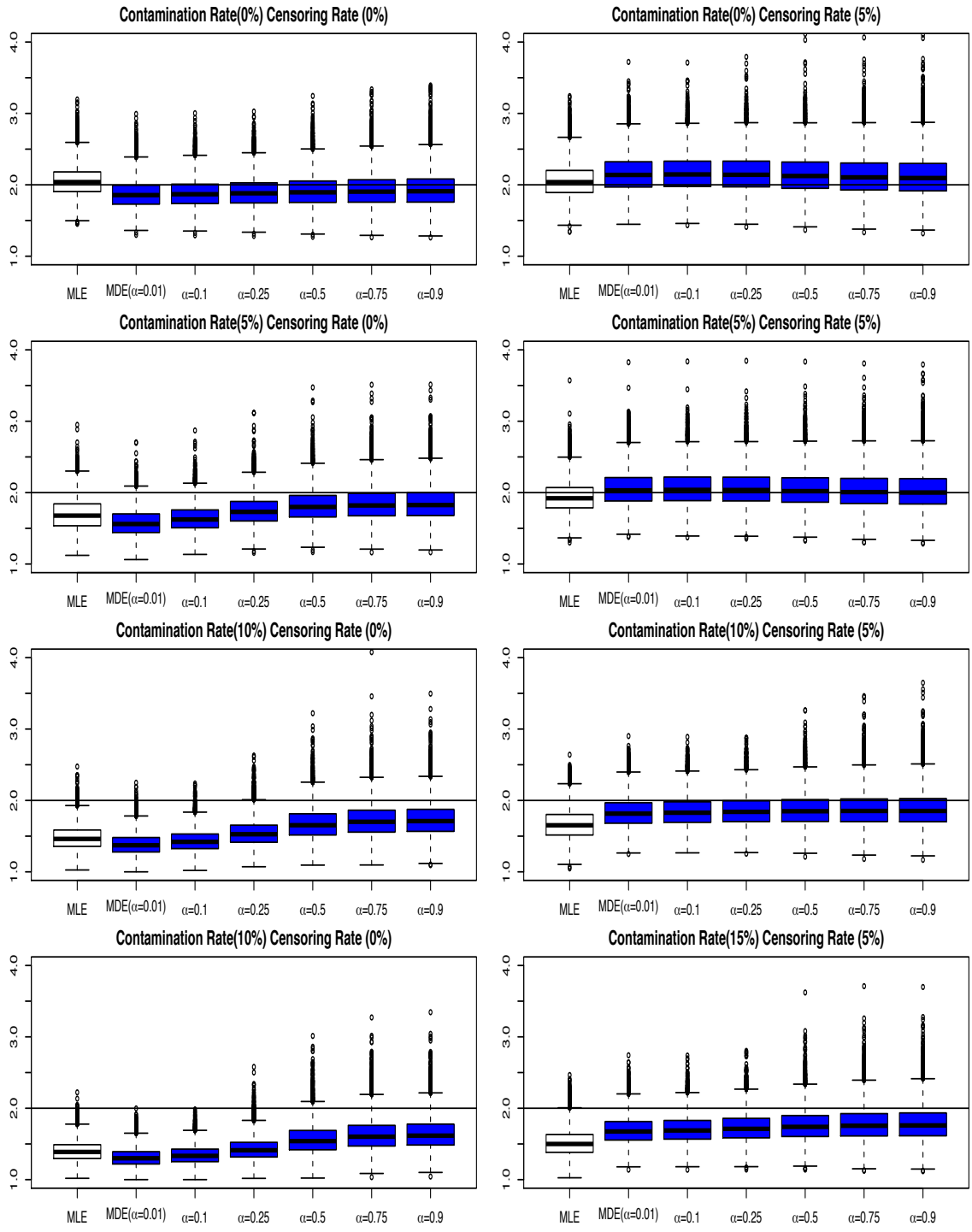

Figure 3.32: Boxplot of 10000 estimates of shape parameters by the MDE_P procedure for the System II with the longer-life contamination model

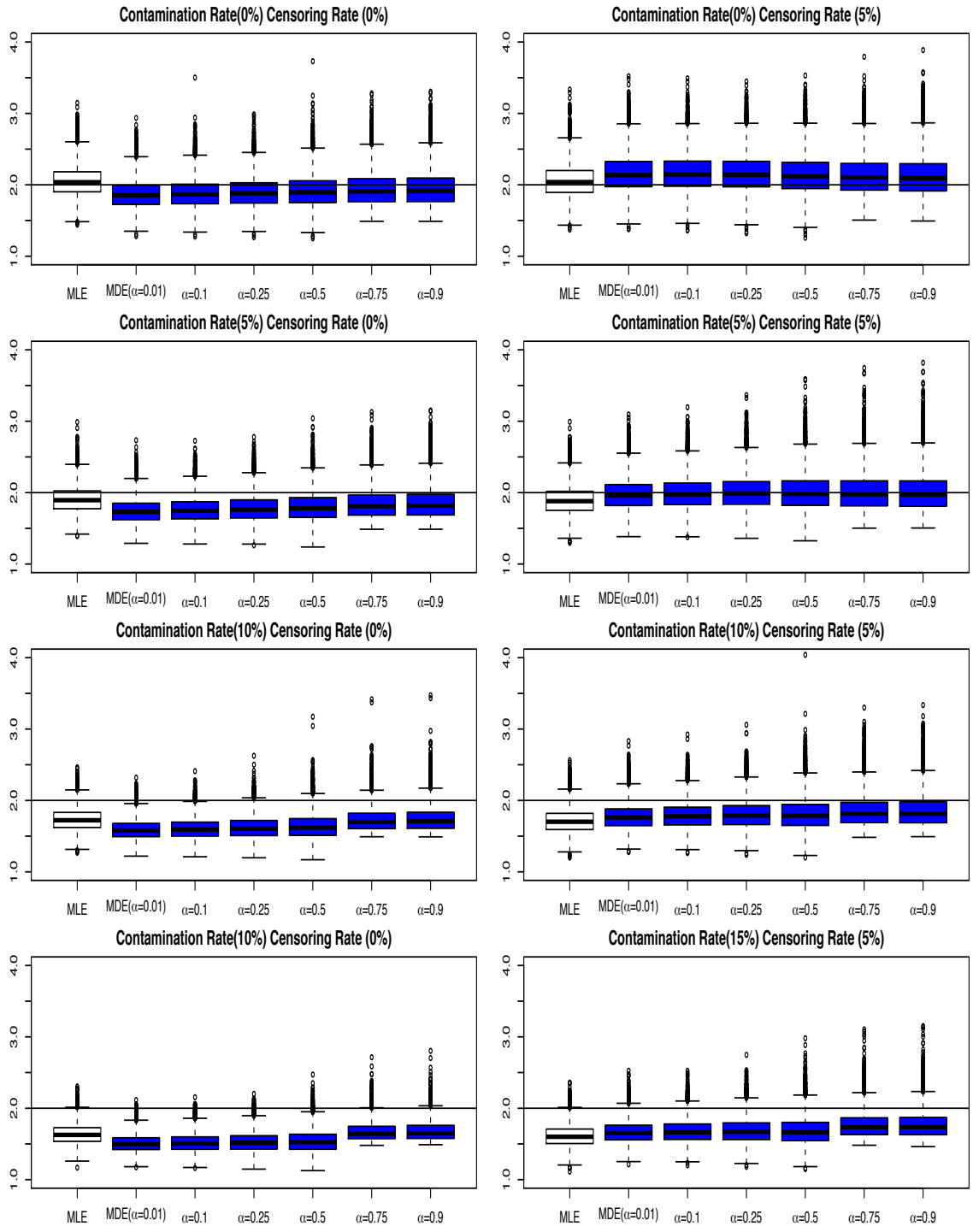

Figure 3.33: Boxplot of 10000 estimates of shape parameters by the MDE_P procedure for the System II with the shorter-life contamination model

The relative efficiencies between the MDE_P and the MLE are presented in Figure 3.34 - 3.37. When the contamination proportion is 0, the relative efficiencies are less than 1 in the both longer-life contamination model and shorter-life contamination model (Figures 3.34 - 3.37). This further supports the result that the MLE gives smaller MSE compared to the MDE_P when there is no contamination. However, when the contamination proportion is large, the MDE_P with large power parameter α has relative efficiency larger than 1, especially in the longer life contamination model. This indicates that the MDE_P with larger power parameter α could perform better than the MLE when there are contaminations in the data.

Different from the MDE_S, the MDE_P is sensitive to the contamination model. In the longer-life contamination model, when the contamination proportion is large, i.e., 15%, the relative efficiency becomes larger than 1 (top panel in Figures 3.26 - 3.37). However, in the shorter-life contamination model (bottom panel in Figures 3.34 - 3.37), the relative efficiencies of MDE_P are less than 1 in most cases.

3.3.2. Results for Estimating The Mean Component Lifetime

To evaluate the performance of proposed estimation procedures for point estimation, the three proposed MDEs – MDE_S, MDE_C and MDE_P – are compared with the MLE in terms of their MSEs for the estimating the mean component lifetime, i.e., $a\Gamma(1+1/b)$, where $\Gamma(\cdot)$ is the gamma function. Specifically, in the ℓ-th simulation, we first estimate the parameter $\boldsymbol{\theta} = (a, b)$ based on different methods, denoted as $\hat{\boldsymbol{\theta}}_{(\ell)} = (\hat{a}_{(\ell)}, \hat{b}_{(\ell)})$, and then the estimated mean component lifetime is computed as $\hat{a}_{(\ell)}\Gamma(1+1/\hat{b}_{(\ell)})$. The estimated MSE of an estimator is computed as

$$\frac{1}{L}\sum_{\ell=1}^{L}\left[\hat{a}_{(\ell)}\Gamma(1+1/\hat{b}_{(\ell)}) - a\Gamma(1+1/b)\right]^2.$$

The simulation results in this subsection are computed based on 10000 realizations ($L = 10000$).

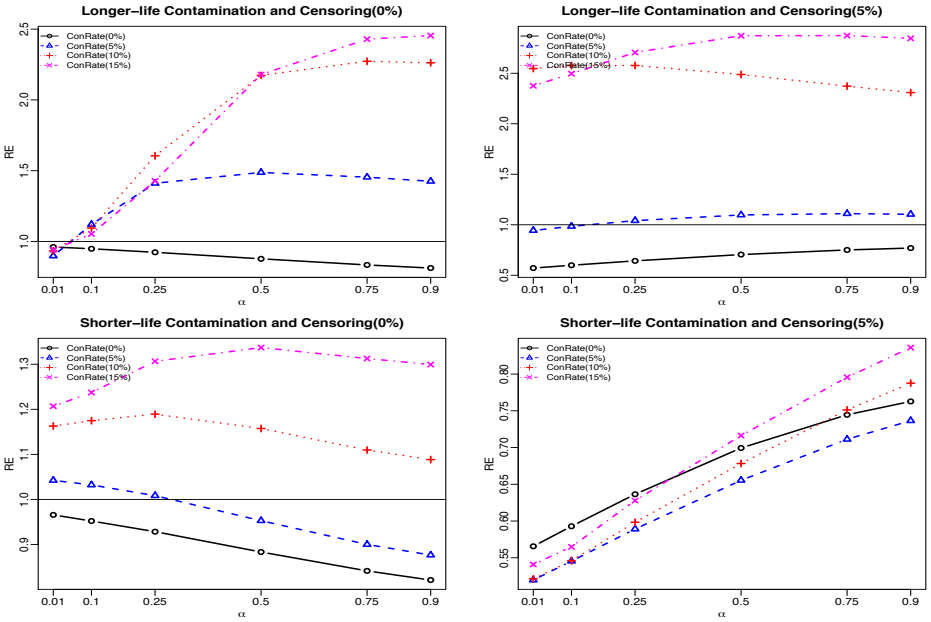

Figure 3.34: Relative efficiencies of estimated scale parameter by the MDE_P procedure for the System I

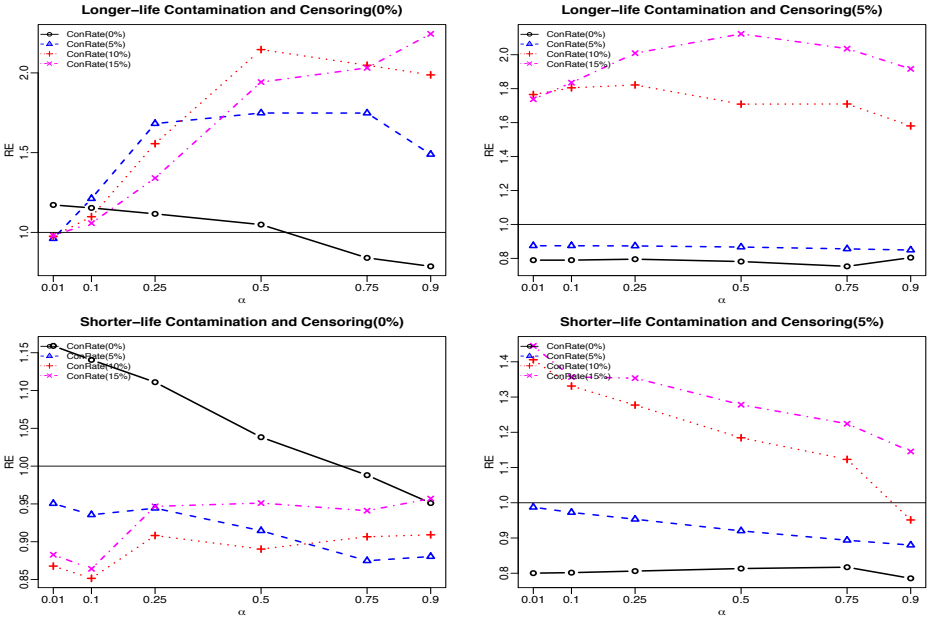

Figure 3.35: Relative efficiencies of estimated shape parameter by the MDE_P procedure for the System I

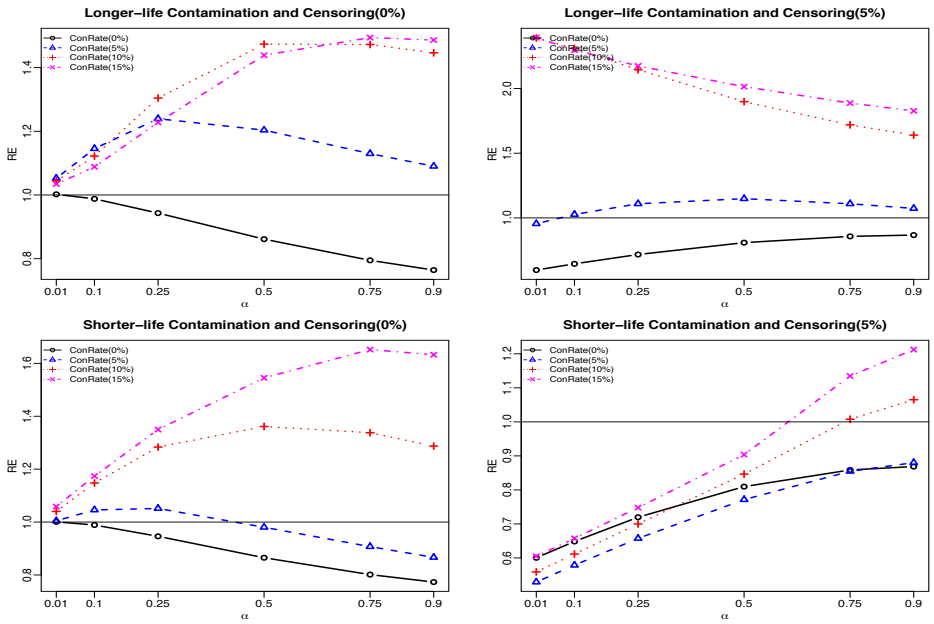

Figure 3.36: Relative efficiencies of estimated scale parameter by the MDE_P procedure for the System II

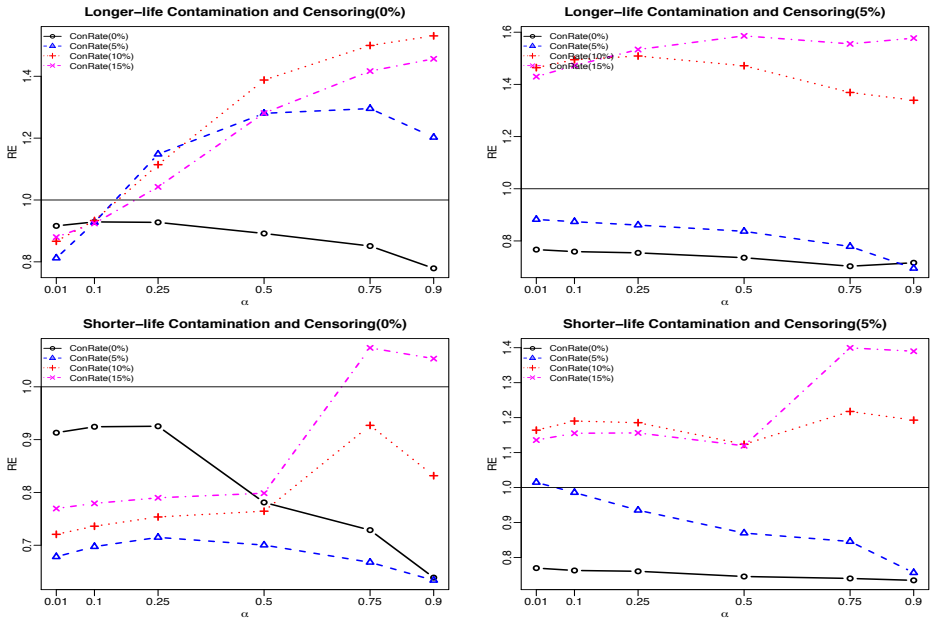

Figure 3.37: Relative efficiencies of estimated shape parameter by the MDE_P procedure for the System II

Similarly, the relative efficiency of MDEs for the mean component lifetime can be defined as

$$RE_{MDE} = \frac{MSE(MLE)}{MSE(MDE)}.$$

The value of relative efficiency greater than 1 indicates that the performance of the MDE is better than the MLE. The relative efficiencies for different censoring rates, different contamination proportions and different values of α for the System I and the System II, and for the longer-life contamination model and the shorter-life contamination model, are plotted in Figures 3.38 - 3.41.

From Figures 3.38 - 3.41, we observe that the performance of the MDE_C is the worst among the three proposed MDEs as the relative efficiencies are below 1 in many cases. Therefore, we focus the discussion of the results below on the MDE_S and MDE_P.

In Figures 3.38 and 3.40, the relative efficiencies of MDE_S, MDE_C and MDE_P with the System I and the System II are presented for the longer-life contamination model, respectively. We can observe that, for the longer-life contamination model, MDE_S and MDE_P have similar performance for both system structures. When there is no contamination (dashed lines with triangles in Figures 3.38 and 3.40), the relative efficiencies are less than 1 for MDE_S and MDE_P, which indicates that the MLE performs better than MDE_S and MDE_P in terms of MSEs. When the contamination rate increases, the relative efficiencies increase and become larger than 1 for MDE_S and MDE_P. Moreover, we observe that the performance of MDE_S and MDE_P improve when α get closer to 1.

These observations are consistent in both no censoring case (Figures 3.38 and 3.40 (a) - (c)) and the 5% censoring case (Figures 3.38 and 3.40 (d) - (f)). However, in the longer-life contamination model, the relative efficiencies in the censoring case are smaller than those in complete data. This indicates that the Type-II censoring reduces the influence of the contamination in the estimating of parameters. It is likely that the contaminated observations with longer life are censored in the Type-II censoring scheme. For example, the relative efficiency of the MDE_S with $\alpha = 0.9$ is close to 15 when the contamination rate is 15% with no censoring, while the relative efficiency of the MDE_S with $\alpha = 0.9$

reduces to 10 when the contamination rate of 15% with 5% censoring.

In Figures 3.39 and 3.41, the relative efficiencies of MDE_S, MDE_C and MDE_P with the System I and the System II are presented for the shorter-life contamination model respectively. In contrast to the longer-life contamination model, MDE_S and MDE_P have different performance in the shorter-life contamination model. In the complete sample case, the MDE_S and MDE_P have relative efficiency greater than 1 when the contamination proportion is over 10% in most cases (Figures 3.39 and 3.41 (a) and (c)). In the Type-II censoring with 5% censoring case, the MDE_S has relative efficiencies greater than 1 when the contamination proportion is 15% and the value of α is close to 1 (Figures 3.39 and 3.41 (d)), while the MDE_P has relative efficiencies less than 1 in most cases (Figures 3.39 and 3.41 (f))

Comparing the performance of all three proposed procedures in the System I (Figures 3.38 and 3.39) and the System II (Figures 3.40 and 3.41), we observe that the MDE_S procedure has consistent performance for both system structures. The MDE_P also has similar performance for the two systems despite some small differences. However, the MDE_C performs differently for the two system structures.

In summary, the proposed estimator MDE_S has better performance compared to MDE_C and MDE_P and it shows advantage over the MLE when there is contamination presented in the data. Moreover, the performance of MDE_S is not much worse than the MLE even when there is no contamination or with a low contamination rate (i.e., relative efficiency less than but close to 1). In the contamination cases, the value of α closer to 1 for the MDE_S has better performance. Therefore, we recommend the use of MDE_S, especially when it is suspect that there is contamination exists in the data. Based on these simulation results and for the simplicity sake, we consider the MDE_S but not the MDE_C and MDE_P in the subsequent study of the performance of standard error estimation and interval estimation.

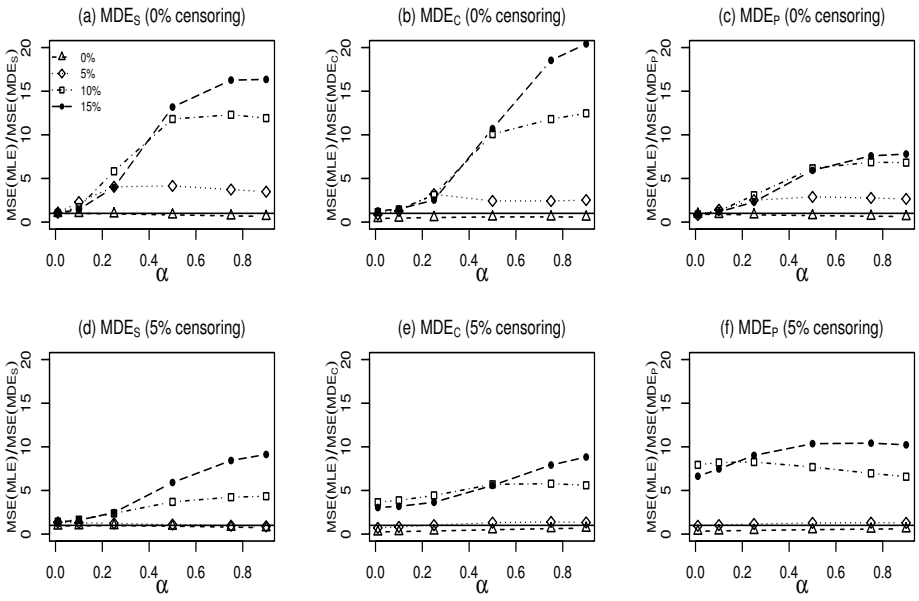

Figure 3.38: Relative efficiencies of estimated mean component lifetime for the System I with the longer-life contamination model

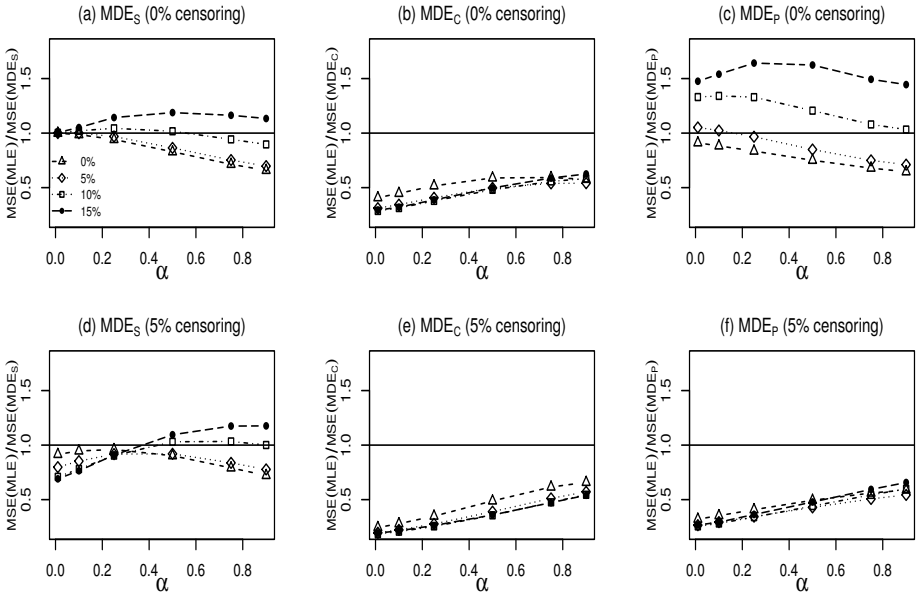

Figure 3.39: Relative efficiencies of estimated mean component lifetime for the System I with the shorter-life contamination model

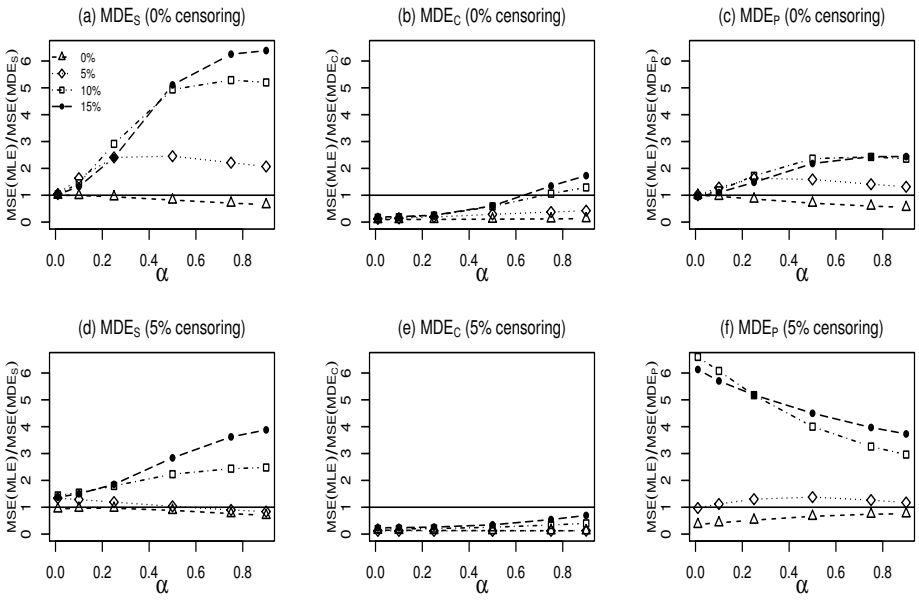

Figure 3.40: Relative efficiencies of estimated mean component lifetime for the System II with the longer-life contamination model

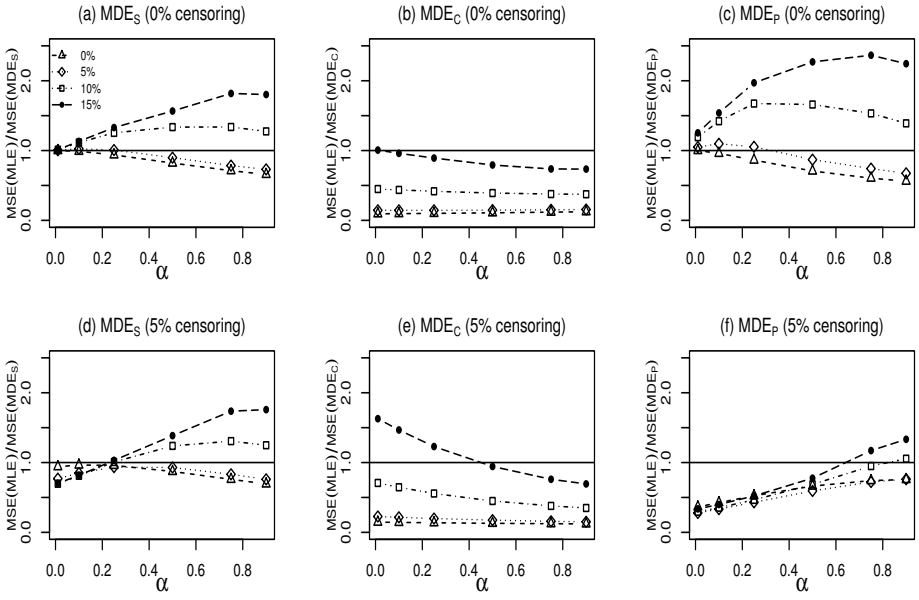

Figure 3.41: Relative efficiencies of estimated mean component lifetime for the system II with the shorter-life contamination model

3.3.3. Results for Standard Error Estimation and Confidence Interval Estimation

3.3.3.1. Determining a Suitable Bootstrap Size for Standard Error Estimation

To determine the required bootstrap size B for the standard error estimation for MDE described in Section 3.2.2.3, based on the discussion in Efron and Tibshirani (1993), we consider evaluating the coefficient of variation of the standard error estimates to obtain a reasonable value of the number of bootstrap replicates.

We consider the coefficient of variation of the standard error estimates, which is computed as the ratio of the variance of bootstrap estimate of standard error $\widehat{SE}_B$ to the expectation of $\widehat{SE}_B$ with different bootstrap size B. The variability of bootstrap estimates can be evaluated by using the coefficient of variation and a suitable value of B is a value such that the variability does not change significantly after increasing the value of B.

A Monte Carlo simulation is carried out to evaluate the coefficient of variation for different bootstrap size B in order to determine the proper number of bootstrap replications. We simulate 200 samples of $m = 50$ system lifetimes based on System 1 (4-component series-parallel III system) with true underlying component lifetime distribution $Weibull(3, 2)$, no contamination and no censoring. For each simulation, given a bootstrap replication number B, the bootstrap standard error estimate of MDE_S is calculated, denoted as $\hat{SE}_B$. Then, with the 200 bootstrap standard error estimates $\hat{SE}_B^{(1)}$, $\hat{SE}_B^{(2)}$, ..., $\hat{SE}_B^{(200)}$, the simulated coefficient of variation is computed as:

$$\widehat{CV}(\widehat{SE}_B) = \frac{\widehat{Var}(\widehat{SE}_B)}{\hat{E}(\widehat{SE}_B)},$$

where

$$\hat{E}(\widehat{SE}_B) = \frac{1}{B}\sum_{i=1}^{200}\widehat{SE}_B^{(i)},$$

$$\text{and } \widehat{Var}(\widehat{SE}_B) = \frac{1}{B}\sum_{i=1}^{200}(\widehat{SE}_B^{(i)} - \hat{E}(\widehat{SE}_B))^2.$$

Figures 3.42 and 3.43 presented the simulated coefficient of variation of the standard error of MDE_S for the scale and shape parameters, respectively. From Figures 3.42 and 3.43, we observe that when the bootstrap size B gets above 250, further increase in the bootstrap size does not bring a substantial reduction in the variation. Hence, we consider the number of bootstrap replications $B = 250$ in the Monte Carlo simulation study for evaluating the performance of confidence intervals.

3.3.3.2. Performance of Standard Error Estimates

To evaluate the performance of the three standard error estimation methods for MDE, we compare the simulated standard errors of the MDE based on the system-level data, MDE_S, and the averaged values of the standard error estimates based on the theoretical results from Basu et al. (1998) (i.e., $\widehat{SE}_A$), based on the observed Fisher information matrix (i.e., $\widehat{SE}_F$), and based on the bootstrap method (i.e., $\widehat{SE}_B$) with the bootstrap size $B = 250$. We simulate 1000 samples of $m = 50$ system lifetimes based on the System 1 (4-component series-parallel III system) with true underlying component lifetime distribution $Weibull(3, 2)$, no contamination and no censoring. The simulation results are presented in Table 3.2.

From the results in Table 3.2, we observe that the standard error estimates based on the theoretical results from Basu et al. (1998) can seriously underestimate the standard error of MDE_S, while the standard error estimates based on observed Fisher information matrix provide reasonable approximation to standard errors of the MDE_S when α is close to 0. Overall, among the three standard error estimation methods for MDE, bootstrap

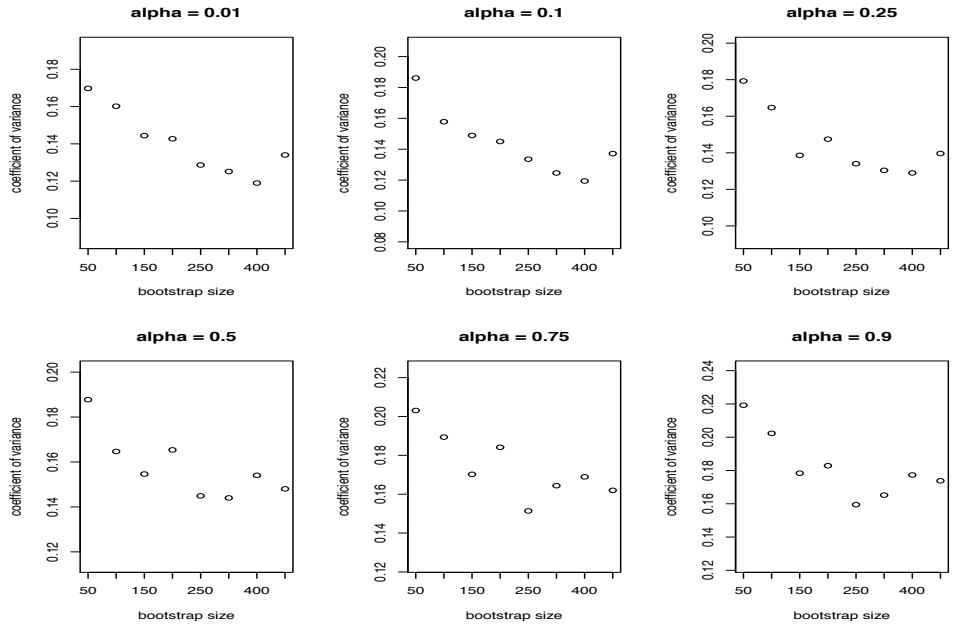

Figure 3.42: Coefficient of variation of $\widehat{SE}_B$ for scale parameter as a function of the number of bootstrap samples B

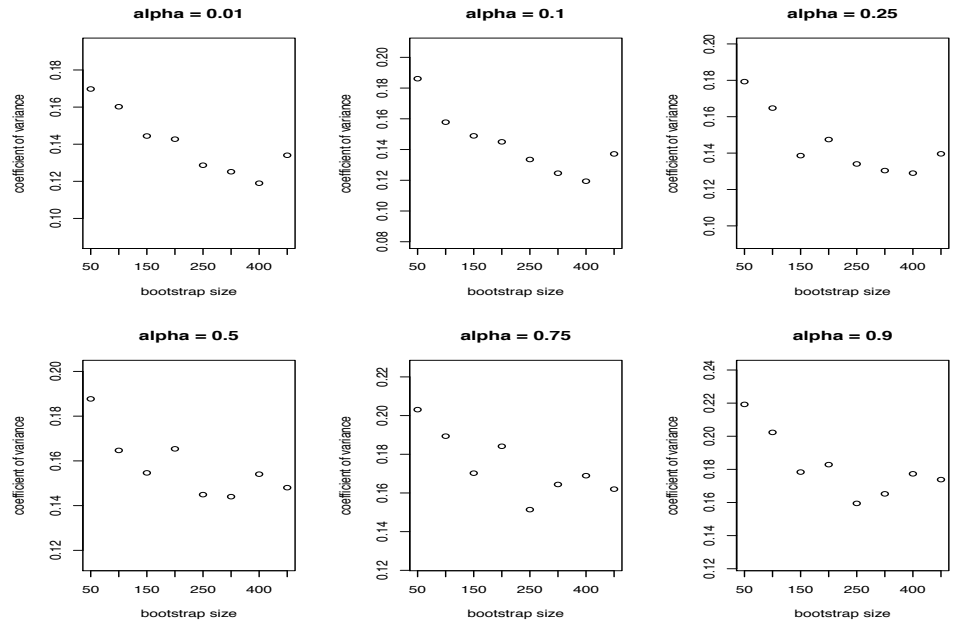

Figure 3.43: Coefficient of variation of $\widehat{SE}_B$ for scale parameter as a function of the number of bootstrap samples B

method with bootstrap size $B = 250$ provides reasonable approximation to standard errors of the MDE_S for all the values of α considered here. Therefore, in the following simulation study for confidence intervals, we use the standard error estimates based on the bootstrap method.

Table 3.2: Simulated standard errors the MDE_S and the averaged standard error estimates based on the theoretical results from Basu et al. (1998) ($\widehat{SE}_A$), based on observed Fisher information matrix ($\widehat{SE}_F$), and based on bootstrap method ($\widehat{SE}_B$) with bootstrap size $B = 250$

	α = 0.01	α = 0.1	α = 0.25	α = 0.5	α = 0.75	α = 0.9
Simulated $\widehat{SE}(\hat{a})$	0.179	0.180	0.184	0.196	0.210	0.219
Average $\widehat{SE}_A(\hat{a})$	0.013	0.011	0.008	0.006	0.005	0.005
Average $\widehat{SE}_F(\hat{a})$	0.214	0.206	0.190	0.172	0.165	0.164
Average $\widehat{SE}_B(\hat{a})$	0.205	0.210	0.197	0.183	0.187	0.189
Simulated $\widehat{SE}(\hat{b})$	0.247	0.248	0.257	0.290	0.326	0.336
Average $\widehat{SE}_A(\hat{b})$	0.009	0.007	0.005	0.003	0.003	0.002
Average $\widehat{SE}_F(\hat{b})$	0.203	0.207	0.215	0.232	0.244	0.248
Average $\widehat{SE}_B(\hat{b})$	0.238	0.230	0.255	0.322	0.375	0.389

3.3.3.3. Performance of Confidence Intervals

In this subsection, the simulated coverage probabilities and the average widths of 95% confidence intervals of the Weibull parameters a and b for the MLE and the MDE based on system-level data (MDE_S) with different values of α are compared. The two systems (System I and System II) and the longer-life and shorter-life contamination models described in beginning of Section 3.3 are considered here. Specifically, a two-sided $100(1-\alpha)\%$ normal approximated confidence interval of a is constructed as

$$[a_l, a_u] = \left[\hat{a} - z_{1-\alpha/2}\widehat{SE}(\hat{a}), \hat{a} + z_{1-\alpha/2}\widehat{SE}(\hat{a})\right],$$

where the estimated standard error $\widehat{SE}(\hat{a})$ is obtained based on the bootstrap method. Similarly, a two-sided $100(1-\alpha)\%$ normal approximated confidence interval of b is constructed as

$$[b_l, b_u] = \left[\hat{b} - z_{1-\alpha/2}\widehat{SE}(\hat{b}), \hat{b} + z_{1-\alpha/2}\widehat{SE}(\hat{b})\right],$$

where the estimated standard error $\widehat{SE}(\hat{b})$ is obtained based on the bootstrap method. The simulated coverage probabilities (CP) is computed as the proportion of cases that the true value of the parameter falls within the confidence interval, and the average width (AW) is computed as $2z_{1-\alpha/2}\widehat{SE}(\hat{a})$ and $2z_{1-\alpha/2}\widehat{SE}(\hat{b})$ for parameters a and b, respectively. The simulation results are presented in Tables 3.3 – 3.6.

From Tables 3.3 – 3.6, we observe that when there is no contamination, the confidence intervals based on MLEs give coverage probabilities close to the nominal 95% for both scale and shape parameters. Compared with MDE_S, the confidence intervals based on MLEs give the highest coverage probabilities and the smallest average widths when there is no contamination (i.e., contamination rate is 0). However, when the contamination rate increases, the coverage probabilities of the confidence intervals based on MLEs decrease for both the scale and shape parameters, and the average widths increase for the scale parameter but decrease for the shape parameter. This result is consistent in both the longer-life and shorter-life contamination models, with and without censoring in System I and System II.

We also observe that the coverage probabilities of the confidence intervals based on MLEs are sensitive to the contamination rate and the type of contamination. In the longer-life contamination model, the coverage probabilities for both scale and shape parameters drop dramatically when the contamination rate increases. For example, in Table 3.3 when the contamination rate is 15% with no censoring, the simulated coverage probability of the confidence intervals based on MLE is only 18% for the scale parameter and 2% for the shape parameter under the longer-life contamination model, while the simulated coverage probability of the confidence intervals based on MLE is 80.7% for the scale parameter and 68.7% for the shape parameter under the shorter-life contamination model.

Similar to the MLEs, the coverage probabilities of the confidence intervals based on MDE_S are also sensitive to the contamination rate and the type of the contamination. For the longer-life contamination model, the confidence intervals of the scale parameter based on MDE_S with power parameter α close to 1 has closer coverage probability to the nominal levels when the contamination rate is high. However, for the shorter-life contamination model, the coverage probability of the confidence intervals of the scale parameter based on MDE_S with power parameter α close to 1 is far away from the nominal level when the contamination rate is high (see, Table 3.3).

We can see that the confidence intervals based on MDE_S have better coverage probabilities than the confidence intervals based on MLE in the longer-life contamination model when the contamination rate is high. For example, when the contamination rate is 15% in the longer-life contamination model, the coverage probability of the confidence interval based on MDE_S with α close to 1 can still maintain 95.7% for scale parameter (Table 3.3) and 91.6% for shape parameter (Table 3.4), while the coverage probability of the confidence intervals of based on MLE is down to 18% for scale parameter and 2% for shape parameter.

In general, for the longer-life contamination model, comparing to the confidence intervals based on MLE, the confidence intervals based on MDE_S have higher coverage probabilities and larger average widths of the confidence intervals (Tables 3.3 and 3.4). Nevertheless, for the shorter-life contamination model, comparing to the confidence intervals based on MLE, the confidence intervals based on MDE_S have lower coverage probabilities.

3.4. Illustrative Example

In this section, a numerical example based on the system lifetime data of the 4-component series-parallel III system with Weibull component lifetime distribution is used to illustrate the estimation methods proposed in this paper. The system lifetime data was originally presented in Balakrishnan et al. (2011b) and further analyzed by Yang et al.

Table 3.3: Simulated coverage probabilities (in %) and average widths of confidence intervals of the scale parameter computed based on MLE and MDE_S with different values of α under the longer-life and shorter-life contamination models for System I

Coverage Probability	Longer-life Contamination Model								Shorter-life Contamination Model							
	No censoring				5% censoring				No censoring				5% censoring			
Contamination Rate	0%	5%	10%	15%	0%	5%	10%	15%	0%	5%	10%	15%	0%	5%	10%	15%
MLE	93.9	88.1	44.9	18.0	93.3	92.0	58.0	24.5	93.7	92.4	86.3	80.7	93.6	92.3	87.8	82.0
MDE_S ($\alpha = 0.01$)	93.9	92.3	59.1	31.7	87.9	93.1	79.5	50.6	93.6	92.2	86.0	80.0	88.6	84.7	75.3	67.5
MDE_S ($\alpha = 0.10$)	93.9	94.7	73.5	45.9	89.7	93.2	81.3	55.5	93.7	92.5	87.1	81.6	89.8	87.0	79.6	72.1
MDE_S ($\alpha = 0.25$)	93.9	95.2	93.1	82.6	91.3	93.2	86.1	70.2	93.3	91.8	83.3	73.2	90.9	89.2	82.8	73.6
MDE_S ($\alpha = 0.50$)	93.3	94.6	95.9	95.8	92.7	93.3	92.6	91.5	92.6	91.4	82.8	71.3	92.0	91.2	85.2	75.7
MDE_S ($\alpha = 0.75$)	92.9	94.0	95.4	95.9	93.1	93.6	94.8	95.5	92.1	90.5	81.4	68.8	92.2	91.4	85.2	74.8
MDE_S ($\alpha = 0.90$)	92.3	93.8	95.3	95.7	93.2	93.6	95.0	95.9	91.6	90.1	80.2	67.6	92.2	91.3	84.6	73.8
Average Width	Longer-life Contamination Model								Shorter-life Contamination Model							
	No censoring				5% censoring				No censoring				5% censoring			
Contamination Rate	0%	5%	10%	15%	0%	5%	10%	15%	0%	5%	10%	15%	0%	5%	10%	15%
MLE	0.69	0.99	1.32	1.50	0.70	0.77	1.06	1.33	2.06	2.14	2.24	2.30	2.09	2.18	2.30	2.37
MDE_S ($\alpha = 0.01$)	0.69	1.08	1.45	1.64	0.63	0.73	1.19	1.45	2.06	2.14	2.22	2.26	1.89	1.97	2.06	2.10
MDE_S ($\alpha = 0.10$)	0.69	0.93	1.33	1.54	0.64	0.74	1.14	1.41	2.08	2.17	2.27	2.32	1.92	2.02	2.12	2.18
MDE_S ($\alpha = 0.25$)	0.71	0.82	1.11	1.35	0.66	0.76	1.06	1.31	2.12	2.23	2.34	2.38	1.99	2.10	2.22	2.27
MDE_S ($\alpha = 0.50$)	0.75	0.82	0.98	1.15	0.71	0.80	1.04	1.23	2.24	2.38	2.52	2.57	2.12	2.25	2.40	2.46
MDE_S ($\alpha = 0.75$)	0.80	0.86	0.98	1.11	0.76	0.87	1.08	1.22	2.39	2.53	2.68	2.75	2.27	2.42	2.58	2.65
MDE_S ($\alpha = 0.90$)	0.83	0.89	1.00	1.11	0.80	0.91	1.10	1.21	2.47	2.61	2.78	2.85	2.38	2.52	2.70	2.77

Table 3.4: Simulated coverage probabilities and average widths of confidence intervals of the shape parameter computed based on MLE and MDE_S with different values of α under the longer-life and shorter-life contamination models for System I

Coverage Probability	Longer-life Contamination Model								Shorter-life Contamination Model							
	No censoring				5% censoring				No censoring				5% censoring			
Contamination Rate	0%	5%	10%	15%	0%	5%	10%	15%	0%	5%	10%	15%	0%	5%	10%	15%
MLE	95.2	36.8	6.5	2.0	95.0	93.0	49.8	20.4	95.2	93.7	82.0	68.7	95.3	93.3	81.6	68.7
MDE_S ($\alpha = 0.01$)	92.4	42.3	4.4	1.0	88.7	91.7	73.0	33.8	92.4	92.1	74.8	52.6	88.9	91.9	91.4	82.0
MDE_S ($\alpha = 0.10$)	92.4	70.0	10.3	2.3	89.3	92.2	72.6	33.2	92.5	91.4	72.2	47.7	89.7	92.3	89.4	77.2
MDE_S ($\alpha = 0.25$)	92.5	91.8	70.3	37.5	89.9	92.6	77.7	40.4	92.2	90.0	65.4	37.6	90.3	91.8	83.7	64.2
MDE_S ($\alpha = 0.50$)	92.5	93.0	91.6	87.5	91.1	92.8	88.8	80.0	91.9	89.8	62.2	31.9	91.2	90.8	75.8	49.7
MDE_S ($\alpha = 0.75$)	92.3	93.0	92.8	91.1	92.1	93.4	91.6	89.7	91.4	88.2	60.3	28.9	91.6	89.5	70.0	41.6
MDE_S ($\alpha = 0.90$)	92.3	93.0	92.6	91.6	92.4	93.3	92.3	90.8	91.2	87.3	59.9	28.7	91.4	88.7	67.6	39.0
Average Width	Longer-life Contamination Model								Shorter-life Contamination Model							
	No censoring				5% censoring				No censoring				5% censoring			
Contamination Rate	0%	5%	10%	15%	0%	5%	10%	15%	0%	5%	10%	15%	0%	5%	10%	15%
MLE	0.95	0.68	0.56	0.53	1.02	0.96	0.77	0.66	0.95	0.90	0.84	0.80	1.02	0.96	0.89	0.85
MDE_S ($\alpha = 0.01$)	1.01	0.78	0.57	0.54	1.25	1.12	0.98	0.79	1.01	0.86	0.71	0.64	1.25	1.04	0.85	0.76
MDE_S ($\alpha = 0.10$)	1.01	0.84	0.60	0.55	1.24	1.11	0.94	0.77	1.01	0.86	0.70	0.62	1.24	1.04	0.84	0.74
MDE_S ($\alpha = 0.25$)	1.05	1.03	0.89	0.74	1.25	1.10	0.91	0.76	1.05	0.89	0.71	0.62	1.25	1.06	0.83	0.73
MDE_S ($\alpha = 0.50$)	1.20	1.18	1.14	1.09	1.33	1.17	1.02	1.00	1.20	1.01	0.75	0.63	1.31	1.12	0.84	0.70
MDE_S ($\alpha = 0.75$)	1.41	1.37	1.31	1.24	1.49	1.34	1.21	1.19	1.39	1.17	0.82	0.65	1.45	1.23	0.90	0.71
MDE_S ($\alpha = 0.90$)	1.51	1.47	1.39	1.32	1.57	1.46	1.31	1.28	1.54	1.28	0.88	0.68	1.55	1.34	0.94	0.73

Table 3.5: Simulated coverage probabilities and average widths of confidence intervals of the scale parameter computed based on MLE and MDE_S with different values of α under the longer-life and shorter-life contamination models for System II

Coverage Probability	Longer-life Contamination Model								Shorter-life Contamination Model							
	No censoring				5% censoring				No censoring				5% censoring			
Contamination Rate	0%	5%	10%	15%	0%	5%	10%	15%	0%	5%	10%	15%	0%	5%	10%	15%
MLE	93.8	88.6	56.6	30.4	93.9	92.9	68.4	40.8	94.0	91.1	78.5	63.8	93.9	92.2	81.3	69.7
MDE_S ($\alpha = 0.01$)	93.6	92.0	70.2	47.6	88.8	93.9	82.2	63.3	93.9	90.3	74.2	55.4	88.8	83.1	60.7	41.5
MDE_S ($\alpha = 0.10$)	93.7	93.9	77.6	57.7	90.2	94.0	83.6	67.0	94.0	91.3	78.5	61.8	90.3	86.1	68.5	51.3
MDE_S ($\alpha = 0.25$)	93.5	95.2	89.7	77.9	91.9	93.9	86.4	75.3	93.8	92.1	84.2	71.7	91.7	90.0	78.6	65.5
MDE_S ($\alpha = 0.50$)	93.1	94.8	95.2	93.0	93.1	94.3	91.8	88.7	93.3	93.1	89.4	82.7	93.3	93.1	88.4	81.2
MDE_S ($\alpha = 0.75$)	92.4	94.4	95.7	95.2	93.4	94.6	94.6	94.2	92.1	89.9	75.6	54.4	92.8	92.0	79.5	60.0
MDE_S ($\alpha = 0.90$)	92.2	94.2	95.7	95.6	93.1	94.5	95.3	95.2	91.7	89.6	75.5	55.0	92.4	91.5	79.2	60.2

Average Width	Longer-life Contamination Model								Shorter-life Contamination Model							
	No censoring				5% censoring				No censoring				5% censoring			
Contamination Rate	0%	5%	10%	15%	0%	5%	10%	15%	0%	5%	10%	15%	0%	5%	10%	15%
MLE	0.71	0.93	1.14	1.27	0.72	0.79	1.00	1.17	2.13	2.23	2.35	2.40	2.16	2.29	2.44	2.51
MDE_S ($\alpha = 0.01$)	0.71	1.00	1.27	1.42	0.65	0.75	1.04	1.22	2.13	2.17	2.17	2.14	1.96	2.02	2.04	2.02
MDE_S ($\alpha = 0.10$)	0.72	0.92	1.20	1.36	0.67	0.76	1.03	1.21	2.15	2.22	2.24	2.21	2.00	2.08	2.12	2.10
MDE_S ($\alpha = 0.25$)	0.74	0.86	1.09	1.26	0.70	0.79	1.02	1.20	2.21	2.30	2.38	2.36	2.09	2.19	2.27	2.26
MDE_S ($\alpha = 0.50$)	0.78	0.87	1.05	1.21	0.75	0.85	1.06	1.22	2.35	2.49	2.63	2.64	2.26	2.40	2.54	2.56
MDE_S ($\alpha = 0.75$)	0.84	0.92	1.08	1.22	0.82	0.93	1.13	1.28	2.51	2.65	2.79	2.78	2.45	2.59	2.74	2.74
MDE_S ($\alpha = 0.90$)	0.87	0.95	1.11	1.24	0.86	0.97	1.16	1.31	2.59	2.74	2.90	2.89	2.56	2.72	2.87	2.88

Table 3.6: Simulated coverage probabilities and average widths of confidence intervals of the shape parameter computed based on MLE and MDE_S with different values of α under the longer-life and shorter-life contamination models for System II

Coverage Probability	Longer-life Contamination Model								Shorter-life Contamination Model							
	No censoring				5% censoring				No censoring				5% censoring			
Contamination Rate	0%	5%	10%	15%	0%	5%	10%	15%	0%	5%	10%	15%	0%	5%	10%	15%
MLE	94.9	48.5	12.1	4.6	95.2	92.0	50.1	21.7	95.1	91.4	65.6	41.8	95.2	91.3	64.3	39.2
MDE_S ($\alpha = 0.01$)	92.2	55.0	9.0	2.7	87.9	92.1	73.2	37.0	92.6	89.6	52.5	24.2	88.7	92.7	81.1	54.0
MDE_S ($\alpha = 0.10$)	92.3	71.8	14.1	4.4	89.2	92.4	71.6	34.8	92.8	89.1	50.3	22.2	89.6	92.5	77.8	47.9
MDE_S ($\alpha = 0.25$)	92.3	90.5	53.5	22.2	90.5	92.8	72.6	35.8	93.1	89.8	51.4	21.5	91.3	92.6	73.2	40.7
MDE_S ($\alpha = 0.50$)	92.3	92.7	86.8	74.4	91.8	92.7	82.8	60.8	93.4	91.3	57.9	25.9	92.9	92.8	70.8	36.1
MDE_S ($\alpha = 0.75$)	92.3	92.9	90.8	86.2	92.7	92.9	89.0	79.7	92.2	87.8	54.2	22.0	92.9	89.8	62.6	27.4
MDE_S ($\alpha = 0.90$)	92.5	92.9	91.5	88.3	92.8	92.9	90.8	84.2	91.9	87.3	56.8	25.3	92.8	89.3	62.8	29.3
Average Width	Longer-life Contamination Model								Shorter-life Contamination Model							
	No censoring				5% censoring				No censoring				5% censoring			
Contamination Rate	0%	5%	10%	15%	0%	5%	10%	15%	0%	5%	10%	15%	0%	5%	10%	15%
MLE	0.82	0.64	0.55	0.52	0.88	0.82	0.69	0.62	0.81	0.77	0.71	0.67	0.88	0.83	0.75	0.71
MDE_S ($\alpha = 0.01$)	0.87	0.71	0.54	0.51	1.07	0.94	0.77	0.67	0.87	0.72	0.58	0.53	1.07	0.87	0.70	0.63
MDE_S ($\alpha = 0.10$)	0.87	0.71	0.55	0.51	1.06	0.93	0.75	0.65	0.87	0.73	0.58	0.53	1.07	0.88	0.70	0.63
MDE_S ($\alpha = 0.25$)	0.91	0.86	0.68	0.58	1.06	0.92	0.73	0.64	0.95	0.78	0.61	0.54	1.09	0.92	0.71	0.62
MDE_S ($\alpha = 0.50$)	1.06	1.02	0.94	0.85	1.13	0.96	0.82	0.74	1.16	0.97	0.69	0.59	1.21	1.05	0.76	0.63
MDE_S ($\alpha = 0.75$)	1.26	1.20	1.09	1.01	1.26	1.10	1.00	0.93	1.43	1.22	0.88	0.71	1.44	1.26	0.92	0.73
MDE_S ($\alpha = 0.90$)	1.40	1.32	1.17	1.07	1.38	1.23	1.11	1.02	1.64	1.43	1.03	0.80	1.66	1.49	1.07	0.83

(2016). The original data set contains $m = 10$ system lifetimes from the 4-component system with system signature $\boldsymbol{s} = (1/4, 1/4, 1/2, 0)$ with component lifetime follows $Weibull(3, 2)$ are presented in Table 3.7. To illustrate the effect of contamination in the statistical inference procedures, we simulated an observation from the $Weibull(9, 2)$ to replace a random selected observation in the original data set. After the random selection process, the observation 1.76789 is replaced by 5.48619. The updated data set with contamination is presented in Table 3.8.

Table 3.7: Simulated system lifetimes with system signature $\boldsymbol{s} = (1/4, 1/4, 1/2, 0)$ with component lifetime distribution $Weibull(3, 2)$

0.72717	1.02050	1.38633	1.61244	1.70590
1.76789	2.67863	3.02676	3.25943	3.78497

Table 3.8: Simulated system lifetimes with system signature $\boldsymbol{s} = (1/4, 1/4, 1/2, 0)$ with component lifetime distribution of $Weibull(3, 2)$ and one contaminated observation from $Weibull(9, 2)$

0.72717	1.02050	1.38633	1.61244	1.70590
5.48619	2.67863	3.02676	3.25943	3.78497

Based on the original and the contaminated data sets in Tables 3.7 and 3.8, the point and interval estimates of the Weibull parameters a and b based on maximum likelihood method and the three proposed minimum divergence estimation methods are presented in Tables 3.10 and 3.12, respectively.

For point estimation, form Tables 3.10 and 3.12, the MLE, MDE_S, MDE_C and MDE_P with different values of α provide similar point estimates of the parameters a and b. By comparing the estimates obtained from the data sets with and without contamination, the difference between MDEs (especially α close to 1) obtained from the data sets with and without contamination is smaller than the difference between MLEs obtained from the data sets with and without contamination in general. For example, the MLE of a is 2.695 for the dataset without contamination and the MLE of a is 3.249 for the dataset with contamination which has a difference 0.554, while the MDE_S with $\alpha = 0.9$ is 2.691 for the

dataset without contamination and the MDE_S with $\alpha = 0.9$ is 3.105 for the dataset with contamination, which has a difference 0.414.

For interval estimation, in both with and without contamination cases (Table 3.10 and Table 3.12), the confidence intervals for the scale parameter based on the observed Fisher information matrix is very close to the one using the bootstrap method. However, the confidence intervals for the shape parameter based on the bootstrap method is wider than those using the observed Fisher information matrix.

The confidence intervals using MDEs with standard error estimates based on the theoretical results is much narrower than the confidence intervals with standard error estimates based on the observed Fisher information matrix and based on the bootstrap method. This observation agrees with the results in the Monte Carlo simulation that the standard error estimates based on the theoretical results are likely to underestimate the standard errors of the MDEs (Table 3.2).

Table 3.9: Point and interval estimates for Weibull scale parameter for the data set presented in Table 3.7

Estimator	$\hat{a}$	95% CI based on $\widehat{SE}_A(\hat{a})$	95% CI based on $\widehat{SE}_F(\hat{a})$	95% CI based on $\widehat{SE}_B(\hat{a})$
MLE	2.695		(1.978, 3.412)	(1.980, 3.410)
MDE_S				
$\alpha = 0.01$	2.696	(2.490, 2.902)	(1.976, 3.416)	(2.014, 3.378)
$\alpha = 0.10$	2.700	(2.504, 2.896)	(1.961, 3.439)	(1.967, 3.433)
$\alpha = 0.25$	2.706	(2.531, 2.881)	(1.937, 3.475)	(1.922, 3.490)
$\alpha = 0.50$	2.710	(2.495, 2.925)	(1.900, 3.520)	(1.780, 3.640)
$\alpha = 0.75$	2.703	(2.507, 2.899)	(1.867, 3.539)	(1.731, 3.675)
$\alpha = 0.90$	2.691	(2.495, 2.887)	(1.850, 3.532)	(1.667, 3.715)
MDE_C				
$\alpha = 0.01$	2.617	(2.421, 2.813)	(2.003, 3.231)	(2.019, 3.215)
$\alpha = 0.10$	2.628	(2.442, 2.814)	(2.002, 3.254)	(2.027, 3.229)
$\alpha = 0.25$	2.647	(2.483, 2.811)	(1.997, 3.297)	(2.024, 3.270)
$\alpha = 0.50$	2.677	(2.538, 2.816)	(1.987, 3.367)	(1.976, 3.378)
$\alpha = 0.75$	2.700	(2.576, 2.824)	(1.972, 3.428)	(1.909, 3.491)
$\alpha = 0.90$	2.709	(2.585, 2.833)	(1.960, 3.458)	(1.896, 3.522)
MDE_P				
$\alpha = 0.01$	2.769	(2.453, 3.085)	(1.892, 3.646)	(1.937, 3.601)
$\alpha = 0.10$	2.782	(2.505, 3.059)	(1.884, 3.680)	(1.877, 3.687)
$\alpha = 0.25$	2.802	(2.579, 3.025)	(1.872, 3.732)	(1.866, 3.738)
$\alpha = 0.50$	2.829	(2.665, 2.993)	(1.851, 3.807)	(1.853, 3.805)
$\alpha = 0.75$	2.848	(2.633, 3.063)	(1.835, 3.861)	(1.815, 3.881)
$\alpha = 0.90$	2.855	(2.649, 3.061)	(1.827, 3.883)	(1.780, 3.930)

Table 3.10: Point and interval estimates for Weibull shape parameter for the data set presented in Table 3.7

Estimator	$\hat{b}$	95% CI based on $\widehat{SE}_A(\hat{b})$	95% CI based on $\widehat{SE}_F(\hat{b})$	95% CI based on $\widehat{SE}_B(\hat{b})$
MLE	2.004		(0.945, 3.063)	(0.566, 3.442)
MDE_S				
$\alpha = 0.01$	1.999	(1.847, 2.151)	(0.942, 3.056)	(0.668, 3.330)
$\alpha = 0.10$	1.946	(1.794, 2.098)	(0.916, 2.976)	(0.430, 3.462)
$\alpha = 0.25$	1.872	(1.733, 2.011)	(0.878, 2.866)	(0.275, 3.469)
$\alpha = 0.50$	1.782	(1.630, 1.934)	(0.832, 2.732)	(0.000, 3.705)
$\alpha = 0.75$	1.718	(1.594, 1.842)	(0.799, 2.637)	(0.000, 5.163)
$\alpha = 0.90$	1.690	(1.566, 1.814)	(0.788, 2.592)	(0.000, 4.666)
MDE_C				
$\alpha = 0.01$	2.340	(2.188, 2.492)	(1.079, 3.601)	(0.310, 4.370)
$\alpha = 0.10$	2.276	(2.124, 2.428)	(1.058, 3.494)	(0.349, 4.203)
$\alpha = 0.25$	2.184	(2.045, 2.323)	(1.024, 3.344)	(0.257, 4.111)
$\alpha = 0.50$	2.065	(1.941, 2.189)	(0.974, 3.156)	(0.000, 4.671)
$\alpha = 0.75$	1.978	(1.854, 2.102)	(0.932, 3.024)	(0.000, 9.267)
$\alpha = 0.90$	1.937	(1.813, 2.061)	(0.911, 2.963)	(0.000, 6.431)
MDE_P				
$\alpha = 0.01$	1.732	(1.462, 2.002)	(0.800, 2.664)	(0.715, 2.749)
$\alpha = 0.10$	1.713	(1.473, 1.953)	(0.787, 2.639)	(0.775, 2.651)
$\alpha = 0.25$	1.688	(1.536, 1.840)	(0.773, 2.603)	(0.373, 3.003)
$\alpha = 0.50$	1.653	(1.501, 1.805)	(0.748, 2.558)	(0.403, 2.903)
$\alpha = 0.75$	1.627	(1.503, 1.751)	(0.731, 2.523)	(0.279, 2.975)
$\alpha = 0.90$	1.615	(1.491, 1.739)	(0.723, 2.507)	(0.028, 3.202)

Table 3.11: Point and interval estimates for Weibull scale parameter for the data set presented in Table 3.8

Estimator	$\hat{a}$	95% CI based on $\widehat{SE}_A(\hat{a})$	95% CI based on $\widehat{SE}_F(\hat{a})$	95% CI based on $\widehat{SE}_B(\hat{a})$
MLE	3.249		(2.172, 4.326)	(2.192, 4.306)
MDE_S				
$\alpha = 0.01$	3.248	(2.851, 3.645)	(2.169, 4.327)	(2.194, 4.302)
$\alpha = 0.10$	3.235	(2.853, 3.617)	(2.154, 4.316)	(2.183, 4.287)
$\alpha = 0.25$	3.210	(2.859, 3.561)	(2.131, 4.289)	(2.129, 4.291)
$\alpha = 0.50$	3.165	(2.861, 3.469)	(2.100, 4.230)	(2.010, 4.320)
$\alpha = 0.75$	3.124	(2.884, 3.364)	(2.072, 4.176)	(1.935, 4.313)
$\alpha = 0.90$	3.105	(2.941, 3.269)	(2.057, 4.153)	(1.855, 4.355)
MDE_C				
$\alpha = 0.01$	3.203	(2.887, 3.519)	(2.261, 4.145)	(2.329, 4.077)
$\alpha = 0.10$	3.207	(2.910, 3.504)	(2.247, 4.167)	(2.292, 4.122)
$\alpha = 0.25$	3.213	(2.965, 3.461)	(2.225, 4.201)	(2.269, 4.157)
$\alpha = 0.50$	3.216	(3.030, 3.402)	(2.194, 4.238)	(2.168, 4.264)
$\alpha = 0.75$	3.206	(2.983, 3.429)	(2.165, 4.247)	(2.090, 4.322)
$\alpha = 0.90$	3.192	(2.969, 3.415)	(2.148, 4.236)	(2.036, 4.348)
MDE_P				
$\alpha = 0.01$	3.368	(2.952, 3.784)	(2.096, 4.640)	(2.168, 4.568)
$\alpha = 0.10$	3.379	(2.973, 3.785)	(2.089, 4.669)	(2.076, 4.682)
$\alpha = 0.25$	3.392	(3.005, 3.779)	(2.080, 4.704)	(2.071, 4.713)
$\alpha = 0.50$	3.406	(3.050, 3.762)	(2.069, 4.743)	(2.008, 4.804)
$\alpha = 0.75$	3.414	(3.080, 3.748)	(2.065, 4.763)	(1.912, 4.916)
$\alpha = 0.90$	3.416	(3.100, 3.732)	(2.062, 4.770)	(1.685, 5.147)

Table 3.12: Point and interval estimates for Weibull shape parameter for the data set presented in Table 3.8

Estimator	$\hat{b}$	95% CI based on $\widehat{SE}_A(\hat{b})$	95% CI based on $\widehat{SE}_F(\hat{b})$	95% CI based on $\widehat{SE}_B(\hat{b})$
MLE	1.607		(0.782, 2.432)	(0.485, 2.729)
MDE_S				
$\alpha = 0.01$	1.604	(1.300, 1.908)	(0.779, 2.429)	(0.404, 2.804)
$\alpha = 0.10$	1.588	(1.284, 1.892)	(0.770, 2.406)	(0.476, 2.700)
$\alpha = 0.25$	1.569	(1.272, 1.866)	(0.761, 2.377)	(0.319, 2.819)
$\alpha = 0.50$	1.550	(1.287, 1.813)	(0.751, 2.349)	(0.000, 3.695)
$\alpha = 0.75$	1.535	(1.411, 1.659)	(0.741, 2.329)	(0.000, 4.102)
$\alpha = 0.90$	1.525	(1.386, 1.664)	(0.736, 2.314)	(0.000, 3.997)
MDE_C				
$\alpha = 0.01$	1.825	(1.593, 2.057)	(0.899, 2.751)	(0.206, 3.444)
$\alpha = 0.10$	1.786	(1.571, 2.001)	(0.879, 2.693)	(0.382, 3.190)
$\alpha = 0.25$	1.732	(1.580, 1.884)	(0.851, 2.613)	(0.162, 3.302)
$\alpha = 0.50$	1.668	(1.504, 1.832)	(0.816, 2.520)	(0.000, 8.867)
$\alpha = 0.75$	1.625	(1.501, 1.749)	(0.791, 2.459)	(0.000, 4.849)
$\alpha = 0.90$	1.606	(1.482, 1.730)	(0.781, 2.431)	(0.000, 5.860)
MDE_P				
$\alpha = 0.01$	1.464	(1.167, 1.761)	(0.697, 2.231)	(0.733, 2.195)
$\alpha = 0.10$	1.455	(1.158, 1.752)	(0.691, 2.219)	(0.626, 2.284)
$\alpha = 0.25$	1.444	(1.147, 1.741)	(0.685, 2.203)	(0.533, 2.355)
$\alpha = 0.50$	1.433	(1.149, 1.717)	(0.676, 2.190)	(0.432, 2.434)
$\alpha = 0.75$	1.428	(1.158, 1.698)	(0.674, 2.182)	(0.292, 2.564)
$\alpha = 0.90$	1.426	(1.170, 1.682)	(0.672, 2.180)	(0.021, 2.831)

Chapter 4

Concluding Remarks and Future Research Directions

4.1. Concluding Remarks

4.1.1. Improved Test for Monotonic Trend in Time Series Data

In the study of testing the monotonic trend, we have illustrated that the Brillinger test (Brillinger, 1989) for monotonic trend in time series can only control the significance level when the record length of time series is large and/or the autocorrelation in the residuals are weak. When the record length of the time series is small and/or when there is strong autocorrelation in the residuals, the Brillinger test based on normal approximation tends to give significance level higher than the nominal 5% level. We have investigated plausible reasons for the inflated significance levels and proposed three different bootstrap-based procedures based on the Brillinger test statistic to test for monotonic trend in time series.

Compared to the observed significance level of Brillinger's test, the estimated significance levels of the three proposed bootstrap-based procedures are much closer to the nominal level, especially when the record length is short and/or the autocorrelation in noise series is strong. When exploring the estimated power values, all the three proposed test procedures give reasonable power under all the settings considered in this dissertation.

In addition, the three proposed bootstrap-based procedures are compared with other trend test procedures for testing the monotonic trend in the literature. We have shown

that compared to other existing trend test procedures, when there are strong autocorrelation in time series, the three proposed bootstrap procedures can control the significance level closer to the nominal level. Overall speaking, the three bootstrap-based procedures give a reasonable modification to the Brillinger test procedure for testing the monotonic trend, and these tests are recommended to use in practice, especially when the record length of the time series is short and/or highly correlated.

4.1.2. Robust Parameter Estimation for System Lifetime Data

In the study of system lifetime data, we study the robust estimation method for the model parameters in the component lifetime distribution based on system lifetime data with known system structure. Minimum density power divergence estimation method is considered and three different minimum density power divergence estimators are proposed. Standard error estimation and interval estimation procedures based on the minimum density power divergence estimators are also studied. The three proposed estimation procedures are compared to the maximum likelihood estimation method via a Monte Carlo simulation study. It is shown that the minimum density power divergence estimation method based on system-level data can provide better performance in both point and interval estimation when there is longer-life contamination in the data. We have also showed that the standard error estimates based on bootstrap method can be adopted for estimating the standard errors of the minimum density power divergence estimators.

There are three procedures proposed based on the minimum density divergence estimator, which are the minimum density divergence estimator at system lifetime level (MDE_S), the minimum density divergence estimator at component lifetime level (MDE_C) and the minimum density divergence estimator with estimated p.d.f. (MDE_P). In terms of point estimation, the MDE_S is the most robust one among the three minimum density divergence estimators under different contamination proportions, different system structures and different censoring rates. For the MDE_C, it is the most sensitive one among the three MDEs in the sense that the performance of MDE_C is different for different con-

tamination models, different system structures and different censoring rates. In addition, the MDE_P procedure has similar performance as the MDE_S in most cases for point and interval estimation. However, for point estimation, the MDE_P performs differently in estimating the parameters and the mean component lifetime with different system structures, while the MDE_S gives consistent estimation with different system structures.

Compared with the MLE for point estimation, the MLE outperforms the MDEs when there is no contamination in the data. However, we observe that the system-level minimum density divergence estimator (MDE_S) is a robust estimator compared to the MLE when there is contamination in the data. For interval estimation, we observe that the contaminated data considerably affect the coverage probabilities of the confidence intervals based on MLE and MDE_S. The confidence intervals based on MDE_S perform better than those based on MLE for contaminated data, especially when the contamination rate is high (say, 10% or 15%) in the longer-life contamination model.

For contamination data with longer lifetimes, MDE_S with value of α close to 1 ($\alpha = 0.75$ or 0.9) is recommended. For contamination data with shorter lifetimes, MDE_S with value of α close to 0 ($\alpha = 0.01$ or 0.1) is recommended. Since the choice of the value α for the MDE_S affect the results for the interval estimation, it is interesting to study the choice of the value of α in the system-level minimum divergence estimator MDE_S. In practice, the sample size m, the system signature $\boldsymbol{s}$, the censoring proportion are known, but the underlying component lifetime distribution and the contamination rate are usually unknown. The performance of the estimators with different values of α can be studied under different underlying component lifetime distributions and contamination rates via simulation, and then a reasonable range of the value of α can be obtained.

4.2. Future Research Directions

4.2.1. Improved Test for Monotonic Trend in Time Series Data

In the Brillinger test, as presented in Eq. (1.3), the smoothed periodogram spectral estimate $\hat{f}_{EE}(0)$ is used to estimate the power spectrum of the noise series at frequency of 0 $f_{EE}(0)$. In order to calculate the smoothed periodogram specral estimate $\hat{f}_{EE}(0)$, the noise series and signal series are first estimated respectively as:

$$\hat{S}(t) = \sum_{s=-V}^{s=V} Y(t+s)/(2V+1), \tag{4.1}$$

and

$$\hat{E}(t) = Y(t) - \hat{S}(t), \tag{4.2}$$

where V is the moving average parameter. With the estimated noise series $\hat{E}(t)$, the Fourier transform of $\hat{E}(t)$ is $\hat{\epsilon}_j = \sum_{t=V+1}^{t=T-1-V} \hat{E}(t)\exp(-2\pi itj/T), j = 0, ..., T$. Then, the smoothed periodogram spectral estimate can be calculated as:

$$\hat{f}_{EE}(0) = \frac{\sum_{j=1}^{L} \frac{1}{2\pi T}|\hat{\epsilon}_j|^2}{\sum_{j=1}^{L}(1-a_j)^2}, \tag{4.3}$$

where $a_j = \frac{sin(2\pi j \frac{2V+1}{2T})}{(2V+1)sin\frac{2\pi j}{2T}}$, and L is the spectrum truncation point.

In our study, the moving average parameter V, which is the length of moving average window for the estimated signal term $S^{(t)}$, is set to be $0.05T$. The spectrum truncation point L, which is used to calculate the smoothed periodogoram that estimates the power spectrum of the estimated noise term, is set to be $2\sqrt{T}$. It would be interesting to further evaluate whether the performance of the Brillinger test is sensitive to the moving average parameter V and the spectrum truncation point L.

In order to evaluate the influences of V and L on the Brillinger test, a simulation of 1000 realizations for the AR(1) model with length $n = 100$:

$$Y(t) = E(t),$$

with

$$(1 - 0.95B)E(t) = a_t,$$

and a_t being a $N(0, 1)$ white noise series are generated. The 1000 realizations of time series are further analyzed using the Brillinger test based on different V and L.

When assessing the effect of the moving average parameter, the truncation point parameter L is fixed at $L = 7$ (Figure 4.1a), which is roughly the value $2\sqrt{100}$. When evaluating the effect of truncation point, the moving average parameter V is fixed at $V = 5$ (Figure 4.1b), which is 5% of the realization length 100. It is shown in Figure 4.1 that the performance of the Brillinger test varies with different values of V and L. With a fixed truncation points $L = 7$, the performance of the Brillinger test becomes better when the moving average parameter V increases (Figure 4.1a). However, with a fixed moving average parameter $V = 5$, the percentage of identifying a significant trend increases as the truncation point L increases (Figure 4.1b). Hence, for future research, it would be interesting to study the impact of the moving average parameter V and the spectrum truncation point L on the results of testing the monotonic trend using the Brillinger method and the three proposed bootstrap procedures based on the Brillinger test statistic.

4.2.2. Robust Parameter Estimation for System Lifetime Data

In lifetime data analysis, when censoring is involved and the last observation is a right-censored observation (for example, a Type II censored sample), it is known that the nonparametric estimate of the c.d.f. $G_T(t)$ becomes a constant for all t greater than the last observed failure time. For this reason, we can consider using a truncated distribution in the minimum density divergence estimation.

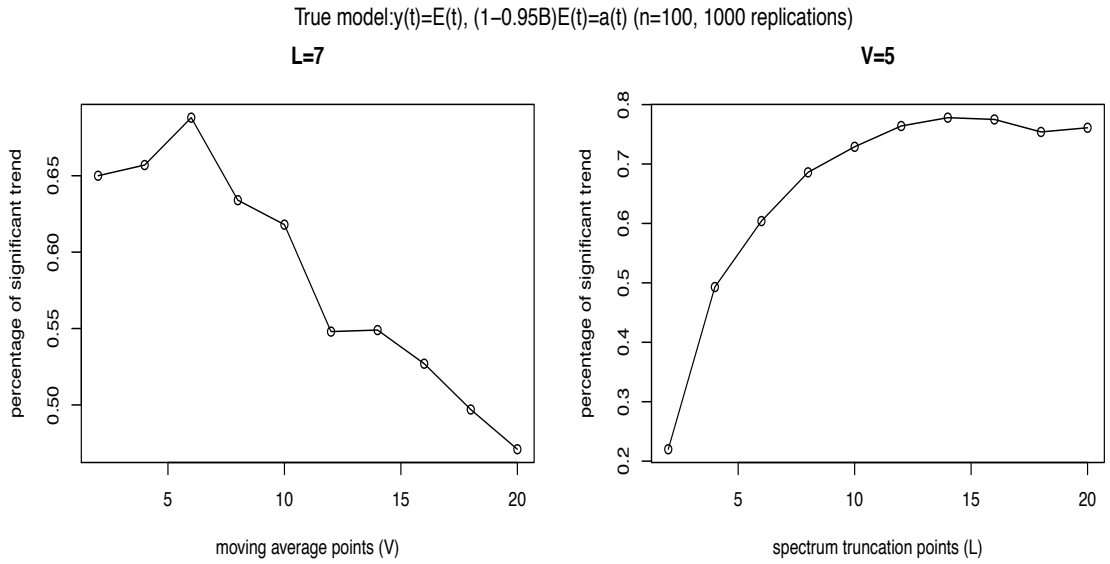

Figure 4.1: Percentage of identifying a significant trend for testing the monotonic trend with (a) the smooth window for spectrum $L = 7$ and the moving average parameter V varying from 2 to 20 in interval of 2 and with (b) the moving average parameter $V = 5$ and the smooth window for spectrum L varying from 2 to 20 in interval of 2

Specifically, suppose we observe the r system lifetimes among the m systems in a life test to obtain a Type II censored sample $T_{1:m} < T_{2:m} < ... < T_{r:m}$. From the result in order statistics, if $T_1, T_2, ..., T_m$ is a random sample of size m with p.d.f. $f(t)$ and c.d.f. $F(t)$, then conditional on the rth order statistic $T_{r:m} = c$, the random variable $T_{j:m}, 1 \leq j \leq r-1$ is the jth order statistic of a random sample of size $r-1$ from a truncated distribution with p.d.f. $f(t)/F(c), t < c$. Hence, we can obtain a minimum density divergence estimator based on $T_{j:m}, 1 \leq j \leq r-1$, given $T_{r:m} = c$, using a truncated distribution. Here, the truncated density for the system lifetime is $f_{T,c}(t;\boldsymbol{\theta}) = f_T(t;\boldsymbol{\theta})/F_T(c;\boldsymbol{\theta}), t \leq c$, and the empirical distribution of the truncated target distribution is $\hat{G}_{T,c}(t) = \hat{G}_T(t)/\hat{G}_T(c), t \leq c$. Let the truncated target density be $g_{T,c}(t)$ and the truncated fitted model be $f_{T,c}(t)$. The estimated density divergence based on Type II censored system lifetime data can be obtained as:

$$\begin{aligned}\hat{d}_\alpha(g_{T,c}, f_{T,c}) &= \int_0^c f_{T,c}(t;\boldsymbol{\theta})^{1+\alpha}dt - \int_0^c \left(1+\frac{1}{\alpha}\right) f_{T,c}(t;\boldsymbol{\theta})^{\alpha} d\hat{G}_{T,c}(t) \\ &\approx \int_0^c f_{T,c}(t;\boldsymbol{\theta})^{1+\alpha}dt - \sum_{j=1}^{r-1} \left(1+\frac{1}{\alpha}\right) f_{T,c}(t;\boldsymbol{\theta})^{\alpha} \tilde{g}_{T,c}(t_j),\end{aligned}$$

where

$$\tilde{g}_{T,c}(t_j) = \begin{cases} \hat{G}_{T,c}(t_j) - \hat{G}_{T,c}(t_{j_1}), & j \le r, \\ 1 - \sum_{j=1}^{r-1} \hat{G}_{T,c}(t_j), & j = r. \end{cases} \tag{4.4}$$

We refer the estimator obtained from the minimum density divergence estimator at system level with truncation as $\hat{\boldsymbol{\theta}}_{ST}$.

Similar to the idea in the system-level MDE, we can estimate the parameters by considering truncation based on the component-level data. The truncated density function at component level is $f_{X,c}(t;\boldsymbol{\theta}) = f_X(t;\boldsymbol{\theta})/F_X(c;\boldsymbol{\theta}), t \le c$ for the fitted model, and is $g_{X,c} = g_X(t)/G_X(c), t \le c$ for the target distribution. Moreover, the empirical distribution can be rescaled as $\hat{G}_{X,c}(t) = \hat{G}_X(t)/\hat{G}_X(c), t \le c$. An estimator of $\boldsymbol{\theta}$ ($\hat{\boldsymbol{\theta}}_{CT}$) can be obtained by minimizing the density divergence measure:

$$\begin{aligned}\hat{d}_\alpha(g_{X,c}, f_{X,c}) &= \int_0^c f_{X,c}^{1+\alpha}(t;\boldsymbol{\theta})dt - \int_0^c (1+\frac{1}{\alpha}) f_{X,c}^{\alpha}(t;\boldsymbol{\theta}) d\hat{G}_{X,c}(t) \\ &\approx \int_0^c f_{X,c}^{1+\alpha}(t;\boldsymbol{\theta})dt - \sum_{j=1}^{r} (1+\frac{1}{\alpha}) f_{X,c}^{\alpha}(t;\boldsymbol{\theta}) \tilde{g}_{X,c}(t_j),\end{aligned}$$

where

$$\tilde{g}_{X,c}(t_j) = \begin{cases} \hat{G}_{X,c}(t_j) - \hat{G}_{X,c}(t_{j_1}), & j \le r, \\ 1 - \sum_{j=1}^{r-1} \hat{G}_{X,c}(t_j), & j = r. \end{cases} \tag{4.5}$$

Furthermore, based on the results in Chapter 3, we make some recommendations for the α parameter in the MDE method. In addition, we observe that the performance of the MDEs depends on the power parameter. Hence, it is interesting to study how to choose the value of α for the MDE. For future research, a systematic way to choose the value of α for the minimum density divergence estimator can be studied. On the other hand, since the simulated coverage probabilities of the confidence intervals based on the estimators studied in this dissertation can be much lower than the nominal level when there is contamination in the data, it is desire to develop better standard error estimation methods and confidence interval estimation methods which can provide better coverage probabilities when there is contamination in the data.

Bibliography

Basu A., Harris I.R., Hjort N.L., Jones M.C. (1998). Robust and efficient estimation by minimising a density power divergence. *Biometrika*, 3:549–559.

Basu S., Basu A., Jones M.C. (2006). Robust and efficient parametric estimation for censored survival data. *Annals of the Institute of Statistical Mathematics*, 58:341–355.

Balakrishnan N., Ng H.K.T., Navarro J. (2011a). Exact nonparametric inference for component lifetime distribution based on lifetime data from systems with known signatures. *Journal of Nonparametric Statistics*, 23:741–752.

Balakrishnan N., Ng H.K.T., Navarro J. (2011b). Linear Inference for type-II censored lifetime data of reliability systems with known signature. *IEEE Transactions on Reliability*, 60:426–440.

Balakrishnan N., Tan T. (2016). A parametric test for trend based on moving order statistics. *Journal of Statistical Computation and Simulation*, 86:642–655.

Bloomfield P., Nychka D.W. (1992). Climate spectra and detecting climate change. *Climate Change*, 21:275–287.

Boland P.J., Samaniego F.J. (2004). The signature of a coherent system and its application in reliability. In: Soyer R. Mazzuchi T.A., Singpurwalla N.D. (eds) Mathematical Reliability: An Expository Perspective. International Series in Operations Research & Management Science, Vol. 67. Springer, Boston, MA.

Bonaccorso B., Cancelliere A., Rossi G. (2005). Detecting trends of extreme rainfall series in sicily *Advance in Geosciences*,2:7–11.

Brillinger D.R. (1989). Consistent detection of a monotonic trend superinposed on a stationary time series. *Biometrika*, 76:23–30.

Burg J.P. (1975). Maximum entropy spectral analysis. *PhD dissertation, Stanford University*.

Chahkandi M., Ahmadi J., Baratpour S. (2014). Non-parametric prediction intervals for the lifetime of coherent systems. *Statistical Papers*, 55:1019–1034.

Cochrane D., Orcutt G.H. (1949). Application of least squares regression to relationships containing auto-correlated error terms. *Journal of the American Statistical Association*, 44:32–61.

Cohen A.C. (1991). Truncated and censored samples: theory and applications. *New York: Marcel Dekker*.

Cohn A.T., Lins F.H. (2005). Nature's style: Natually trendy. *Geophysical Research Letters*, 32:L23402.

Efron B., Tibshirani R.J. (1993). An Introduction to the Bootstrap. *New York: Chapman & Hall*.

Feidas H., Makrogiannnis T., Bora-Senta E. (2004). Trend analysis of air temperature time series data in greece determined by ground and satellite data. *Theoretical and Applied Climatology*, 79:185–208.

Hamed K.H., Rao A.R. (1998). A modified mann-kendal trend test for autocorrelated data. *Journal of Hydorlogy*, 204:182–196.

Hofmann G., Balakrishnan N. (2006). A nonparametric test for trend based on initial ranks. *Journal of Statistical Computation and Simulation*, 76:829–837.

Kaplan E.L., Meier P. (1958). Nonparametric estimation from incomplete observations. *Journal of the American Statistical Association*, 53:457–481.

Kendall M.G. (1955). Rank correlation methods. *Griffin, London*.

Kochar S., Mukerjee H., Smaniego F.J. (1999). The signature of a cohenrent system and its application to comparison among systems. *Naval Research Logistics*, 46:507–523.

Kullback S., Leibler R.A. (1951). On information and sufficiency. *Annals of Mathematical Statistics*, 22:79–86.

Mann H.B. (1946). Nonparametric test against trend. *Econometrica*, 13:245–259.

Meeker W.Q., Escobar L.A. (1998). Statistical Methods for Reliability Data. *New York: John Wiley & Son*.

Navarro J., Ruiz J.M., Sandoval C J. (2007). Properties of coherent systems with dependent components. *Communnications in Statistics - Theory and Methods*, 36:175–191.

Ng H.K.T., Navarro J., Balakrishnan N. (2012). Parametric inference from system lifetime data under a proporitonal hazard rate model. *Metrika*, 75:367–388.

Park R.E., Mitchell B.M. (1980). Estimating the autocorrelated error model with trended data. *Journal of Econometrics*, 13:185–201.

Samaniego F.J. (2007). System signatures and their applications in engineering reliability. *Springer, New York*.

Sheather S.J., Jones M.C. (1991). A reliable data-based bandwidth selection emthod for kernel density estimation. *Journal of the Royal Statistical Society Series B*, 53:683–690.

Sun H., Pantula S.G. (1999). Testing for trends in correlated data. *Statistics and Probability Letters*, 41:87–95.

Woodward W.A., Gray H.L. (1993). Global warming and the problem of testing for trend in time series data. *Journal of Climate*, 6:953–962.

Woodward W.A., Gray H.L. (1995). Selecting a model for detecting the presence of a trend. *Journal of Climate*, 6:1929–1937.

Woodward W.A., Bottone S., Gray H.L. (1997). Improved tests for trend in time series data. *Journal of Agricultural, Biological and Environmental Statistics*, 2:403–416.

Woodward W.A. (2013). Trend detecting. Encyclopedia of Environmetrics, 6.

Xu X.Z., Takeauchi K., Ishidaira H. (2002). Long term trends of annual temperature and precipitation time series in Japan. *Journal of Hydroscience and Hydraulic Engineering*, 20:11–26.

Yang Y., Ng H.K.T., Balakrishnan N. (2016). A stochastic expectation-maximization algorithm for the analysis of system lifetime data with known signature. *Computational Statistics*, 31:609–641.

Yang Y., Ng H.K.T., Balakrishnan N. (2019). Expectation-maximization algorithm for system-based lifetime data with unknown system structure. *AStA Advances in Statistical Analysis*, 103:69–98.

Zhang J., Ng H.K.T., Balakrishnan N. (2015). Statistical inference of component lifetimes with location-scale distribution from censored system failure data with known signature. *IEEE Transactions on Reliability*, 64:613–626.